Formation and Signaling of Electrophilic Lipids in Immunity

by

Gregory James Buchan

Bachelor of Science, University of Akron, 2014

Submitted to the Graduate Faculty of

School of Medicine in partial fulfillment

of the requirements for the degree of

Doctor of Philosophy

University of Pittsburgh

2019

UNIVERSITY OF PITTSBURGH

SCHOOL OF MEDICINE

This dissertation was presented

by

Gregory James Buchan

It was defended on

November 8, 2019

and approved by

Thomas W. Kensler, Professor – Dept. Pharmacology and Chemical Biology

(Currently at Fred Hutchinson Cancer Research Center)

Seema S. Lakdawala, Assistant Professor – Dept. Microbiology and Molecular Genetics

Paul R. Kinchington, Professor – Dept. Ophthalmology and Dept. Microbiology and Molecular Genetics

Robert J Binder, Associate Professor – Dept. Immunology and Dept. Pharmacology and Chemical Biology

Dissertation Co-Director, Bruce A. Freeman, Professor and Chair – Dept. Pharmacology and Chemical Biology

Dissertation Co-Director, Stacy G. Wendell, Assistant Professor – Dept. Pharmacology and Chemical Biology

Formation and Signaling of Electrophilic Lipids in Immunity

Gregory James Buchan, PhD

University of Pittsburgh, 2019

Many diseases are caused by aberrant inflammation. Novel drug strategies are transitioning from global suppression and single-target inhibition to fine tuning the immune response by modifying several key pathways in order to minimize tissue injury. Recently, classes of pleiotropic, electrophilic lipids (mainly nitroalkenes and α, β-unsaturated ketones), are emerging as prominent immunomodulators that both dampen inflammation and initiate cytoprotective responses. Electrophilic lipids alkylate nuclear factor kappa-light-chain-enhancer of activated B cells (NF-κB) causing a decrease in inflammation. Furthermore, kelch-like ECH-associated protein 1 (Keap1) is also alkylated by electrophilic lipids, causing the release of nuclear factor (erythroid-derived 2)-like 2 (Nrf2) and the activation of hundreds of genes involved in repairing and preventing cellular injury.

Moreover, endogenous lipid mediators such as Lipoxin A_4 (LXA_4) have successfully limited tissue injury in animal models of sepsis, acute lung injury, and asthma. The primary metabolite of LXA_4, 15-oxo-LXA_4, is electrophilic and its role in immune responses is understudied. Herein, I demonstrate that 15-oxo-LXA_4 acts in a similar manner to other electrophilic lipids and limits LPS-induced inflammatory responses in murine macrophages. These data suggest electrophilic metabolites of endogenous lipid mediators such as LXA_4 may be partially responsible for their anti-inflammatory and cytoprotective actions.

Nitroalkenes alkylate NF-κB and Keap1, resulting in dampened inflammatory responses and active tissue repair. In fact, Nitro-Oleic Acid (NO_2-OA) is currently in clinical trials for focal

segmental glomerulosclerosis, asthma and pulmonary hypertension. Much of the preclinical research for nitroalkenes has been carried out in epithelial, endothelial, or macrophages so their effect on dendritic cell function is largely unknown. The data provided within suggest that NO_2-OA limits DC activation. These changes are consistent with other electrophilic lipids and suggest a common role in modifying immune responses.

Lastly, I tested the efficacy of NO_2-OA in treating influenza-induced lung injury in mice. Survival increased compared to vehicle controls and pro-inflammatory cytokine production was decreased. These results demonstrate the potential of NO_2-OA to improve outcomes of severe viral infection, characterized by aberrant inflammation. Further research on NO_2-OA, 15-oxo-LXA_4 and other electrophiles will enhance the knowledge of these agents and inform future clinical trials and drug discovery efforts.

Table of Contents

List of Tables

List of Figures

Preface

I would like to thank my mentors, Stacy G. Wendell, PhD and Bruce A. Freeman, PhD for their continued support over the past 4 years. They always encouraged me to pursue novel and impactful ideas and supported me professionally. Moreover, I credit my committee for valuable insight into pharmacology, toxicology, immunology, virology, and cell signaling – I have benefited greatly from an interdisciplinary project. In fact, support from the committee, especially from Seema S. Lakdawala, PhD, Stacy, and Bruce, led to a successful grant submission and awarding of an F31. Thomas W. Kensler, PhD and Paul R. Kinchington, PhD were always asking difficult questions that forced me to think of larger concepts as well as important details that influenced my research. Robert J. Binder, PhD contributed greatly to my knowledge of flow cytometry and DC immunity. I also gained an abundance of technical and experimental knowledge from the Freeman laboratory, especially from Sonia Salvatore and the late Franca Bisello. Francisco Schopfer, PhD, set up collaborations with colleagues in Denmark that led to me being second author on a PNAS publication. Furthermore, this dissertation would not be possible without the immense scientific contributions from Crystal Uvalle, Veronika Cechova, Adolf Koudelka, PhD, Michelle Manni, PhD, Hiroshi Yano, PhD, Gracie Liu, PhD, James O'Brien, Steve Mullett, Soma Jobbaby, PhD, Julia Woodcock, PhD, and Madeline Ellgass.

The Department of Pharmacology and Chemical Biology administrative staff was immensely helpful. Shannon Granahan ensured milestones were hit and progress was being made, along with Patrick Pagano, PhD. Holly Gergely and Jennifer Cristali were essential in the submission of my F31. Jim Kaczynski always let me get sandwiches and coffee before seminars began and, with Barb Martin, enabled my Keurig coffee addiction. I would still be trying to

download software, wrestling with the department sonicator and washing my lab equipment if it weren't for Rich Smith, Brian Taylor, and Ricky Serventi. Finally, health insurance and traveling to conferences were made possible because of Ginnie Reiner, Jeanette McDew, and Lynda Sorch. Departmental support was awesome and allowed me to dedicate my time to research.

Finally, I would like to acknowledge my family that has supported me through this entire process and continues to do so as I continue my career. My wife, Erin, followed me with the utmost support and trusted me when we came to Pittsburgh in pursuit of a scientific career. She has been an amazing mother to our son, Connor, and has been there through all of the ups and downs of this process. I would never have been able to graduate without her support and she kept me healthy by making me dinners for late night lab sessions. Being able to lean on Erin was essential for my continued motivation and being able to finish. She enabled my Karaoke habit with Ravi Patel, PhD, Shelby Hemker, PhD, Ryan Staudt, PhD, and Hiroshi. She also bought me a piano after my major thesis project took a turn for the worse so I could regain my confidence and motivation. Her and both of our families have sacrificed so much of their time to make sure I could reach my goals and for that, I am forever grateful.

1.0 Introduction

1.1 Inflammation and Injury

Inflammation is an essential response to tissue injury and infection. A myriad of external stimuli such as air pollution, viruses, and trauma can incite an inflammatory response. Furthermore, internal irritants such as stress, atherosclerosis, and changes in metabolism (e.g. type II diabetes) will initiate similar actions. The cardinal signs of inflammation include redness, pain, heat, swelling, and loss of function. These symptoms are caused by the production of cytokines and chemokines that activate the local environment and recruit leukocytes to clear the insult. All symptoms eventually decrease as the infection or injury is cleared; however, the strength and duration of the response can vary – sometimes in a negative manner. Excessive responses can result in acute episodes that cause significant bystander tissue damage while chronic responses skew the normal immune response to an altered, malignant state [1, 2]. Therefore, much of our health depends on the well-orchestrated and near-perfect collaboration between all aspects of the immune response [3-6]. In fact, immunity involves every aspect of cellular signaling from growth, proliferation, and metabolism to programmed cell death, making drug discovery and pharmacological examination of novel therapeutics difficult. A better understanding of how inflammation is controlled will likely lead to novel therapeutics for hundreds of diseases and it is imperative to evaluate new treatments in the context of immunity.

1.1.1 Inflammatory Signaling

Inflammation begins with the detection of cellular injury (e.g. xenobiotic toxicity, trauma), infection, internal stress from metabolic imbalances, protein overload (endoplasmic reticulum stress), or genome instability [4, 6]. Cellular damage, infection, and other noxious stimuli are detected by damage-associated or pathogen-associated molecular patterns (DAMPs and PAMPs) by a variety of receptors on the surface of many cell types, including immune cells. For example, airway epithelial cells and antigen-presenting cells (APCs) express toll like receptors (TLRs) that bind PAMPs such as lipopolysaccharide (LPS), cytosolic DNA, and double-stranded RNA [7-10]. Many DAMPs are released during cell death and include uric acid, ATP, extracellular DNA, oxidized phospholipids (oxPLs), and a variety of different proteins such as interleukin (IL)-33 [1, 11-13]. Together with a host of transcription factors and intracellular signaling cascades, these detectors will initiate the inflammatory response by alerting innate immune cells.

After detecting cellular damage and other noxious stimuli, cells will produce a host of pro-inflammatory mediators including lipid mediators, cytokines, and chemokines. This is done by activating transcription factors such as nuclear factor kappa-light-chain-enhancer of activated B cells (NF-κB) downstream of pattern recognition receptors and their associated kinases (e.g. MyD88 for TLR4). In addition to the transcription of pro-inflammatory genes, cells will be mobilized for changes in proliferation, metabolism, and migration depending on the acting stimulus [14, 15]. This simplified scenario will result in the production of cytokines like interleukin (IL)-12, IL6, monocyte chemoattractant protein 1 (MCP1), and tumor necrosis factor alpha (TNFα). Moreover, enzymes such as cyclooxygenase (COX)-2 and inducible nitric oxide synthase (NOS2) will be induced and begin synthesizing their products (i.e. prostaglandins and nitric oxide). These actions will attract neutrophils, activate resident macrophages and dendritic cells (DCs), and

alert nearby monocytes to differentiate into a myriad of effector cells. Then, these innate cells will converge to eliminate the damaging stimuli as well as initiate adaptive immune responses in the event the same stimulus is seen again. Under normal conditions, these responses will clear the insult and initiate cellular repair mechanisms that return tissues to homeostasis. Until inflammation is resolved, the cycle of stimulation, cellular activation, production of cytokines, reactive oxygen and nitrogen species, and lipid mediators will continue indefinitely (**Fig 1**).

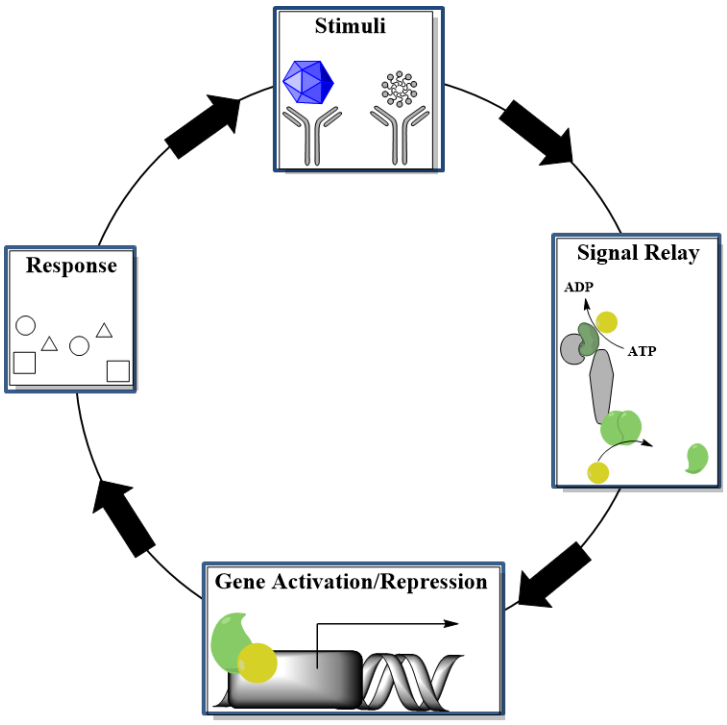

Figure 1: Positive feedback loop of inflammation

A stimulus (DAMP or PAMP) will intiate a signal relay (e.g. NF-κB), usually involving phosphorylation cascades, that will alter the expression of hundreds if not, thousands of genes within the cell in order to respond to injury or stress. A response consisting of free radicatl generation, cytokine production, and cellular recruitment will insue and continue until inflammation resolves; otherwise, irreversible tissue damage will result.

1.1.2 Aberrant Inflammation

When inflammation fails to resolve, damage to cells and tissues occurs through excessive generation of reactive oxygen and nitrogen species, cell death, and the sustained recruitment of leukocytes and cytokine production [16, 17]. For example, viral-induced acute lung injury can result in acute respiratory distress syndrome due to an exuberant host response [18]. In this case, neutrophils and dendritic cells become pathogenic by generating massive amounts of free radical species that promote tissue injury [19-22]. In multiple sclerosis (MS), DCs activate T lymphocytes that cause myelin sheath degeneration [23, 24]. The pathogenesis to MS is closely linked to the amplification of effector T cells and the sustained production of pro-inflammatory cytokines (e.g. IL12, IL23, IL6, interferon [IFN]γ) from DCs [23, 24]. Most inflammatory diseases – acute, chronic, and autoimmune – are linked with the prolonged and aberrant production of cytokines and a sustained presence of immune cells. Therefore, novel therapeutics are targeting macrophages and dendritic cells for their central role in initiating both innate and adaptive immunity.

1.1.3 Key regulators of immunity

Cytokine and chemokine production, in addition to the release of lipid mediators like prostaglandins and pro-resolving mediators, activate and instruct immune cells. Mainly, neutrophils, macrophages, and DCs will be the first to respond to injury or infection, depending on the nature and location of the insult. These cells can be residents of the tissue (e.g. Alveolar macrophages – lung, Langerhans DCs – skin) or circulate within the bloodstream until chemokines induce their migration. As more cells are needed, monocytes or other precursors from the bloodstream or bone marrow can differentiate into more specialized cell subsets, depending on the

needs of the immune response – all defined by tissue type, local environment, duration, and strength of signals received by each individual cell. Both macrophages and DCs are absolutely essential for initiating immune responses and activating adaptive immunity by presenting antigen to T and B lymphocytes.

1.1.3.1 Dendritic Cells and Macrophages

DCs are specialized cells defined by their ability to sample the environment for antigens and initiate immune responses. Activated DCs are programmed to rapidly react and regulate the immune response according to the given stimulus [25-27]. Upon ligation of TLR ligands, DCs will alter their metabolism in order to accommodate the rapid expansion of membranes, cytokine production, the growing ATP demand, and reducing factors such as NADPH [28-31]. During and after metabolic reprogramming, DCs will continue to generate cytokines and chemokines (e.g. IL6, IL12, IL23, IL15) that recruit and activate natural killer cells, surrounding macrophages, neutrophils, and lymphocytes. Some DCs will migrate to nearby lymph nodes to initiate adaptive immunity by presenting antigen to T and B cells – bridging all aspects of the immune response [32-34]. Because of their essential role in innate and adaptive immunity, DCs are becoming targets for novel therapeutics that aim to modulate aberrant immune responses [35]. In fact, there are instances of acute and chronic inflammation where limiting DC function is effective in minimizing tissue damage caused by excessive cytokine production and free radical production [19, 36-38].

Macrophages, like DCs, are often positioned in tissues where they can quickly respond to pathogens or injury. For example, alveolar macrophages of the lung will become activated upon viral infection or inhalation of air pollutants. These cells will also utilize TLRs and other pattern recognition receptors in order to instruct intracellular signaling cascades that induce or repress

hundreds of genes. Cytokine production will alert nearby cells and macrophages will begin phagocytosing damaged cells and/or pathogens, while DCs are activating T and B lymphocytes [39-42]. The function and method of activation for DCs and macrophages are very similar, in fact, both undergo aerobic glycolysis after LPS administration and produce cytokines and chemokines to initiate immunity. Furthermore, they possess similar surface markers (e.g. CD11c, CD11b, MHCII) and are a heterogeneous population when cultured *in vitro* [43-46]. Therefore, therapeutics designed for one or the other may impact both populations, making understanding macrophage and DC pharmacodynamics during treatment essential.

1.1.3.2 Immunometabolism

Metabolism plays a major role in the regulation of immunity [47-49]. As tissues respond to damage and pathogens, energy requirements are shifted to meet the demanding use of lipids, proteins, nucleotides, and reducing factors (e.g. NADPH) by cells. Immune cells undergo rapid growth and proliferation, in addition to producing RS, cytokines, and lipid mediators, requiring massive generation of cellular building blocks [50-52]. Similar to cancer cells, many immune cells will enter aerobic glycolysis to meet their new energy quota [49]. In general, cells will shunt glucose into glycolysis despite having enough oxygen for the TCA cycle and oxidative phosphorylation. However, there are tiers and gradients to this response and recent data suggests different subsets of immune cells will have optimized and disparate metabolic states [53-58]. For example, inflammatory T cell phenotypes, TH17 and TH1, undergo aerobic glycolysis whereas, TH2 and TREG (allergic and anti-inflammatory phenotypes) will rely on oxidative phosphorylation and fatty acid catabolism [53, 59].

Furthermore, pro-inflammatory macrophages (M1) can be distinguished from their reparative counterparts (M2) by their metabolic patterns. Much like TH1 and TH17 cells, M1 macrophages will utilize glycolysis more than oxidative phosphorylation [55, 60]. A plethora of studies have demonstrated how manipulating proteins that regulate metabolism can augment immune responses. Dimethyl fumarate (DMF), a synthetic analog of the electrophilic metabolite, fumarate, can alkylate GAPDH and inhibiting IFN signaling in DCs [61, 62]. Targeting molecular target of rapamycin (mTOR), hypoxia inducible factor (HIF) α, pyruvate kinase, or succinate dehydrogenase all affect T cells, DC, and/or macrophages [55, 63-76]. Immunometabolism plays a key role in inflammation and has been reviewed extensively [48-51, 54, 56, 58, 59, 70, 77]. Hence, novel therapeutics based on metabolism are being designed to combat inflammatory diseases involving DCs, macrophages, and T lymphocytes.

1.2 Returning to homeostasis after inflammation

It is becoming clear that repair mechanisms and the resolution of inflammation begin not long after the innate response begins [78-83]. In fact, many transcription factors meant for cellular recovery are induced by the same proteins (e.g. NF-κB) that initiated the inflammatory response. For example, nuclear factor (erythroid-derived 2)-like 2 (Nrf2) is activated when reactive species (RS), such as superoxide and nitric oxide (produced from NAPDH oxidases [NOX enzymes] and NOS2 - both induced by NF-κB), oxidize KELCH-like associated protein 1 (KEAP1), and is allowed to enter the nucleus and bind to promotors with antioxidant response elements (AREs) in DNA [84, 85]. After Nrf2 binds to an ARE, hundreds of genes are activated that result in the production of antioxidants and other cellular-repair enzymes [86]. NF-κB also initiates the

production of IL-10 and tissue growth factor (TGF) β as well as induces COX and lipoxygenase (LOX) enzymes that oxidize arachidonic acid and other polyunsaturated lipids (e.g. docosahexaenoic acid), resulting in several pro-resolving lipid mediators (e.g. Lipoxin A_4) – all of which aid in returning cells to homeostasis [87-89]. Hence, complete inhibition of NF-κB would result in the cessation of pro-inflammatory lipids such as prostaglandins and leukotrienes, as well as the anti-inflammatory mediators. Therefore, total suppression of the immune response may result in ineffective clearing of potential stimuli, perturbation of normal homeostatic functions of cell signaling pathways, or inhibition of resolution itself – all of which may contribute to chronic malformations of physiology.

1.2.1 Nrf2 signaling and inflammation

The Nrf2 signaling pathway plays a critical role in protecting cells from injury, activating antioxidant defenses, and detoxifying toxins and xenobiotics [86, 90, 91]. Under homeostatic conditions, Nrf2 is bound to Keap1 in the cytoplasm, ubiquinated, and marked for degradation [84]. After encountering certain stimuli (e.g. electrophile formation, oxidative stress), cysteines within Keap1 are oxidized, Nrf2 translocates to the nucleus, and binds to AREs in hundreds of genes (**Fig 2**) [84, 85, 90-92]. Genes activated represent phase II enzymes involved in the catabolism of xenobiotics, such as heme oxygenase 1 (HO1) and NAD(P)H quinone oxidoreductase 1 (NQO1), glutathione metabolism (e.g. glutamyl-cysteinyl ligase modifier subunit - GCLM), and antioxidant enzymes (e.g. catalase) [86]. All of these changes function to restore the cell to homeostasis and minimize the collateral damage caused by the original stimulus.

There is growing evidence suggesting Nrf2 plays a key role in regulating inflammation. It has been demonstrated that Nrf2 and NF-κB communicate and regulate each other during immune

responses [93, 94]. Furthermore, modulation of Nrf2 signaling can increase or decrease damage done in models of inflammation including influenza infection, sepsis, MS, and asthma [93, 95-99]. Nrf2 activation can limit pro-inflammatory cytokine production, modulate central metabolism, and alter several key regulatory modules within the cell (e.g. NF-κB) – making Nrf2 an important immunomodulator [100-104].

1.2.2 Inhibition of NF-κB

NF-κB is a central regulator of not only inflammation but cellular growth and survival as well [88]. NF-κB generally consists of a dimer of the p65 and p50 subunits (RelA and RelB) and held together in the cytoplasm by IκB [88]. Signal transduction between TLRs and NF-κB is largely controlled by protein cascades mediated by kinases and adaptor proteins that relay their message via phosphorylation (**Fig 2**). Upon activation, a phosphorylation cascade occurs and NF-κB translocates to the nucleus where it binds to the promotor region (κB) of hundreds, if not thousands of genes, altering their transcription [15, 105-109]. After pathogen or injury detection (e.g. TLR signaling), the inhibitor of NF-κB (IκB) kinase (IKK) is phosphorylated leading to the phosphorylation and subsequent degradation of IκB [110]. After IκB is degraded, p65/p50 dimers are free to enter the nucleus and activate inflammatory gene expression. Non-canonical NF-κB signaling can consist of p50/p50 dimers, and p50/p52 – all with varying effects on inflammation [111]. In regards to inflammation, NF-κB activation will lead to increased expression of *Nos2*, *Cox2 Il6, Tnfa, Il1b,* and other primary inflammatory executors. Despite the pathway being

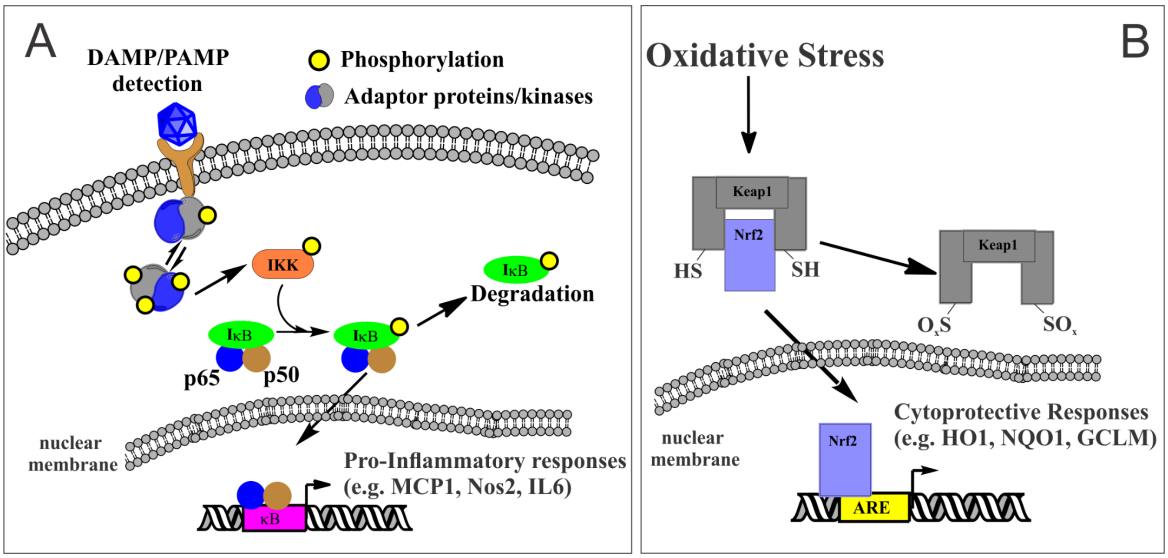

Figure 2: Simplified model of NF-κB and Nrf2 signaling

DAMPs (such as oxidized phospholipids, oxPL) and PAMPs (e.g. viruses) will bind TLRs and intiate a signaling cascade that leads to NF-κB activation (A). Oxidative stress and other components of inflammation will lead to Keap1 oxidation, Nrf2 release and activation (B). These factors, among others, will ensure a well-orchestrated response that minimizes bystander damage and maximizes injury clearance.

immensely complex and multilayered, it has become a primary target in developing anti-inflammatory and immunomodulatory therapeutics [15, 109, 112, 113].

1.3 Formation and signaling of electrophilic lipids

Two main classes of endogenously-produced electrophilic lipids are the α, β-unsaturated ketones and nitroalkenes (**Fig 3**). Both are formed either through enzymatic oxidation and reduction reactions or free-radical induced oxidation and nitration reactions [114-116]. Once

formed, the electrophilic moiety rapidly alkylates nearby nucleophiles. Many key regulatory proteins utilize cysteine residues to carry out their function. The thiol groups (especially deprotonated, thiolate anion) within these proteins will form a covalent, Michael adduct with electrophilic lipids (**Fig 4**). After alkylation, protein function may be unchanged, activated, or inhibited, depending on cellular conditions – culminating in major cellular changes. Many electrophilic lipid mediators are formed during inflammation and play a role in maintaining cellular homeostasis and dampening tissue injury.

Electrophiles (electron poor) contain electron-withdrawing groups (e.g. nitro-, carbonyls, cyano-) that render specific carbons more capable of forming a Michael adduct with nucleophilic (electron rich) functional groups such as thiols. The covalent, Michael adduct can be reversible when "soft" electrophiles modify "soft" nucleophiles; however, hard electrophiles and hard nucleophiles will typically form irreversible covalent adducts – based on electronegativity, steric hindrance, and other chemical factors [117-119]. Only recently, have soft electrophiles been appreciated for their reversible, and often anti-inflammatory properties because drug developers were concerned mostly with hard electrophiles and their toxicity due to the formation of irreversible adducts [118, 120]. Many hard electrophiles alkylate nucleotide bases or completely inactivate cell signaling pathways. For example, terminal aldehydes (i.e. formaldehyde) are extremely toxic because they alkylate many proteins and DNA [121]. Most biological macromolecules contain nucleophilic moieties with the potential to donate electrons to electrophiles, forming covalent bonds. These include but are not limited to thiol (especially deprotonated thiolate anion) groups present within cysteines; the imidazole ring within histidine; and amine groups of lysine and nucleotide bases. Hard electrophiles are usually charged and bind hard nucleophiles while soft electrophiles typically have delocalized charges and bind soft

electrophiles [122]. Therefore, soft electrophiles can modify cell signaling pathways without complete inactivation, making them useful tools to dampen multiple pathways at once (polypharmacology) without the toxic effects of a complete loss in activity [123].

1.3.1 Endogenous electrophile formation

Although much is known about the enzymatic and non-enzymatic oxidation of unsaturated lipids, lipid nitration is less understood [124-129]. The structural characteristics of the unsaturated lipid define the reaction products and their formation is largely dependent on the differing chemical activities between bis-allylic and conjugated diene systems. Two different mechanisms have been proposed for the nitration of polyunsaturated bis-allylic lipids [130]. In short, the nitro-group can either be added directly or indirectly following oxidation and double bond rearrangement – both eventually leading to an electrophilic, nitroalkene moiety. α,β-unsaturated ketones can be formed through enzymatic reactions (e.g. oxidation of 15-hydroxyeicosatetraenoic acid [15-HETE] into 15-oxoETE via 15-prostaglandin dehydrogenase [15-PGDH]) or free-radical induced events such as lipid peroxidation (**Fig 3**) [128, 129, 131]. Inflammation induces NOS2 and NOX enzymes that produce nitric oxide ($^{\cdot}NO$) and superoxide ($O_2^{\cdot -}$) that, after several free radical-based reactions, form the nitrogen dioxide and hydroxyl radicals (**Figure 3**). These radicals will nitrate or oxidize double bonds that are electron poor, creating electrophilic nitroalkenes and oxidized fatty acids. Hydroxy fatty acids can then be reduced via dehydrogenases (e.g. 15-PGDH) to form electrophilic, α, β – unsaturated ketones. Alternatively, hydroxy fatty acids, like the cyclopentenones, are formed enzymatically via COX2 or LOX and then reduced into electrophilic α, β-unsaturated ketones via dehydrogenases as above.

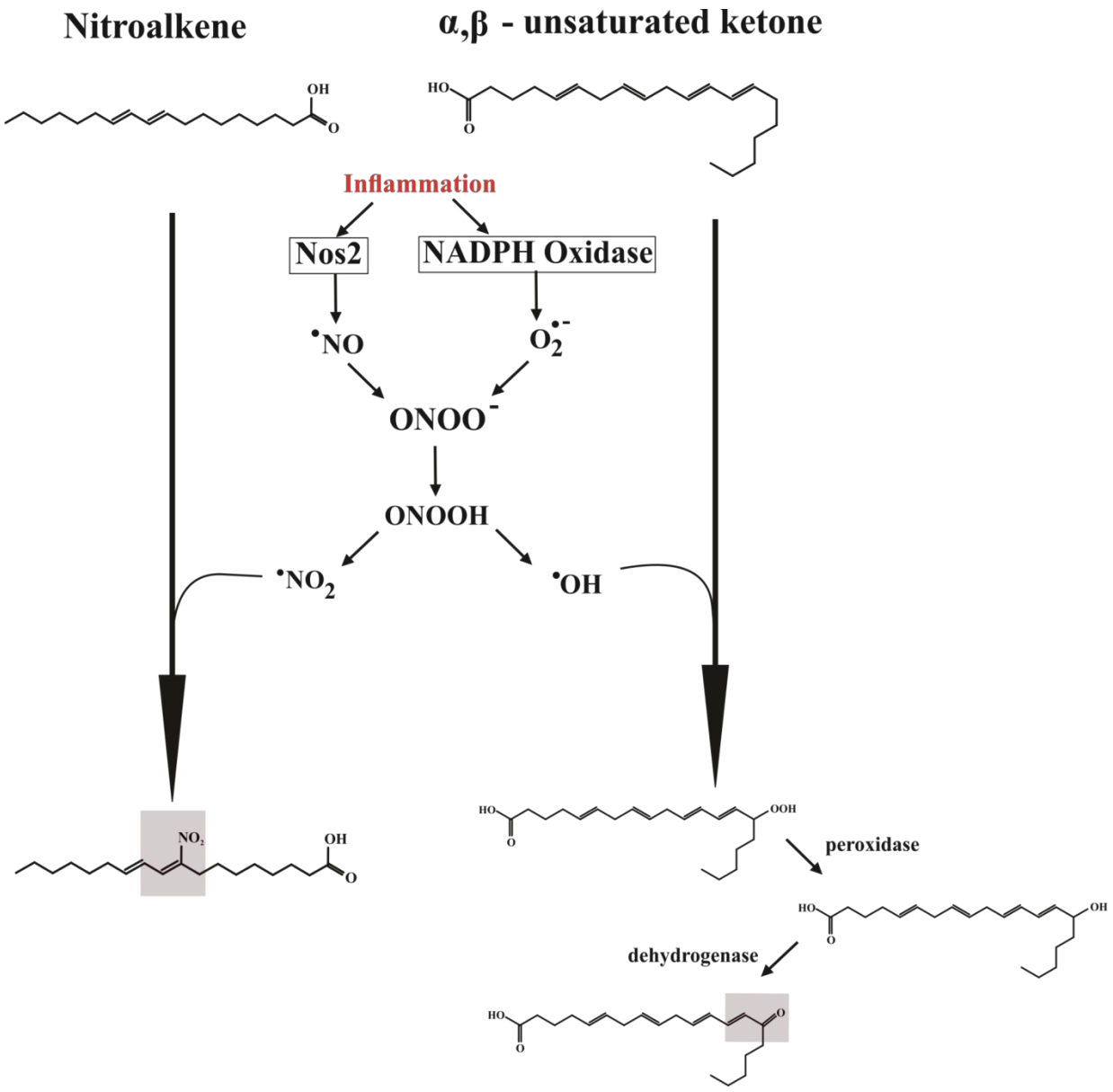

Figure 3: Electrophilic lipid formation

Both nitroalkenes and α,β-unsaturated ketones are formed during inflammation when unsaturated fatty acids react with reactive oxygen and nitrogen species formed from NOS2 and NOX enzymes. Electrophilic α,β-unsaturated ketones are also formed via enzyme-catalyzed (e.g. LOX, COX2) reactions.

1.3.2 Electrophilic lipid signaling

There is a myriad of electrophiles, formed endogenously, that differ in reactivity, reversibility of covalent reactions, concentration, and half-life. Many are toxic, including formaldehyde, acetaldehyde, hydroxynonenal (HNE), and malondialdehyde because they form irreversible protein and DNA adducts that accumulate in the cell over time. Some are viewed as biomarkers of oxidative stress, such as HNE and malondialdehyde, although their signaling role is not exactly clear. Finally, in recent years anti-inflammatory and cytoprotective electrophilic lipids are garnering interest for treating chronic and acute diseases of inflammation. These electrophiles include nitro-lipids and α, β-unsaturated ketones that, unlike the above hard electrophiles, can reversibly alkylate cysteines in key regulatory proteins, through Michael adduct formation (**Fig 4**). I further detail the actions of electrophilic lipids below.

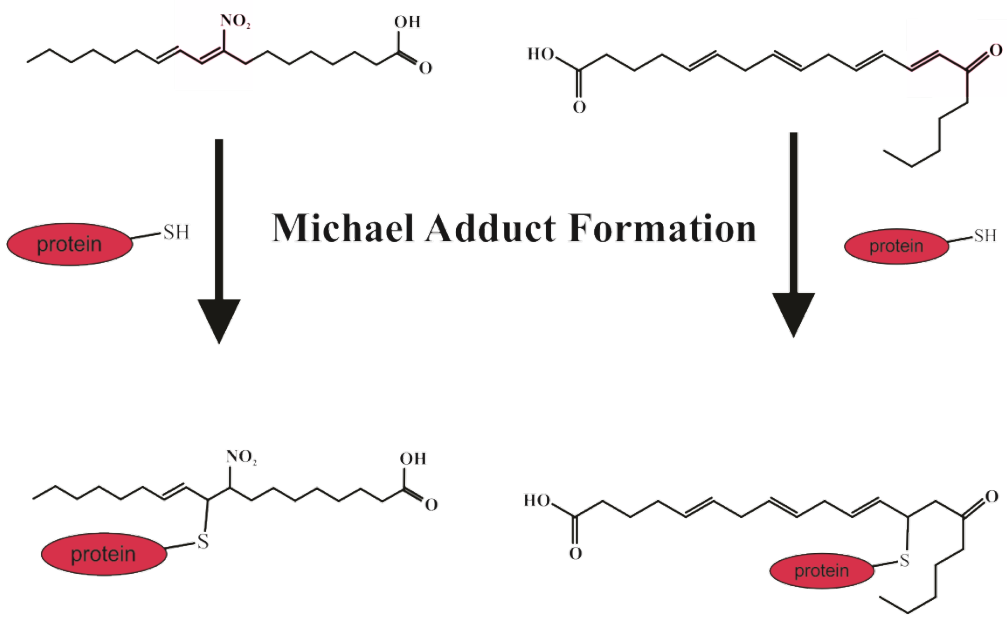

Figure 4: Michael Adduct Formation

Electrophilic lipids alkylate nucleophilic cysteine residues on proteins.

1.3.2.1 Limiting Inflammation

NF-κB is a central regulator of inflammation and can react to and initiate a variety of oxidative signaling events [14, 132]. Furthermore, NF-κB signals by forming dimers and translocating to the nucleus, binding κB promoter regions, ultimately leading to the activation of hundreds of genes – all of this activity is affected by RS and, in some cases, inhibited by electrophilic lipids. The canonical NF-κB pathway is initiated when IKK phosphorylates IκB, leading to its degradation and release of the p65/p50 dimer to the nucleus[88]. Nitroalkenes bind Cys179 of IKKβ, Cys62 of p50 and Cys38 and Cys105 of p65[133, 134]. Due to alkylation, nuclear translocation of the p65/p50 dimer is reduced along with the expression of pro-inflammatory genes

including IL6, MCP1, NOS2, COX2, and TNFα – shown in multiple *in vitro* and *in vivo* studies during the past decade [133, 135-140].

Several α, β-unsaturated ketones have also shown a remarkable ability to dampen inflammation through the inhibition of NF-κB, including prostaglandin metabolite, 15-deoxy-Δ-12,14-prostaglandin J_2 (15d-PGJ_2), and metabolites of polyunsaturated lipids (e.g. 15-oxoETE). Several groups demonstrated 15d-PGJ_2, an electrophilic metabolite of PGJ_2, Inhibits multiple steps along the NF-κB pathway [113, 141]. Rossi, *et al.* showed that Cys179 of IKKβ forms a Michael adduct with 15d-PGJ_2, leading to decreased IKKβ activation and consequently, NF-κB activation [141]. Straus, *et al.* similarly demonstrated 15d-PGJ_2 alkylates Cys38 of p65, and Cernuda-Morollon, *et al.* showed Cys62 of the p50 subunit is also alkylated by 15d-PGJ_2, resulting in decreased inflammation [113, 142]. Lastly, oxidized products of polyunsaturated lipids are often electrophilic and possess an ability to inhibit NF-κB signaling. 15-HETE is oxidized to 15-oxoETE, an electrophilic lipid, with the ability to dampen several aspects of inflammation including IL6, MCP1, and TNFα production – likely through inhibition of p65/p50 translocation [143, 144]. Together, these examples provide a strong argument for NF-κB being a common target for a wide class of electrophilic lipids, despite their assumed promiscuity in non-specifically binding proteins with available cysteines.

1.3.2.2 Protecting cell and tissue integrity

In addition to NF-κB inhibition, many electrophilic lipids are known to activate the Nrf2 antioxidant pathway. Nitroalkenes alkylate Cys151, Cys273, and Cys288 of Keap1, causing Nrf2 translocation to the nucleus, binding of the ARE, and activation of hundreds of antioxidant and

cytoprotective genes including HO1, GCLM, NQO1, and glutathione S-transferase (GST) [134, 145, 146]. Moreover, 15d-PGJ_2 can covalently modify Keap1 and activate the Nrf2 pathway [147-149]. In fact, there is a review describing strategies to use nitroalkenes or 15d-PGJ_2 to ameliorate inflammatory disorders due to their ability to protect cells via the Nrf2 pathway [147]. Electrophilic metabolites of unsaturated lipids such as 15-oxoETE also activate Nrf2 in addition to their ability to inhibit the NF-κB pathway [143, 144]. Nrf2, like NF-κB, seems to be a common target of electrophilic lipids with the end result being cytoprotection and dampened inflammation.

1.3.2.3 Inactivation of STING signaling and other pathways

In a recent article, myself and colleagues from Denmark, demonstrated that nitroalkenes can alkylate stimulator of IFN genes (STING), inhibiting its dimer formation, and ultimately IFN response factor (IRF) 3 activation [115]. STING detects pathogen DNA/RNA intracellular and initiates IFN responses [150-153]. Covalent modification of Cys88 and Cys91 within STING, disallow palmitoylation and clustering. Without palmitoylation, STING does not signal appropriately and is unable to fully activate IRF3, leading to diminishing production of IFN as well as other pro-inflammatory cytokines. Furthermore, nitroalkenes are reported to bind peroxisome-proliferated activator receptor (PPAR) γ to activate anti-inflammatory programs, initiate heat shock response, inactivate xanthine oxidase, and alter mitogen-activated protein kinase (MAPK) signaling – all of these responses potentially play a role in the cumulative anti-inflammatory and cytoprotective effects of nitroalkenes [116, 154-157].

1.4 Therapeutic potential of electrophiles for inflammatory disorders

The ability of several classes of electrophiles to alter several branches of immunity (e.g. Nrf2 activation and NF-κB) are making the case that they are efficient immunomodulators and can play a role in mitigating inflammatory diseases. For example, DMF was recently approved for the treatment of MS (Tecfidera®) and NO_2-OA (CXA-10), a nitroalkene, is in phase II clinical trials for pulmonary arterial hypertension, asthma, and focal segmented glomerulonephritis (PRIMEx – NCT03449524, FIRSTx – NCT03422510, ALMA – NCT03762395). Both maintain cellular homeostasis and limit the damaging effects of inflammation. Moreover, other natural electrophiles such as curcumin and sulforaphane (SFN) found in spices and cruciferous vegetables, respectfully, are excellent Nrf2 activators and have been shown to limit tissue damage in several models of inflammation [158-160]. Most importantly, many of these electrophilic entities have great toxicity profiles in addition to their profound anti-inflammatory and cytoprotective effects.

1.4.1 Nitroalkenes

The nitroalkenes (e.g. NO_2-OA) are an emerging class of electrophilic lipids showing promise in both pre-clinical animal models and phase II human studies (PRIMEx – pulmonary hypertension, FIRSTx – focal segmental glomerulosclerosis, ALMA – asthma) [134, 161]. Nitroalkenes actively promote resolution through Nrf2 activation and limit inflammation through a variety of mechanisms including NF-κB inhibition [116]. Cell culture studies have shown that NO_2-OA alkylates Cys273 and Cys288 of Keap1, making it an efficient Nrf2 activator [145]. NO_2-OA can form covalent Michael adducts with p65 (Cys38, Cys105) and IKKβ (Cys179) – leading to a limitation in NF-κB function [133, 140]. Recently, myself and others showed that nitroalkenes

alkylate Cys88 and Cys91 of STING, inhibiting its palmitoylation and the downstream production of IFN [115]. Furthermore, researchers have demonstrated nitroalkenes activate PPARγ, initiate heat shock signaling, and inhibit xanthine oxidase – all with the potential of having profound effects in immunity [116, 154, 155]. Therefore, NO_2-OA and other nitroalkenes directly alter immune responses by alkylating cysteines on key regulatory proteins.

Over a decade of *in vitro* and *in vivo* models have illustrated the potent anti-inflammatory and cytoprotective responses of nitroalkenes. NO_2-OA was effective in reducing cellular proliferation and tumor growth in a mouse model of triple negative breast cancer [133]. NO_2-OA and NO_2-cLA (another electrophilic nitroalkene) inhibited phosphorylation and dimerization of IRF3, leading to a significant depression in IFN production in bone marrow derived macrophages, THP1 human monocytes, and human, STING-associated vasculopathy with onset in infancy (SAVI) fibroblasts (pathogenesis due to excessive IFN production) [115]. Furthermore, nitroalkenes limit inflammation in several models of metabolic syndrome and fatty liver disease – including mouse models of non-alcoholic fatty liver disease and atherosclerosis [162, 163].

1.4.2 α,β-unsaturated ketones

Many unsaturated lipids formed during inflammation (e.g. prostaglandins) or derived from the diet (e.g. DHA, EPA) can be metabolized into electrophilic lipids [164]. Lipoxin A_4, a pro-resolving lipid mediator derived from AA during inflammation, is oxidized into 15-oxo-LXA_4, an electrophilic αβ-unsaturated ketone, by 15-PGDH [165]. 15-oxoETE is formed from the oxidation of 15-HETE and 15d-PGJ_2 is formed from AA oxidation into PGD_2 and the eventual oxidation and dehydration of its metabolite, PGJ_2 [143, 144, 148]. All of the above electrophilic lipids (with 15-oxoLXA_4 described in this thesis) activate Nrf2 and inhibit NF-κB signaling and how similar

effects to DMF and the nitroalkenes in limiting inflammation. 15-oxoETE limited LPS-induced inflammation in RAW cells (murine macrophages) in addition to PMA-induced activation of THP1 (human monocyte cell line) [143, 144]. 15d-PGJ_2 alkylates the p65 and p50 subunit of NF-κB, directly inhibits IκB, and covalently modifies Keap1 – all culminating in Nrf2 activation and multi-target inhibition of inflammation [113, 142, 148, 149].

DMF is a 6 carbon, α,β-unsaturated ketone approved for the treatment of MS (Tecfidera) [166, 167]. Studies have shown DMF can inhibit several aspects of the inflammatory response in a variety of different cells, including DCs, macrophages, and T cells. Due to DMF's electrophilic nature, much of its intracellular effects are attributed to alkylating cysteine residues on key regulatory proteins [168]. DMF inhibits NF-κB by forming a covalent Michael adduct with Cys38 of the p65 subunit, resulting in decreased expression of TNFα and MCP1 and inhibition of cancer cell growth [112]. Furthermore, DMF has been shown to alkylate Cys151, Cys273, and Cys288 on Keap1 – all of which would allow Nrf2 nuclear translocation and the activation of over a hundred antioxidant and cytoprotective genes [169]. Mitigation of MS pathogenesis by DMF is most likely caused from a combination of activating Nrf2, inhibiting NF-κB, modulating metabolism, and other, yet to be discovered pathways. New studies have confirmed Nrf2 activation when DMF is administered to mice in an experimental autoimmune encephalomyelitis model of MS [170].

From *in vitro* and *in vivo* pre-clinical studies to phase II clinical trials and FDA-approved therapeutics, electrophiles are becoming prominent agents in treating inflammatory diseases. It is becoming clear that both nitroalkenes and α, β-unsaturated ketones modify macrophages and DCs by alkylating key regulatory proteins such as NF-κB and Keap1, resulting in global changes in inflammation, metabolism, and cellular repair pathways. Future research needs to better

characterize how electrophilic lipids are formed endogenously in various states of inflammation, how they signal in immune cell subsets, and evaluate the therapeutic potential of these species in disease models.

1.5 Hypothesis and aims

Inflammation, although necessary, is a critical component in a variety of disease states including, cancer, acute crises (e.g. acute respiratory distress syndrome [ARDS]), chronic, and autoimmune disorders. Classic treatments for inflammation are either suppressive (steroids) or symptomatic (non-steroidal anti-inflammatory drugs [NSAIDS]). Recent trials have evaluated a variety of small molecule and monoclonal antibody-based, targeted therapies that have shown modest success but also many side effects. Electrophilic lipids are an emerging class of immunomodulating agents that can hit multiple targets of inflammation and promote tissue repair with minimal side effects (**Fig 5**). My thesis evaluates three separate hypotheses, adding importance to electrophilic lipids in immunity.

First, electrophilic metabolites of pro-resolving lipid mediators are active and play a role in mitigating aspects of inflammation (Chapter 3). The aims of this chapter are 1) demonstrate 15-oxo-LXA_4, the primary metabolite of Lipoxin A_4 is electrophilic; 2) characterize the ability of 15-oxo-LXA_4 to dampen LPS-induced inflammation and activate Nrf2-regulated cytoprotective responses; and 3) show these actions are independent of canonical, G-protein coupled receptor (GPCR)-dependent, Lipoxin A_4 signaling. These aims are carried out with a common, murine macrophage model using LPS as the inflammatory stimuli. PCR, western blot, ELISA, and LC/MS are used to evaluate each aim.

Second, electrophilic lipids alter DC function (Chapter 4). The aims of this chapter are 1) examine the effects of NO_2-OA on DC activation and surface marker phenotype; 2) demonstrate the impact of NO_2-OA on cytokine production in LPS-activated DCs; and 3) characterize the mechanism of action for nitroalkenes in DCs. A combination of flow cytometry, ELISA, and western blotting was used to carry out this project with a simple, murine bone-marrow derived DC model.

Finally, electrophilic lipids will mitigate influenza-induced, acute lung injury by dampening inflammation (Chapter 5). The aims of this chapter are to 1) test the efficacy of NO_2-OA in a murine model of severe influenza infection, 2) understand the impact of NO_2-OA administration on cytokine production, and 3) characterize changes in leukocyte recruitment to the lung during infection. Influenza A virus (H1N1 – Puerto Rico/08/1934) was used to infect mice and NO_2-OA was delivered by oral gavage. Weight loss was recorded and used to determine survival outcome. ELISA and flow cytometry were used to characterize inflammation.

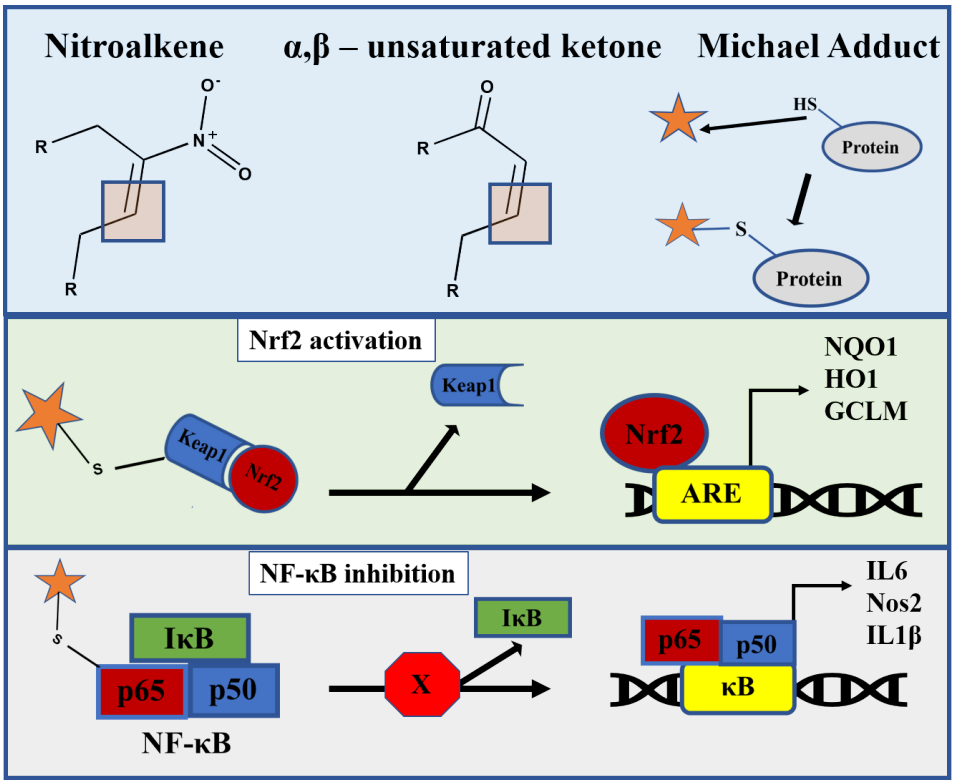

Figure 5: Electrophilic lipid modify key proteins in immunity

Nitroalkenes and α,β-unsaturated ketones activate Nrf2 and inhibit NF-κB – altering immunity. The main mechanism of action for electrophilic lipids is protein alkylation (Michael adduct formation).

2.0 Materials and Methods

2.1 Cells and Reagents

RAW 264.7 (ATCC) murine macrophages grown in DMEM (10% FBS) were used for *in* vitro macrophage studies. LPS was from Sigma (Cat# L4391, Lot 067M4036V). Lipoxin A_4 was purchased from Cayman Chemical Company (#90410) and 15-oxo-LXA_4 was synthesized as a methyl ester (15-oxo-LXA_4-ME) for cellular delivery as described recently [171]. The formyl peptide receptor (FPR) 2 antagonist, WRW^4 was purchased from Tocris (#2262). Madin-Darby Canine Kidney (MDCK, ATCC) were provided by Seema Lakdawala, Ph.D. and Influenza/A/Puerto Rico/08/1934 (PR8) was purchased from the ATCC. Glycerol Trioleate was purchased from Sigma and used as the vehicle for oral delivery of NO_2-OA.

2.2 Bone marrow-derived dendritic cells (BMDCs)

All mouse experiments were in accordance with protocols approved by the University of Pittsburgh IACUC committee. Femurs from male, C57BL/6 (Jackson, 8-12 weeks of age) mice were flushed through a 40 or 70 μm filter using RPMI 1640 (10% FBS + 1% penicillin/streptomycin) to obtain bone marrow. Cells were spun for 10 minutes at 400 x g at 4°C and erythrocytes were lysed using ammonium-chloride-potassium (ACK) lysis buffer (2-3 mL/mouse, 1-2 minutes at 37°C). After lysis, 5 volumes of media were added to deactivate lysis and the cells were spun again, as above. Cells were passed through a filter once more and

suspended as 500,000 cells/mL with 20 ng/mL of granulocyte-macrophage colony stimulating factor (GM-CSF) (Peprotech). In a 6-well plate, 4 mL (2 million cells) were added to each well and the cells were incubated for 5 days at 37°C with 5% CO_2. On day 3, 4 mL of media with 40 ng/mL GM-CSF was added to each well. Cells were scraped and harvested on Day 5 and subjected to various treatments. Flow Cytometry verified the cells were >60% CD11c+ and, in agreement with recent work describing the heterogeneity of these cells, consisted of 2-3 cell populations that varied in CD11b and major histocompatibility complex (MHC) II expression [46, 172, 173]. On Day 5, BMDCs were harvested and one million cells were plated in a 6-well plate at a concentration of 500,000 cells/mL RPMI (10% FBS). Cells were treated with or without 100 ng/mL LPS (Sigma L4391, *E. coli* O111:B4), oleic acid (5 μM), and varying concentrations of NO_2-OA. Cells were scraped at various time points and either prepared for flow cytometry, enzyme-linked immunosorbent assay (ELISA), liquid chromatography coupled with mass spectrometry (LC/MS), or western blot after separating cells and media by spinning for 10 minutes at 400 x g at 4°C.

2.3 Human DC Studies

Human DCs were prepared from frozen CD14+ monocytes purified from peripheral blood mononuclear cells (PBMCs) of healthy donors in collaboration with approved protocols under the direction of Robert Mailliard, PhD according to standard protocol using MACS® separation with CD14 microbeads (Miltenyi Biotec 130-050-201) [174]. Monocytes were thawed and cultured in IMDM media with 10% FBS, 2.5% gentamycin, 1000 U/mL GM-CSF (Genzyme NDC 58468-0180-1) and 20 ng/mL IL4 (R&D Systems 204-IL) for 5 days at a concentration of 500,000

cells/mL – creating immature dendritic cells (iDCs). On Day 5, iDCs were activated with a combination of LPS, CD40L, and/or IFNγ and treated with 2.5 μM NO_2-OA or ethanol control. On day 7, cells were harvested for flow cytometry or further activated with J558 cells for 24 hr in order to evaluate IL12 production from the media via ELISA.

2.4 RAW Cell Signaling Studies

RAW cells (2 million/well in 6 well plate) grown overnight in 10% FBS/DMEM were treated with or without LPS (10 ng/mL), 15-oxo-LXA_4-Me (25 μM), LXA_4 (0.1-25 μM), and WRW^4 (1 μM) for various time points in 1% FBS/DMEM. Media was collected for ELISA and cell lysates were collected for western or PCR analysis. For western analysis, cells were scraped into ice cold radioimmunopreciptation assay (RIPA) buffer (150 mM NaCl, 1% NP-40, 0.5% sodium deoxycholate, 0.1% SDS, 50 mM Tris, pH = 8) with protease (Pierce) and phosphatase inhibitors (Roche). For PCR analysis, cells were scraped into Trizol (Invitrogen). Cytokines were measured with ELISA. Vehicle concentrations were kept under 0.3% ethanol. In all antagonist studies, cells were treated with WRW^4 for 30 minutes prior to treatment.

2.5 Cell Viability

For RAW cell studies, cytotoxicity was determined using the MTT [3-(4,5-dimethylthiazol-2-yl)-2,5-diphenyltetrazolium bromide] assay according to the manufacturer's instruction. Cells were plated in a 96 well plate (50,000/well) and treated with 25 μM 15-oxo-

LXA_4-Me and LPS (10 ng/mL) for 24 hr. Viable cells convert substrate into a product that absorbs maximally at 570 nm. The results were compared directly between LPS + vehicle (<0.3% ethanol) and LPS + 15-oxo-LXA_4-Me as absorbance units. For BMDC studies, viability was determined using the Zombie Red Live/Dead stain from Biolegend (423110).

2.6 Western Blot

Cell lysates (prepared by scraping into 300 µL RIPA buffer with NuPage Sample Buffer and reducing agent) were further ruptured via sonication (30 sec on 30 sec off, repeat 3x, pwr=80-100, QSonica, 4°C) and protein was clarified by centrifugation 21,000 x g for 5 min at 4°C. Samples were heated 95°C for 5 minutes and 20 µL of each sample was loaded onto a polyacrylamide gel (Nupage 4-12%) and electrophoresis was performed for 1-2 hr with 180V. Protein was transferred to nitrocellulose at 100V for 1 hr at 4°C. Membranes were washed with Tris-buffered saline with tween-20 (TBST) buffer and blocked with either 5% Milk or 5% casein in TBST for 1 hr at room temperature. Membranes were washed and primary antibodies were added overnight at 4°C. Horseradish peroxidase (HRP)-linked secondary antibodies were added the following day, incubated with ECL substrates, and imaged with a Bio-Rad ChemiDoc. Details regarding dilutions of each antibody and purchasing information are in **Table 1**.

Table 1: Antibody Details

Company	Target	Primary Dilution	Catalog	kDa	Secondary Dilution
Abcam	**NQO1**	1/5000	ab80588	31	1/6000
Invitrogen	**GCLM**	1/1000	PA5-26111	30	1/3000
Enzo Life Sciences	**HO1**	1/1000	ADI-SPA-895-F	32	1/6000
Sigma	**ACTIN**	1/2000	A4700	42	1/2000
Cell Signaling	**NOS2**	1/1000	13120	140	1/2000

2.7 PCR

Cell lysates were prepared by scraping into 1 mL TRIzol (Invitrogen). RNA was obtained per manufacturer instruction and measured using a NanoDrop (Thermo). cDNA was prepared according to iScript (Bio-Rad) instructions using 500 ng of purified RNA. Taqman (Applied Biosystems) assays and fast master mix were used to analyze gene expression using 250 ng cDNA. Primers are listed in **Table 2** and relative quantification was calculated using established methods [175].

Table 2: PCR primers

Gene	Catalog	Reference Number	Dye
Actin	4352341E	Mm00607939_s1	VIC
Nqo1	4331182	Mm01253561_m1	FAM
Ho1	4331182	Mm00516005_m1	FAM
Gclm	4331182	Mm01324400_m1	FAM
Tnfa	4331182	Mm00443258_m1	FAM
Il6	4331182	Mm99999064_m1	FAM
Nos2	4331182	Mm00440502_m1	FAM
Mcp1	4331182	Mm00441242_m1	FAM
Il1b	4331182	Mm00434228_m1	FAM

2.8 Flow Cytometry

2.8.1 BMDC Studies

For each experiment, 2-3 technical replicate wells were combined (2-3 million cells), centrifuged, and suspended in PBS at 1-5 million cells/mL. Then, 200 µL was plated onto a LegendPlex, V-bottom plate (BioLegend) and spun at 400 x g for 5-10 minutes at 4°C. Zombie Red (1:400) was used as the viability stain in the majority of experiments and cells were stained for 20 minutes at room temperature. Fluorescence-activated cell sorting (FACS) buffer (2% FBS, 1 mM EDTA, 0.1% sodium azide in PBS) was added to deactivate the viability stain and cells were spun again. Then, Fc Block (anti-CD16/32, BioLegend, 1:100) was added in FACS buffer to cells in order to block non-specific immunoglobulin receptors for 20 minutes on ice. After spinning, cells were stained in 100 µL for 20-30 minutes on ice with various panels. In all cases, pooled BMDCs were used for all single stain and FMO controls. After staining, cells were fixed for 20 minutes on ice with Cytofix (BD), washed, and analyzed using a BD Fortessa. At least 50,000 events were recorded for each sample. The following antibodies were used: CD11c-FITC (N418, 1:200, Biolegend), CD11b-BUV395 (M1/70, 1:800, BD), MHCII-APC-Cy7 (IA/IE, M5/114.15.2, 1:1600, Biolegend), CD40-APC (3/23, 1:200, Biolegend), CD80-BUV737 (16-10A1, 1:800, BD), and CD86-PE (GL-1, 1:800, Biolegend). Flow Cytometry experiments were performed within the University of Pittsburgh, School of Medicine, Department of Immunology Flow Cytometry Core on a BD LSR Fortessa.

2.8.2 Influenza Studies

Bronchoalveolar lavage fluid (BALF) was collected from mice (1 mL Hanks buffered saline solution, HBSS with 30 mM EDTA) and centrifuged 400 x g 10 min at 4ºC. Pellets were suspended in ACK lysis buffer for 1 min on ice followed by 800 µL PBS and centrifugation as above. Pellets were resuspended in 200 µL PBS and added to a V-bottom plate (BioLegend). Spleen cells were harvested in a similar manner and used for single stain and fluorescent minus one (FMO) controls. Plates were spun as above and stained with Zombie Aqua (Biolegend, 1:200) in 100 µL PBS for 20 minutes at room temperature in the dark. FACS buffer (100 µL) was added and cells were spun as above. Fc Block (1:100) was added to all samples in 100 µL FACS buffer and set for 20 min on ice. Cells were spun and then stained for 30 min on ice in 100 µL FACS with the following antibodies: CD45-BV605 (1:200), CD11b-APC-Cy7 (1:200), CD11c-Pacific Blue (1:200), Ly6g-AF700 (1:200), F4/80-PE-Cy7 (1:200), CD4-APC (1:200), CD8-FITC (1:200), and CD19-BV421 (1:200) – all from BioLegend. Counting beads (BioLegend) were added to the final suspension (25 µL beads/ 175 µL cell suspension) to obtain absolute counts. Experiments were performed within the University of Pittsburgh, School of Medicine, Department of Immunology Flow Cytometry Core on a BD LSR Fortessa.

2.9 ELISA

Instructions were followed for each kit: MCP1 (88-7391-88), TNFα (88-7324-88), IL1β (88-7013-77), IL6 (88-7064-88), IL12p70 (88-7121), IL10 (88-7105), and IL23p19 (88-7230) – all from Invitrogen. Samples were diluted to be within the linear range of the standard curve. A

Bio-Plex mouse cytokine 23-plex (Bio-Rad) was used to measure cytokines from murine BALF and analyzed with the Luminex platform.

2.10 Glutathione (GSH) Adduct Formation

To form the GSH adduct, GS-15-oxo-LXA$_4$, 10 µM 15-oxo-LXA$_4$-Me was incubated with 100 µM GSH in 50 mM potassium phosphate buffer (pH = 8) for 1 hr at 37°C [133, 143]. Adducts were extracted using solid phase extraction and analyzed with multiple reaction monitoring (MRM) 658/308. Relative levels of 15-oxo-LXA$_4$ were quantified by normalizing MRM 349/233 to LXA$_4$-d5 (MRM 356/114) and 13,14-dihydro-15-oxo-LXA$_4$ (MRM 351/235) in the same manner.

2.11 Lipid Extraction and Liquid Chromatography/Mass Spectrometry

2.11.1 LC/MS - RAW Cells

RAW cells were plated as above and treated with 25 µM 15-oxo-LXA$_4$. Media and cell lysates were scraped into cold PBS over a time course (0, 0.5, 1, 2, 3, and 6 hr). To 1 mL of cell lysate or media, 10 µL of LXA$_4$-d$_5$ (1 µg/mL stock) and 5-oxoETE-d$_7$ (2 µg/mL stock) were added as internal standards. To each sample, 4 mL of chloroform:methanol (2:1) was added, vortexed and centrifuged for 10 min at 2800 x g at 4°C. The organic layer was dried under nitrogen and solvated in 100 µL methanol the day of analysis. Aqueous layers were subjected to C18 solid phase

extraction (Thermo Scientific Hypersep), eluted in methanol, dried, and solvated in methanol for further analysis. Samples were analyzed on a 6500+ QTRAP coupled to an Exion LC (Sciex). Injections were applied to a Luna C18 column (2x100 mm, Phenomenex) with a linear gradient using acetonitrile (0.1% acetic acid) as solvent B and water (0.1% acetic acid) as solvent A. Samples were loaded at 20% B and the gradient increased to 80% B over 10 minutes, was held at 100% B for 2 minutes, and equilibrated at 20% B for 3 minutes at a rate of 0.6 mL/min. LXA_4 and LXA_4-derived metabolites were measured using negative electrospray ionization under the following MS conditions: CUR 40, CAD med, IS 4500, GS1 70, GS2 65, Temp 600 °C, DP -80, EP -7, CE -17, CXP -7. MS conditions were the same for measuring 15-oxoLXA_4 GSH adducts; however, MS analysis was run in positive electrospray ionization mode and source temperature was set to 550°C. GSH adduct separation took place at a flow rate of 0.25 mL/min and the LC gradient was linear starting at 20%B at 5 min and increasing to 98%B at 25 min. The gradient was held at 100%B for 2 minutes and equilibrated at 20%B until 35 min. To form GS-15-oxo-LXA_4, 10 μM 15-oxoLXA_4-Me was incubated with 100 μM GSH in 50 mM potassium phosphate buffer (pH = 8) for 1 hr at 37°C[133, 143]. Adducts were extracted using solid phase extraction and analyzed with MRM 658/308. Relative levels of 15-oxoLXA_4 were quantified by normalizing MRM 349/233 to LXA_4-d5 (MRM 356/114) and 13,14-dihydro-15-oxo-LXA_4 (MRM 351/235) in the same manner.

2.11.2 LC/MS – BMDCs

BMDCs for metabolomics experiments were scraped and harvested as above. After spinning, media samples were frozen at -80°C and the pellets were washed with cold PBS and then lysed in 80% ice cold methanol (0.1% formic acid) with 100 μM of internal standard mix (taurine-

d4, lactate-d3, alanine-d3, and creatinine-d3). On the day of analysis, 100 µL of media was added to 400 µL of 80% methanol/0.1% formic acid with internal standards. Media and lysate samples were vortexed for 30 seconds, spun at 21,000 x g for 10 minutes at 4°C and supernatants were analyzed using LC/MS. Analyses were performed by untargeted LC-HRMS. Briefly, Samples were injected via a Thermo Vanquish UHPLC and separated over a reversed phase Thermo Hypercarb porous graphitic column (2.1×100mm, 3.0µm particle size) maintained at 50°C. For the 20 min LC gradient, the mobile phase consisted of the following: solvent A (0.1% formic acid in water) and solvent B (0.1% formic acid in acetonitrile). The gradient was the following: 0-12.0 min 5% B, to 1000% B, 12.0-15.0 min hold at 100% B, 15.0-15.1100% to 5% B, 15.1-20.0 min 5%B. Spectra were acquired on a Thermo IDX tribrid mass spectrometer, using both positive and negative ion mode, scanning in Full MS mode (2 µscans) from 70 to 800 m/z at 120,000 resolution with an AGC target of 5e4. Source ionization settings were 3.5/2.6 kV spray voltage respectively for positive and negative mode. Source gas parameters were 20 sheath gas, 10 auxiliary gas at 300°C, and 4 sweep gas. Calibration was performed prior to analysis using the Pierce™ Positive and Negative Ion Calibration Solutions (Thermo Fisher Scientific). Integrated peak areas were then extracted manually using Quan Browser (Thermo Fisher Xcalibur ver. 2.7).

2.12 GPCR Binding Assay

Human FPR2 was expressed in Sf9 insect cells (Invitrogen) using the Bac-to-Bac baculovirus expression system (ThermoFisher). Cell cultures were grown in ESF 921 serum-free medium (Expression Systems) to a density of 4×10^6 cells/mL and then infected with the baculovirus expressing FPR2. The cells were collected by centrifugation at 8000 x g for 10min

after 48 hours. For ^{35}S-GTPγS binding assays, ~200 μg/ml of human FPR2 cell membrane was incubated with 200 nM purified Gi protein for 20 min on ice in buffer containing 20 mM HEPES, pH 7.5, 150 mM NaCl, 5mM $MgCl_2$, 3 μg/ml BSA, 0.1μM TCEP, and 5μM GDP. Next, 25 μL aliquots were transferred to 225 μL reaction buffer containing 20 mM HEPES, pH 7.5, 150 mM NaCl, 5mM $MgCl_2$, 3 μg/ml BSA, 0.1μM TCEP, 1μM GDP, 35 pM ^{35}S-GTPγS and ligands (LXA_4 and 15-oxo-LXA_4 at 2 μM, WKYMVm, a peptide agonist of FPR2, at 5 μM). After additional 15 min incubation at 25 °C, the reaction was terminated by adding 6 ml of cold wash buffer containing 20 mM HEPES, pH 7.5, 150 mM NaCl and 5mM $MgCl_2$, and filtering through glass giber prefilters (Millipore Sigma). After washing four times with 6 ml cold wash buffer, the filters were incubated with 5 ml of CytoScint liquid scintillation cocktail (MP Biomedicals) and counted on a Beckman LS6500 scintillation counter. The data analysis was performed using GraphPad Prism 6 (GraphPad Software). One-way ANOVA was applied for experimental comparisons. Results are shown as mean ± SD from 3 independent experiments.

2.13 Murine model of influenza infection

Female, BALB/cJ mice (Jackson, 6-8 weeks old) were infected via intranasal injection (50 μL) with a lethal dose of PR8 (300 $TCID_{50}$ = 1.5 MLD_{50}). Sterile PBS was used as vehicle control. Mice were weighed daily and euthanized when they lost more than 25% of their original weight per IACUC protocol. Treatment begin 4 hr prior to initial infection and continued twice daily (every 12 hr). Doses were approximated by using 20 g as average mouse weight and delivering 5 mg/100 μL (25 mg/kg in glycerol trioleate); however, they were not recalculated each day as the mice lost weight. For timeline studies, mice were euthanized via pentobarbital injection followed

by cardiac puncture. Tissues were harvested at various days during the infection. Blood was collected from cardiac puncture and plasma was obtained by collecting in heparin-laced tubes (to avoid premature clotting) and spinning 15,000 x g for 5 min at 4ºC. Then bronchoalveolar lavage (BAL) was performed to obtain BAL fluid (BALF) for cytokine and titer determination. The left lung was process for flow cytometry and the right lung was divided by lobe and frozen in liquid nitrogen.

2.14 Viral propagation and titer determination

PR8 was propagated in MDCK cells and titered according to established protocols [176]. Infectivity was determined using the dose at which 50% of the cells were infected (tissue culture infectious dose $(TCID)_{50}$). Confluent monolayers of MDCK cells were infected with decreasing doses of PR8 in a 96 well plate (n=4 each dose) and infected cells were counted after 4 days of culture. Cells were ruled infected or not based on destruction of the monolayer determined with microscopy. The dose that results in 50% death in mice (Mouse lethal dose 50, MLD_{50}) was determined using increasing doses of PR8 (n=10).

2.15 Statistics

2.15.1 Statistics – Lipoxin Studies

Standard deviation (SD) is shown in all experiments except where box and whisker plots are used in which the full range of data is shown with the median. Normality tests (Shapiro-Wilk) were performed prior to statistical analysis and non-parametric tests were utilized when abnormal distributions were observed. Student's T Tests were utilized for comparisons between two groups while One-way or Two-way ANOVA with multiple comparisons (Tukey's for 2-way or normally distributed 1-way, Sidak's for non-parametric 1-way) was used for 2 or more variable experiments across groups. GraphPad was used for all tests. Experiments were repeated at least three times (biological replicates) unless otherwise noted.

2.15.2 Statistics – BMDC studies

Shapiro-Wilk normality tests were run to determine if non-parametric or parametric tests should be used. In each case, normal or non-parametric (Kruskal Wallis) one-way ANOVA were run to determine statistical significance. SD is shown in all graphs unless noted otherwise. Each experiment was performed independently at least 3 times unless noted.

2.15.3 Statistics – Influenza studies

Survival curve significance was determined using the Log-Rank, Mantel Cox analysis. Differences in cytokines and cell populations were analyzed with one-way or two-way ANOVA. SD is shown in each experiment. All analyses were performed with Prism (GraphPad).

3.0 15-oxo-Lipoxin$_4$, an electrophilic metabolite of Lipoxin A$_4$, induces anti-inflammatory and cytoprotective responses in LPS-treated murine macrophages

Gregory J Buchan**, Adolf Koudelka, Veronika Cechova, James P O'Brien, Marina C Sarcinella, Mohamad Rawas-Qalagi, Bhupinder Singh, Heng Liu, Steven R Woodcock, Cheng Zhang, Bruce A Freeman, and Stacy G Wendell.* ***J Biol Chem, Submitted 11/20/19

3.1 Introduction

Inflammation is a process associated with the pathogenesis of virtually every disease [2, 4, 16]. Most therapies directed towards the inflammatory process are designed to inhibit pro-inflammatory signaling via inhibition of cytokines, bioactive lipids and other factors. It has only been within the last several decades that research has focused on the resolution of inflammation as a pharmacological target. Resolution was once thought to be a passive process, but it has since been realized that, just as there are key signaling pathways that orchestrate the inflammatory response, there are also pathways that regulate resolution. A defect in resolution permits an uncontrolled inflammatory response that can lead to tissue damage [83]. Rather than completely suppressing inflammation, pro-resolving mediators restore cells and tissue to a homeostatic state where inflammation is curbed and repair mechanisms are activated [177].

Key regulators of both inflammation and resolution are bioactive lipids including prostaglandins, leukotrienes, nitro-lipids, resolvins, and lipoxins. Resolvins and lipoxins, as well as protectins and maresins, are di- and tri-hydroxy specialized pro-resolving mediators (SPMs) formed from enzymatic oxidation of docosahexaenoic acid (DHA), docosapentaenoic acid (DPA)

and arachidonic acid (AA) [78]. In fact, lipoxin A_4 (LXA_4), a trihydroxytetraene lipid derived from AA was discovered in human neutrophils and the first to be described in the literature as a SPM [178, 179]. LXA_4 and its isomer, Lipoxin B_4, were observed under inflammatory conditions where COX and LOX enzymes were both active and able to sequentially oxidize AA – typically via transcellular biosynthesis [180, 181]. Later studies demonstrated that aspirin could also lead to lipoxin formation upon acetylation of the COX2 prostaglandin active site to produce 15(*R*)-HETE, which would later be oxidized by lipoxygenases to different isomers of LXA_4, the epi-lipoxins [182, 183]. These bioactive lipids are mainly thought to signal through G protein coupled receptor (GPCR)-dependent pathways to promote and resolve inflammation [184].

Since the early 1980's, many cell culture and preclinical studies have demonstrated the pharmacological effects of LXA_4 to inhibit inflammation and promote resolution. Nearly 40 years of research has shown that LXA_4 can dampen inflammation in a variety of *in vivo* disease models including: acute lung injury, asthma, subarachnoid hemorrhage, acute renal failure, and cancer [87, 185-191]. Consequently, LXA_4 reinvigorated targeting the resolution of inflammation (rather than its prevention) for diseases defined by aberrant inflammation; thus promoting the discovery and characterization of a variety of novel, lipid mediators that reduce inflammation and promote tissue repair and protection [82, 192-195].

Despite massive success in animal models of disease, LXA_4 is yet to be FDA-approved as a therapeutic for any inflammatory disorder and has not seen comparable success in clinical trials [196-198]. A possible reason for this may be the understudied pharmacokinetics of LXA_4. Since the discovery of LXA_4, only 7 studies examined the metabolism of these species *in vitro* and even less performed any detailed, pharmacokinetic profile in animal models [165, 199-204]. A primary metabolite of LXA_4 is 15-oxo-LXA_4, which is formed through the action of 15-

hydroxyprostaglandin dehydrogenase (15-PGDH). 15-PGDH is best known for the oxidation of prostaglandin E_2 (PGE_2) to 15-oxoPGE_2 and 15-hydroxyeicosatetraenoic acid (15-HETE) to 15-oxoeicosatetraenoic acid (15-oxoETE) [144, 205]. Similarly, 15-PGDH oxidized the hydroxyl group at the C15 position in LXA_4, resulting in the formation of 15-oxo-LXA_4, which has been previously described as an inactive product [165].

Importantly, both 15-oxoPGE_2 and 15-oxo-LXA_4 contain an α,β-unsaturated ketone moiety that renders these metabolites electrophilic. An abundance of literature has clearly demonstrated that electrophilic lipids, including 15d-PGJ_2, 11- and 15-oxoETE, nitro-lipids, and DMF (a non-lipid, α,β-unsaturated ketone) have biological activity that promotes anti-inflammatory signaling primarily through GPCR-independent signaling [116, 143, 144, 148, 166, 206-208]. Electrophilic lipids signal through Michael addition adduct formation with reactive, nucleophilic cysteines that can be found in redox regulatory transcription factors and enzymes NF- κB and Nrf2 [116, 131, 134, 143, 209]. Herein, we demonstrate that 15-oxo-LXA_4 is a bioactive metabolite of LXA_4 that promotes GPCR-independent, anti-inflammatory signaling, in LPS-activated macrophages.

3.2 15-oxo-LXA_4-Me is rapidly metabolized to 15-oxo-LXA_4 and retains its electrophilic properties

15-oxo-LXA_4-Me pharmacokinetics was first evaluated *in vitro* at the same concentration used in subsequent studies (**Fig 6**). The methyl ester derivative is quickly converted to 15-oxo-LXA_4 within cells, likely via intracellular esterases, as shown by the appearance of 15-oxo-LXA_4 and the emergence of the reduced product, 13,14-dihydro-15-oxo-LXA_4. Most of 15-oxo-LXA_4 is metabolized, extruded from the cell, or adducted to proteins or small molecular weight thiols (due

to Michael Addition) within the first 6 hours after administration (**Fig 6A**). Glutathione adducts were also detected in the media (**Fig 7**), providing further evidence that 15-oxo-LXA_4 is electrophilic after release from the methyl ester derivative. Together, these data demonstrate that addition of the methyl ester derivative (15-oxo-LXA_4-Me) is sufficient to yield 15-oxo-LXA_4. Finally, I show 15-oxo-LXA_4 is electrophilic (same molecular weight and retention time as prepared standard, **Fig 7**) and has the potential to signal through protein alkylation like other electrophilic lipids.

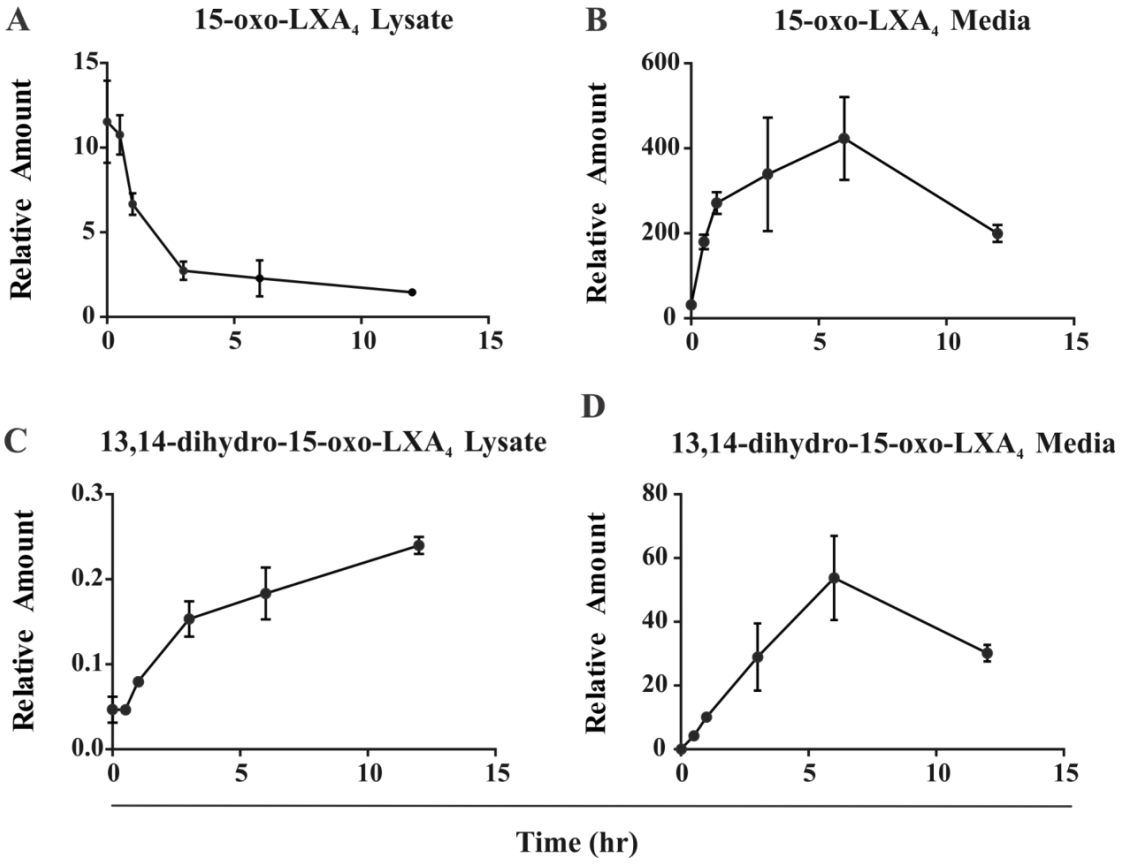

Figure 6: 15-oxo-LXA4-Me is rapidly metabolized to 15-oxo-LXA4 and retains its electrophilic properties

25 μM 15-oxo-LXA4-ME was added to RAW cells (murine macrophages) and incubated for the indicated time. Cell media and lysate was collected and prepared for LC/MS analysis. Free 15-oxo-LXA4 was measured in cell lysate (A) and media (B). The reduced metabolite of 15-oxo-LXA4, 13,14-dihydro-15-oxo-LXA4 was also measured over time in both cell lysate (C) and media (D). Relative amounts were calculated by dividing the peak area for each analyte by that of the internal standard, LXA4-d5. Data are from one of two independent experiments (n=3) and SD is shown.

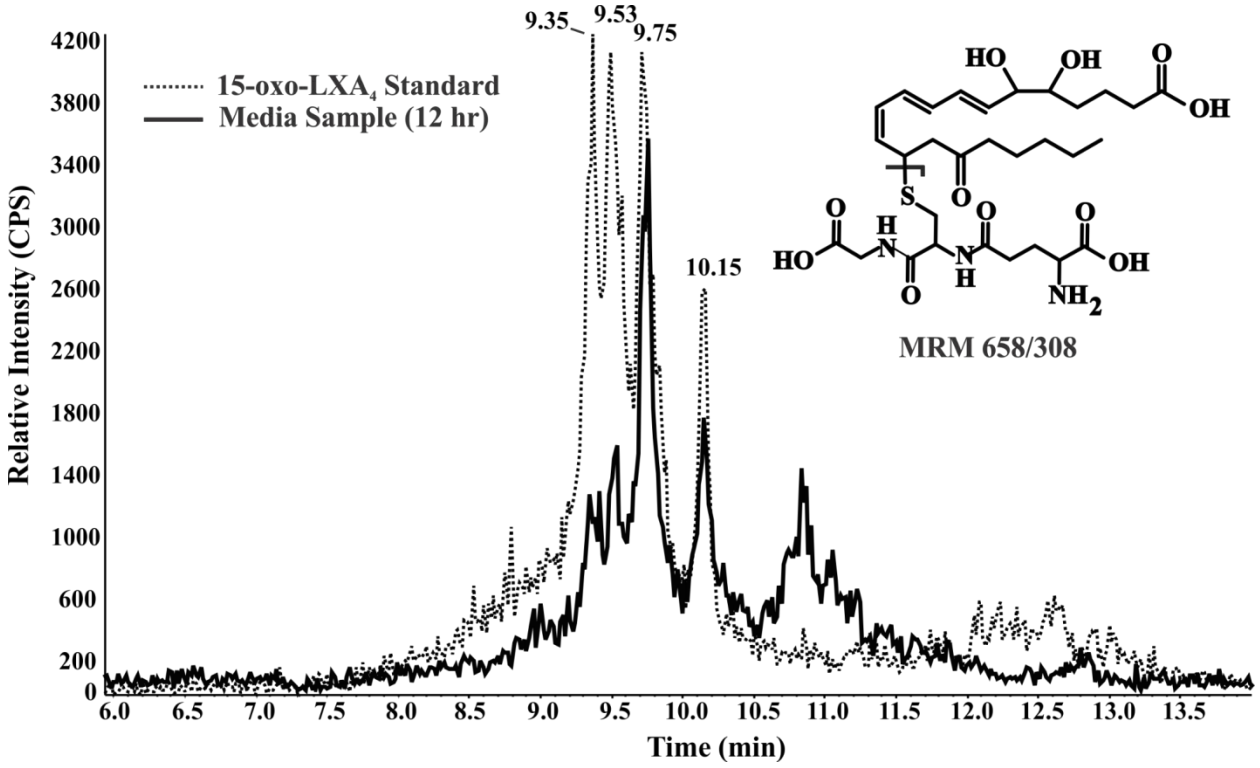

Figure 7: 15-oxo-LXA$_4$-Me is rapidly metabolized into 15-oxo-LXA$_4$ and forms glutathione adduct

Chromatogram for 12 hr media sample from the pharmacokinetic study in **Fig 6** and prepared standard. The dotted line tracing represents profile of a standard made by reacting GSH and 15-oxo-LXA$_4$-Me in phosphate buffer. The solid line tracing represents the 12 hr media sample. Inset displays the MRM transition shown in the chromatogram along with the proposed point of fragmentation (bold line). MRM 658/308 represents formation of the GSH adduct (GS-15-oxo-LXA$_4$) with subsequent cleavage of GSH. Overlapping peaks at 9.35, 9.53, 9.75, and 10.15 min suggest the analyte in the standard and sample are structural similar. These data represent one experiment.

3.3 15-oxo-LXA$_4$ inhibits LPS-induced inflammation

Murine macrophages were treated with LPS (10 ng/mL) with or without 15-oxo-LXA$_4$-Me and the degree of inflammation was measured by evaluating the expression and protein production of IL6, MCP1, TNFα, IL1β, and inducible nitric oxide synthase (NOS2) over time (**Fig 8**). As expected, LPS induced the expression and production of each cytokine as compared to the untreated controls. Pro-inflammatory gene induction was evident at 6 hr and continued through 24 hr. 15-oxo-LXA$_4$-Me significantly reduced the expression and protein levels of NOS2 (**Fig 8A, B**). *Mcp1* mRNA expression was significantly reduced by 15-oxo-LXA$_4$-Me at all times evaluated throughout the study; however, protein levels were only significantly reduced after 12 hr post LPS administration (**Fig 8C, D**). *Il6* expression was markedly reduced at most time points; however, statistically significant reductions were only seen at 18 hr after LPS and 15-oxo-LXA$_4$-Me treatment. Results from ELISA demonstrated that there were significant reductions in IL6 at 18 and 24 hr after LPS administration, but not before hand (**Fig 8E, F**). There were only significant changes in *Tnfα* expression 12 hr after LPS (**Fig 9C**). Lastly, *Il1β* mRNA expression was also decreased upon 15-oxo-LXA$_4$-Me from 12-24 hr after LPS treatment (**Fig 9B**). Finally, there was no loss in viability at 24 hr with LPS and 15-oxo-LXA$_4$-Me treatment (**Fig 9D**). These data show that 15-oxo-LXA$_4$ dampens proinflammatory gene expression and cytokine production, consistent with other anti-inflammatory, electrophilic lipids known to alkylate and inhibit the activation NF-κB.

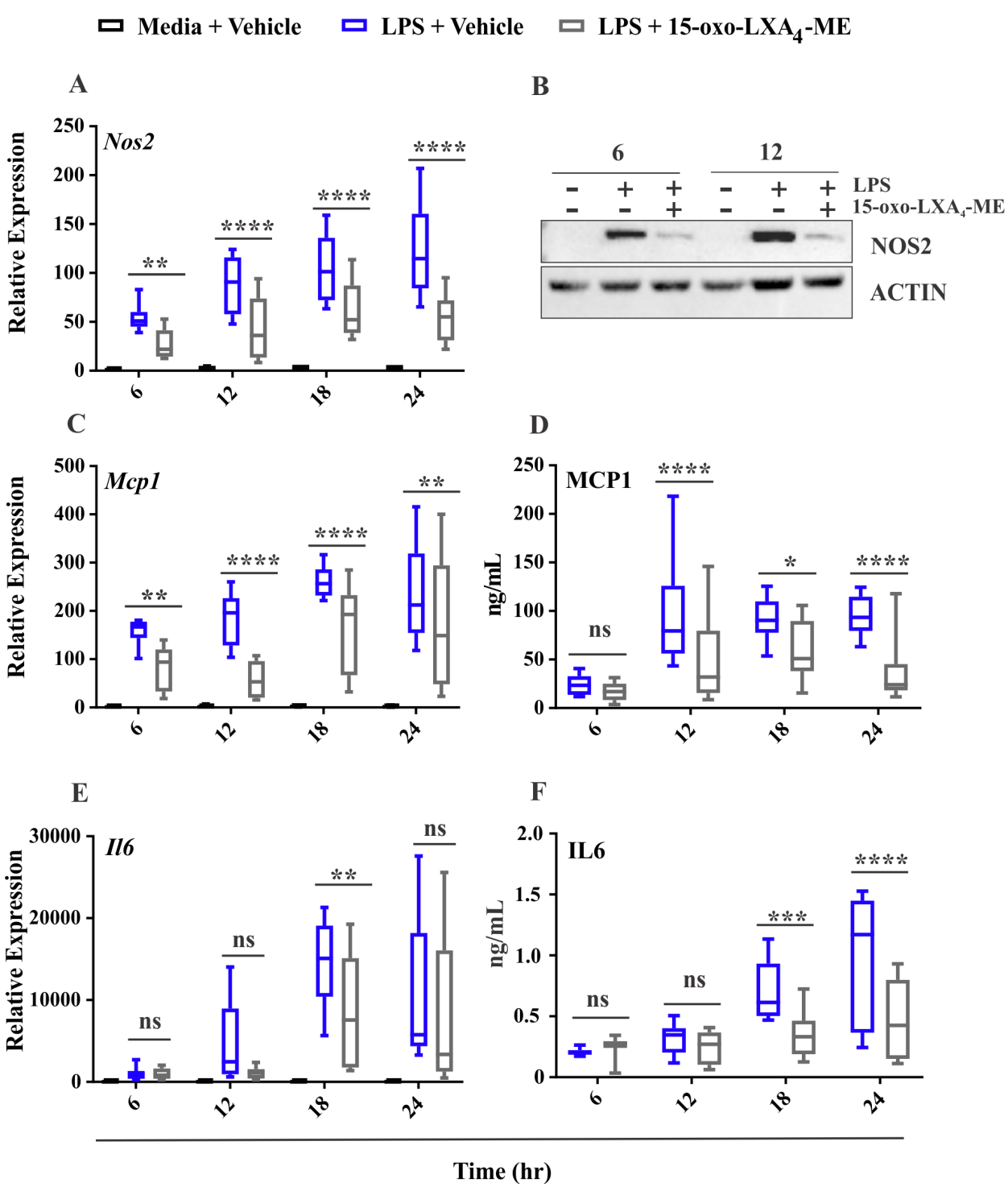
Media + Vehicle
LPS + Vehicle
LPS + 15-oxo-LXA4-ME
A
Nos2
Relative Expression
250
200
150
100
50
0
**
****
****
****
6
12
18
24
B
6
12
LPS
15-oxo-LXA4-ME
NOS2
ACTIN
C
Mcp1
Relative Expression
500
400
300
200
100
0
**
****
****
**
D
MCP1
ng/mL
250
200
150
100
50
0
ns
****
*
****
E
Il6
Relative Expression
30000
20000
10000
0
ns
ns
**
ns
F
IL6
ng/mL
2.0
1.5
1.0
0.5
0
ns
ns
***
****
Time (hr)

Figure 8: 15-oxo-LXA$_4$ represses pro-inflammatory signaling

25 μM 15-oxo-LXA4-ME was added to RAW cells at the time as 10 ng/mL LPS. Samples were harvested at various time points and processed. Relative expression of *Nos2* (A), *Mcp1*(C), and *Il6* (E) mRNA normalized to *Actin*. (B) Western blot for NOS2 with ACTIN loading control measured at 6 and 12 hr after treatment. ELISA data from media for MCP1 (D) and IL6 (F). Two-way ANOVA was performed on gene expression and ELISA data, ns = not significant, *p<0.05, **p<0.01, ***p<0.001, ****p<0.0001. Bars represent statistical difference between LPS alone and LPS-treated groups. Data were normalized to media no LPS samples. PCR and ELISA data are from 3-4 independent experiments with n=4. Western blot is a representative image from three independent experiments. Full western blot images are shown in **Fig 9**.

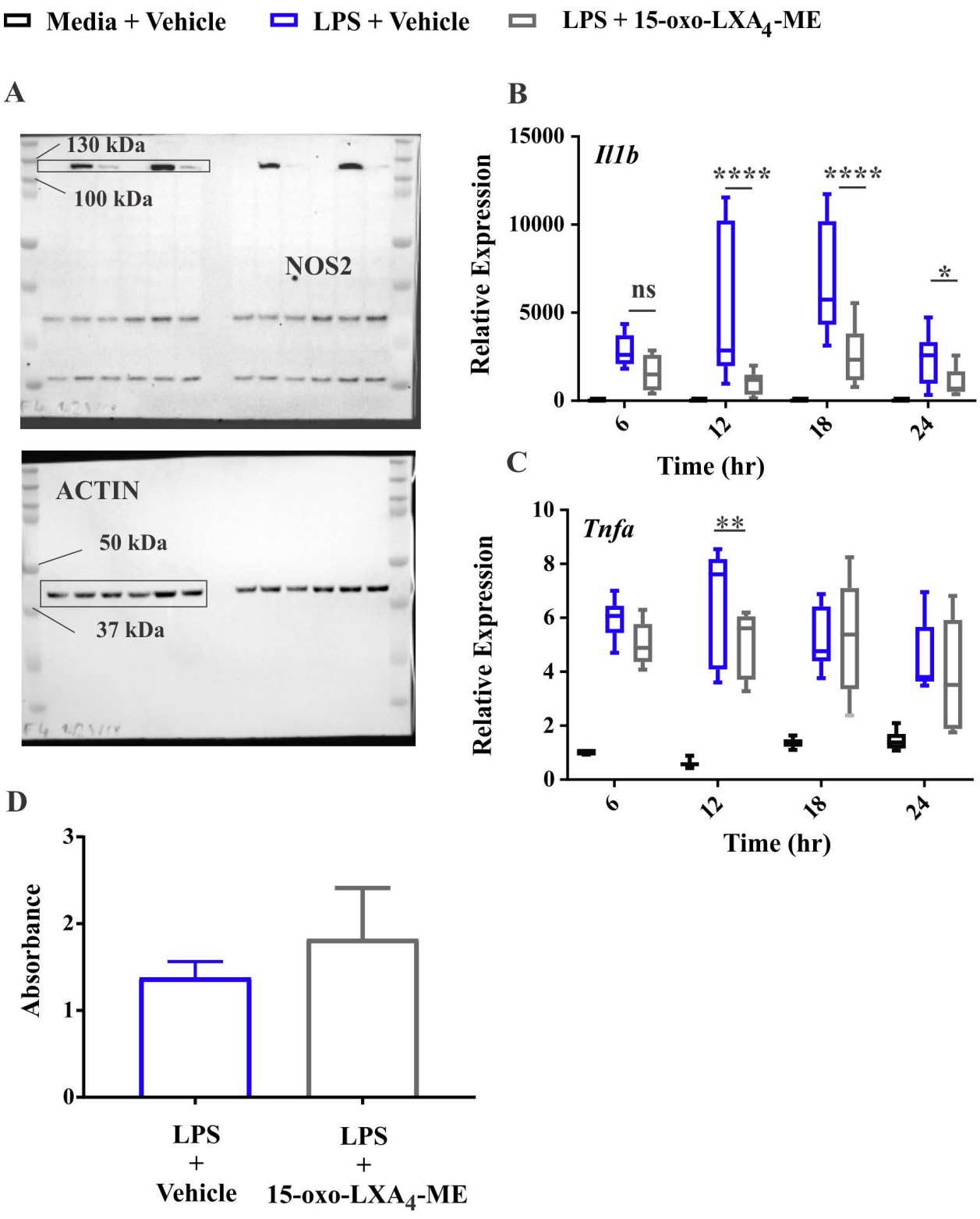
Media + Vehicle
LPS + Vehicle
LPS + 15-oxo-LXA4-ME
A
130 kDa
100 kDa
NOS2
ACTIN
50 kDa
37 kDa
B
Il1b
Relative Expression
15000
10000
5000
0
ns
****
****
*
6
12
18
24
Time (hr)
C
Tnfa
Relative Expression
10
8
6
4
2
0
**
6
12
18
24
Time (hr)
D
Absorbance
3
2
1
0
LPS + Vehicle
LPS + 15-oxo-LXA4-ME

Figure 9: 15-oxo-LXA$_4$ represses pro-inflammatory signaling (supplement to Fig 8)

Full western blot images for NOS2 and ACTIN (in **Fig 8**) (A). Boxes represent the images shown in **Fig 8**. PCR data for the mRNA expression of *Tnfa* and *Il1b* (B, C). Western blot data are representative of three independent experiments. Absorbance values from MTT assay (n=3, three independent experiments) (D). PCR data are representative of 3-4 independent experiments with n=4. ** $p < 0.01$ between LPS + vehicle and LPS + 15-oxo-LXA$_4$-Me (One-way ANOVA).

3.4 15-oxo-LXA$_4$ activates Nrf2

We assessed Nrf2 activation by measuring downstream target genes, *Nqo1*, *Gclm*, and *Ho1* using PCR (**Fig 10**). While LPS itself did not induce any expression of the above genes nor their protein products, 15-oxo-LXA$_4$-Me indeed increased the mRNA expression of each gene at various time points as well as the protein. *Nqo1* induction via 15-oxo-LXA$_4$-Me peaked 12 hr post LPS administration and was significantly higher than the control at each time point measured (**Fig 10A**). *Gclm* and *Ho1* mRNA expression peaked at 6 hr; however, only early time points (6 hr – *Ho1*; 6, 12 hr – *Gclm*) were significantly higher than the control group (**Fig 10C, E**). To further validate induction of each gene, protein levels were evaluated using western blot. NQO1, HO1, and GCLM were all higher than control groups when compared with 15-oxo-LXA$_4$-Me-treated groups (**Fig 10 B, D, F**). Together, these results demonstrate the ability of 15-oxo-LXA$_4$ to induce Nrf2-dependent proteins that are involved in cellular repair and recovery during and after inflammation.

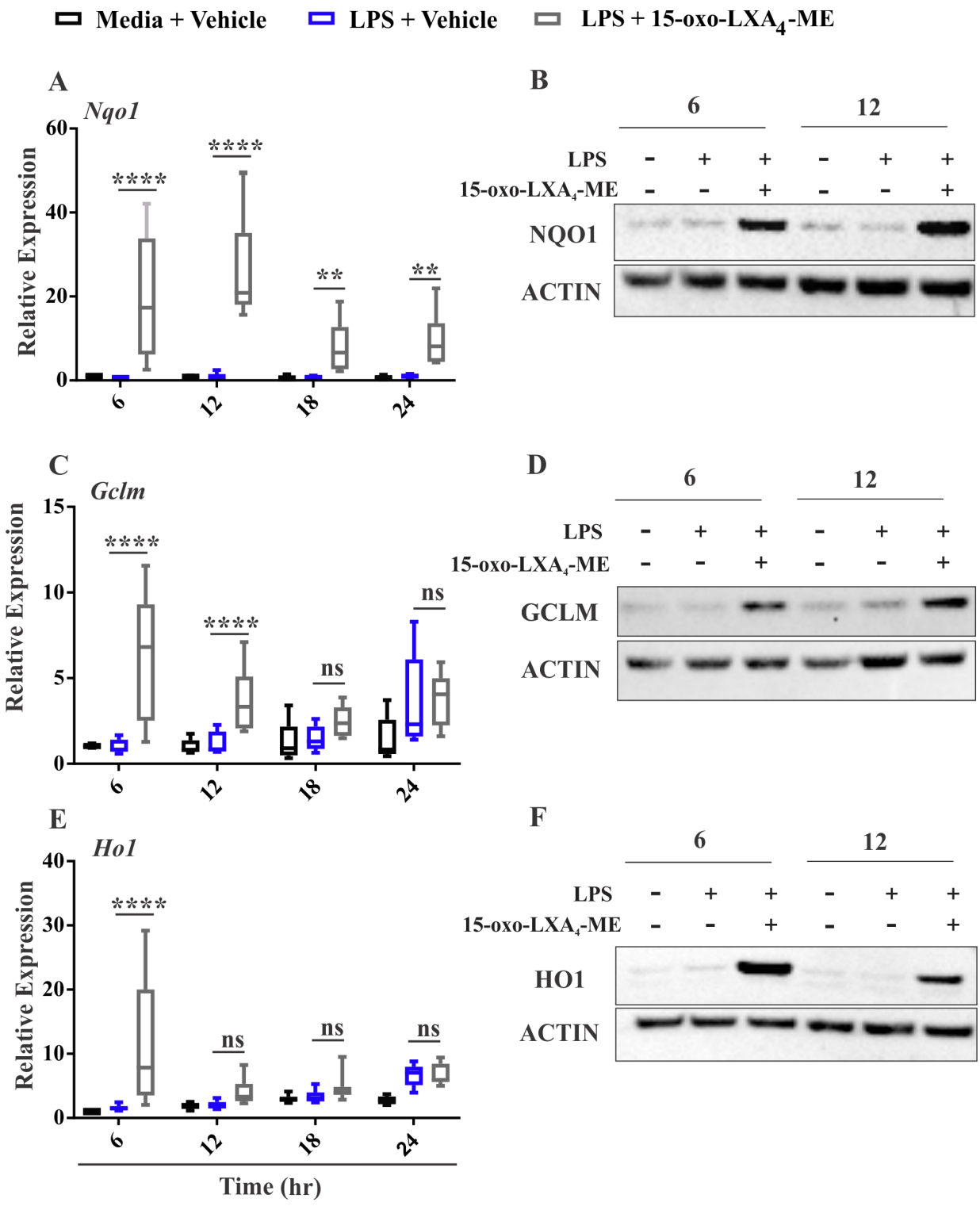
Media + Vehicle
LPS + Vehicle
LPS + 15-oxo-LXA4-ME
A
Nqo1
Relative Expression
60
40
20
0
****
****
**
**
6
12
18
24
B
6
12
LPS - + + - + +
15-oxo-LXA4-ME - - + - - +
NQO1
ACTIN
C
Gclm
Relative Expression
15
10
5
0
****
****
ns
ns
6
12
18
24
D
6
12
LPS - + + - + +
15-oxo-LXA4-ME - - + - - +
GCLM
ACTIN
E
Ho1
Relative Expression
40
30
20
10
0
****
ns
ns
ns
6
12
18
24
Time (hr)
F
6
12
LPS - + + - + +
15-oxo-LXA4-ME - - + - - +
HO1
ACTIN

Figure 10: 15-oxo-LXA$_4$ induces Nrf2 signaling

25 μM 15-oxo-LXA$_4$-ME was added to RAW cells at the time as 10 ng/mL LPS. Samples were harvested at various time points and processed. Relative mRNA expression (normalized to *Actin*) of *Nqo1* (A), *Gclm* (C), and *Ho1* (E). Western blot for NQO1 (B), GCLM (D), and HO1 (F) with ACTIN loading control measured at 6 and 12 hr after treatment. Two-way ANOVA was performed on gene expression, ns = not significant, *p<0.05, **p<0.01, ***p<0.001, ****p<0.0001. Bars represent statistical difference between LPS alone and LPS + 15-oxo-LXA$_4$-Me-treated groups. Data were normalized to media no LPS samples. PCR data are from 3-4 independent experiments with n=4. Western blot is a representative image from three

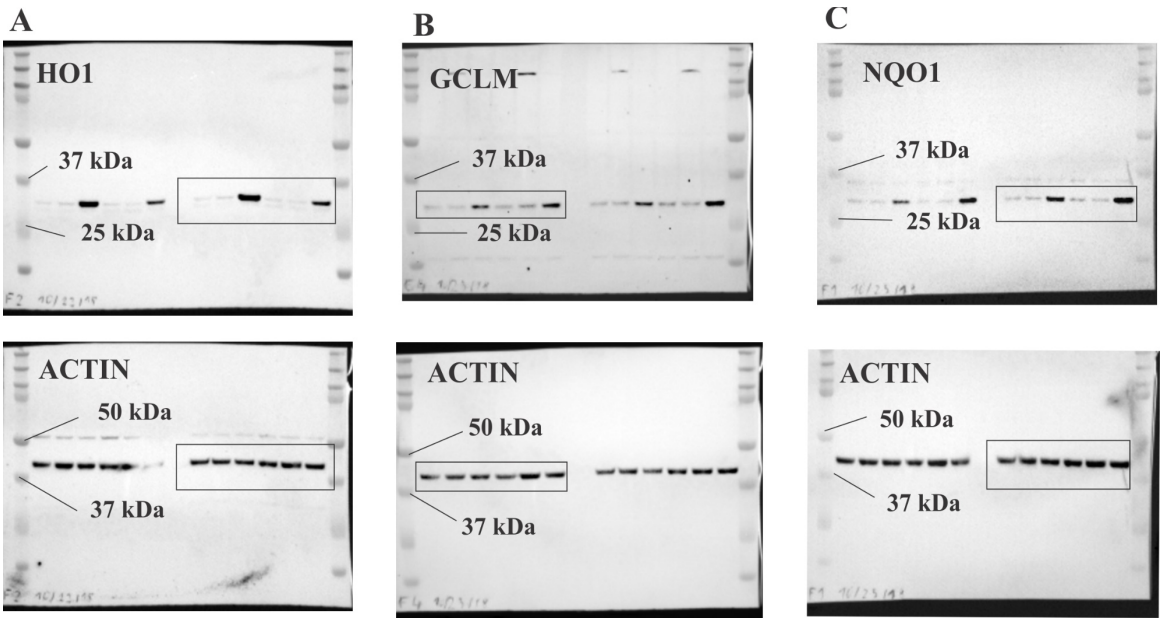

Figure 11: Full western blots for Fig 10

3.5 Pro-resolving actions of 15-oxo-LXA$_4$ are FPR2-independent

Western blot analysis with antibodies from two different companies showed that FPR2 was present within RAW cells (**Fig 12A**). Next, a GPCR activity assay was completed to evaluate the ability of 15-oxo-LXA$_4$-ME to bind FPR2, compared with LXA$_4$ and the positive control, WKYMVm peptide (**Fig 12B**). Both LXA$_4$ and 15-oxo-LXA$_4$-ME showed minimal FPR2 binding compared to WKYMVm peptide (**Fig 12B**). Then, murine macrophages were treated with the FPR2 antagonist, WRW^4 (1 μM), for 30 minutes prior to LPS and 15-oxo-LXA$_4$-ME administration in order to inactivate FPR2. Nrf2 target genes were induced upon 15-oxo-LXA$_4$-ME treatment; however, this induction was not reduced with WRW^4 addition (**Fig 12C, D**). The mRNA expression of *Mcp1* and *Nos2* were once again decreased with the addition of 15-oxo-

LXA_4-ME and not altered upon treatment with the FPR antagonist (**Fig 12F, G**). In line with the gene expression data, 15-oxo-LXA4-Me-induced changes in protein levels of NQO1, GCLM, HO1, and NOS2 were all unaltered with WRW^4 treatment (**Fig 12E**)**.** These data show that, despite being a weak agonist for FPR2 compared to WKYMVm, 15-oxo-LXA_4-ME can activate Nrf2-dependent responses and inhibit pro-inflammatory mRNA expression in the absence of FPR2 signaling.

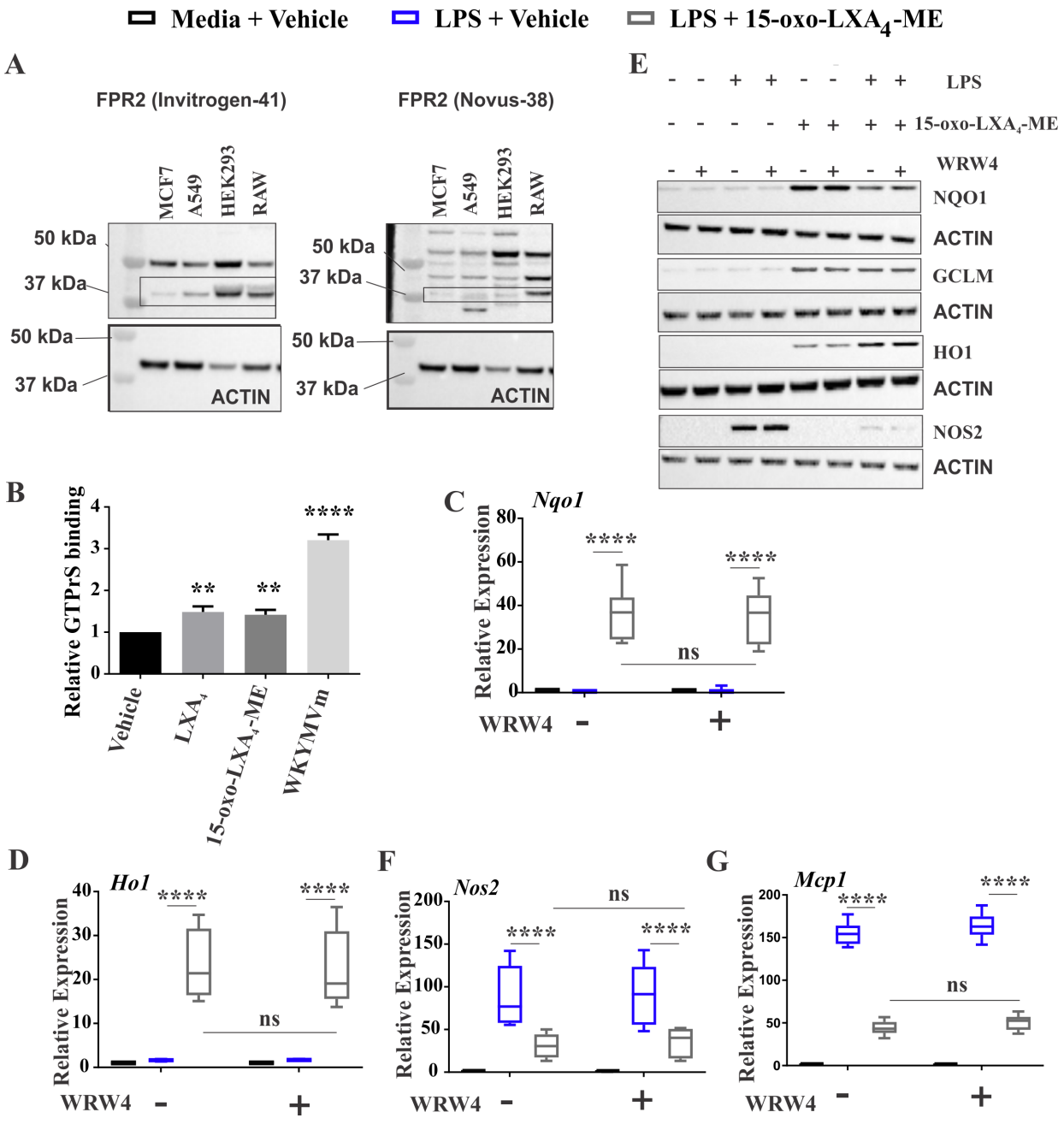
Media + Vehicle
LPS + Vehicle
LPS + 15-oxo-LXA4-ME
A
FPR2 (Invitrogen-41)
FPR2 (Novus-38)
MCF7
A549
HEK293
RAW
50 kDa
37 kDa
ACTIN
E
LPS
15-oxo-LXA4-ME
WRW4
NQO1
ACTIN
GCLM
HO1
NOS2
B
Relative GTPrS binding
Vehicle
LXA4
15-oxo-LXA4-ME
WKYMVm
C
Nqo1
Relative Expression
ns
D
Ho1
F
Nos2
G
Mcp1

Figure 12: Signaling actions of 15-oxo-LXA$_4$ are FPR2-independent

25 μM 15-oxo-LXA$_4$-ME was added to RAW cells at the time as 10 ng/mL LPS. Samples were harvested at various time points and processed. Various cell lysates (non-treated) were used for the western blot for FPR2 antibodies (A). GPCR response assay (B). Expression of Nrf2 target genes, *Nqo1* and *Ho1* normalized to *Actin* (C, D). Western blots for Nrf2 target proteins, NQO1, GCLM, and HO1 (E). mRNA expression of *Nos2* (F) and *Mcp1* (G). Western blot of NOS2 (E). Gene expression data are the combined results of 3-4 independent experiments (n=4). Western blot analyses are representative of 3 independent experiments. -/+ represent the addition of FPR2 antagonist, WRW^4 (1 μM). NS = not significant, **** = $p<0.001$ between vehicle LPS and 15-oxo-LXA$_4$-ME +LPS groups. Full western blot images are in **Fig 13.**

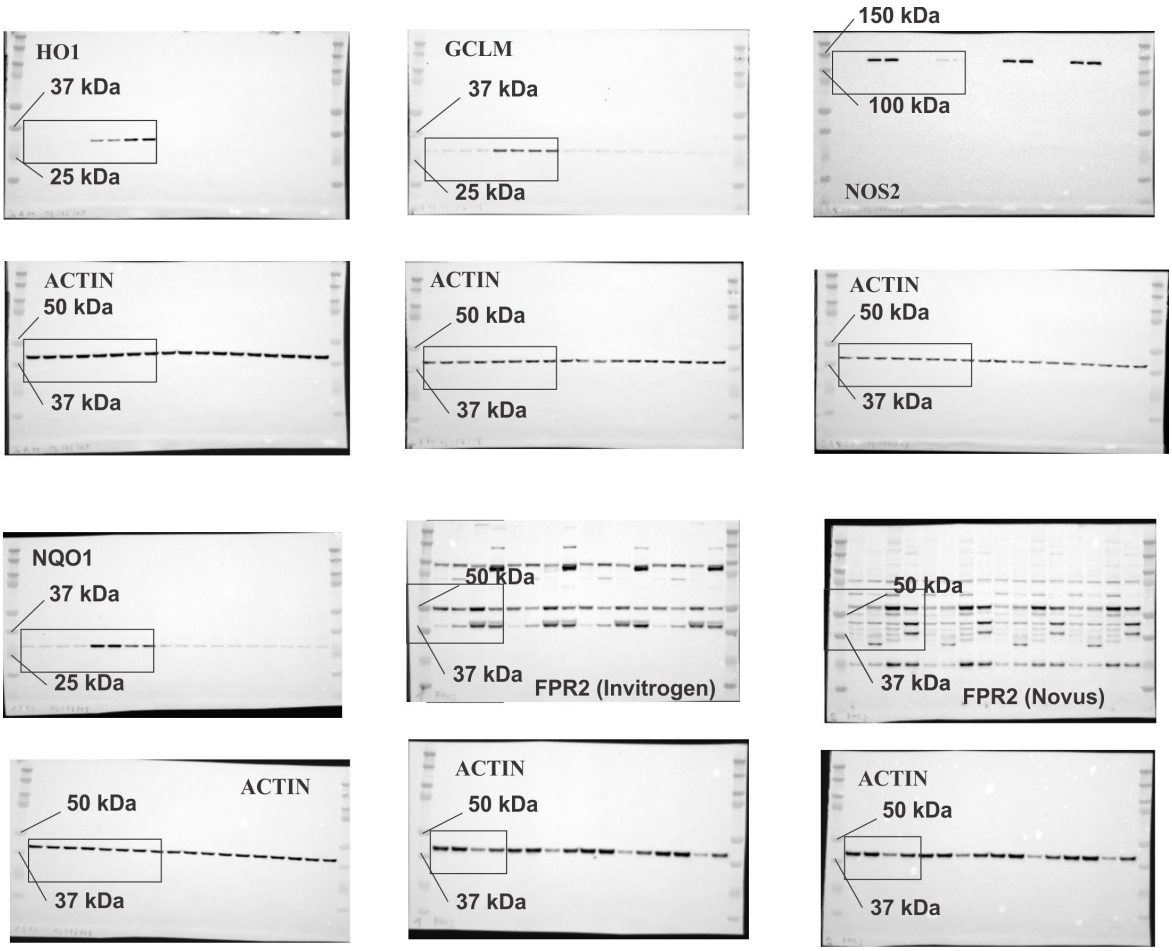

Figure 13: Supplement blots for Figure 12

Full western blot images are shown for **Fig 12** with the outline representing the image shown within the figure.

3.6 LXA_4 does not affect LPS-induced inflammation or Nrf2 activation

Unexpectedly, LXA_4 was unable to repress LPS-induced inflammation nor induce Nrf2 target gene expression within RAW cells in this study (**Fig 14**). Gene expression data for *Ho1* and *Nos2* (representative of Nrf2 and NF-κB pathways, respectively) at 6 hr post LPS/LXA_4

administration was analyzed and no changes were seen with addition of 1 μM LXA_4 (**Fig 14A, B**). Western blot analysis at 12 hr corroborated gene expression data, showing no changes in HO1 or NOS2 protein expression (**Fig 14C**). These results illustrate that in my model of LPS-induced activation of murine macrophages, LXA_4 neither activates Nrf2 nor inhibits pro-inflammatory responses. In fact, these actions are elicited through the primary metabolite of LXA_4, 15-oxo-LXA_4 (an electrophilic, α,β-unsaturated ketone) in the absence of FPR2 signaling.

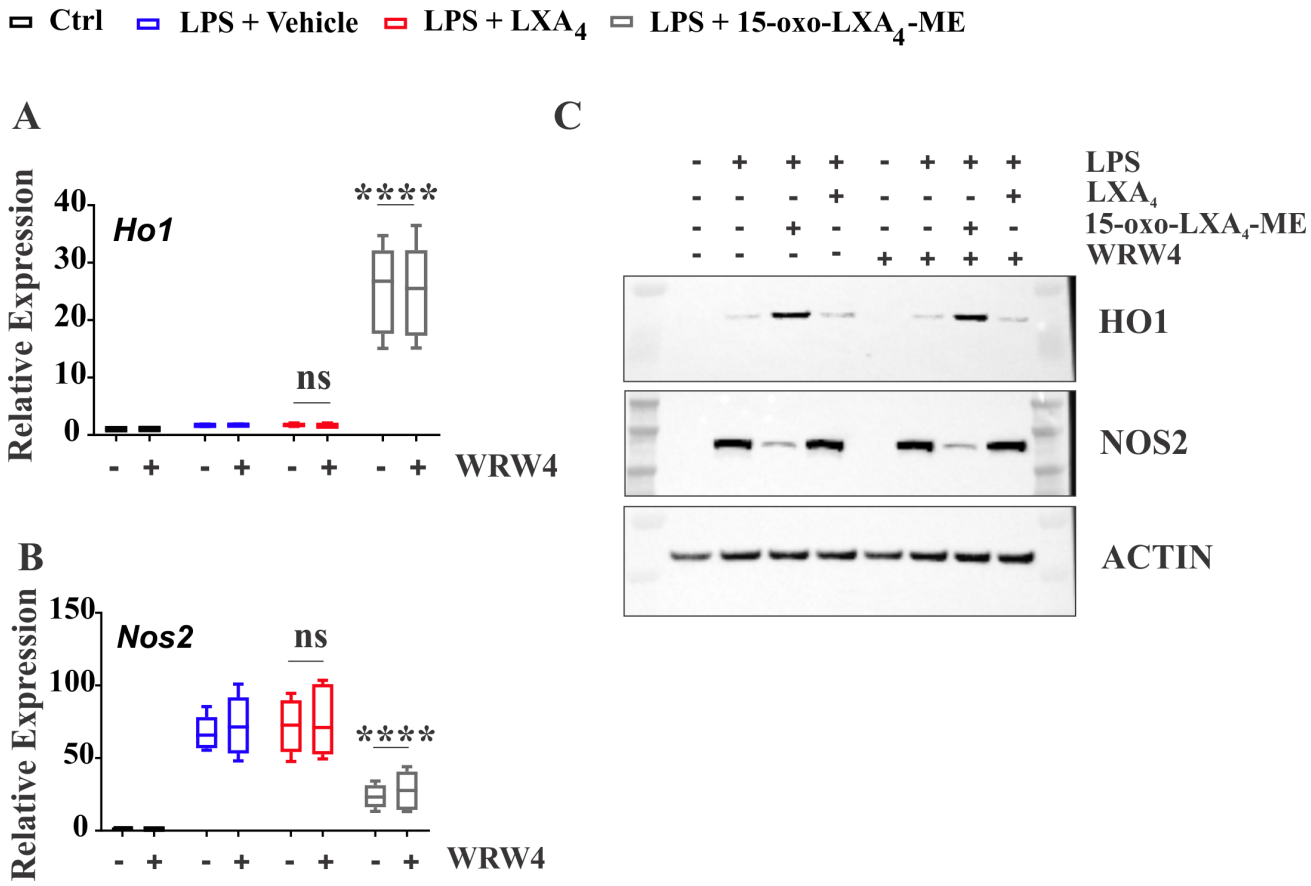

Figure 14: LXA4 does not affect LPS-induced inflammation or Nrf2 activation

25 μM 15-oxo-LXA4-ME or 1 μM LXA4 was added to RAW cells at the time as 10 ng/mL LPS. The FPR2 antagonist, WRW4 was added 30 minutes prior to treatment and media was replaced. Samples were harvested at various time points and processed Gene expression data for *Ho1* (A) and *Nos2* (B), 6 hr after administration of 1 μM LXA4 and LPS. Western blot showing protein levels of HO1 and NOS2 12 hr after 1 μM LXA4 and 10 ng/mL LPS addition (C). Gene expression data are combined from two independent experiments. Western blot images are representative of two independent experiments. Full blots are shown in **Fig 15**.

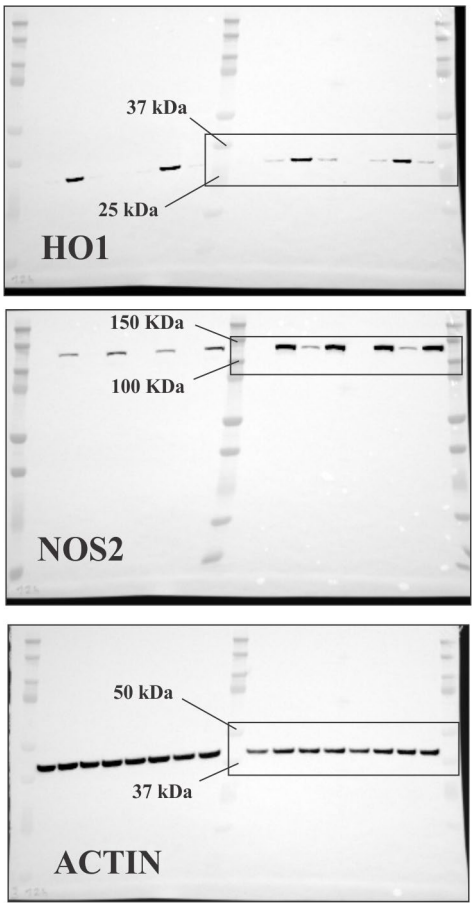

Figure 15: Full images for Fig 14

3.7 Discussion

There is increasing evidence to support that targeting inflammation with compounds that dampen (rather than inhibit) various pro-inflammatory pathways can be beneficial for many disease states including acute lung injury, various autoimmune disorders (e.g. MS and asthma), and infection [87, 170, 192, 194, 210-219]. This "fine-tuning" of the host response (immunomodulation) offers increased therapeutic potential over global suppression from agents

like corticosteroids and highly specific inhibitors (e.g. TNFα monoclonal antibodies) by hitting multiple targets involved in inflammation (e.g. polypharmacology) without ablating regulatory roles of an individual cytokine and/or cell signaling cascade [123]. DMF is a prime example of an immunomodulatory compound that targets multiple proteins (likely through cysteine alkylation), reducing the production of IL12 and IL23, as well as the recruitment of cytotoxic T cells in models of MS [37, 61, 166, 170, 213, 220, 221]. Together, it is clear that modulating immunity, without specific (GPCR-dependent) or global suppression (i.e. corticosteroids), has substantial potential for treating many inflammatory disorders.

During inflammation, electrophilic lipids are formed through enzymatic and/or reactive oxygen or nitrogen species-dependent mechanisms. For example, prostaglandins can be metabolized into electrophilic, α,β-unsaturated ketones (e.g. 15d-PGJ_2, 15-oxoPGE_2) through enzymes like 15-PGDH, and conjugated linoleic acid (cLA) can be nitrated in vivo to form the anti-inflammatory signaling mediator, nitro-cLA [116, 148, 222, 223]. 11-HETE and 15-HETE (derived from AA oxidation) can also be oxidized into 11-oxoETE and 15-oxoETE, respectfully, from 15-PGDH [143, 144, 206]. Likewise, LXA_4 is oxidized by 15-PGDH to form 15-oxo-LXA_4, an electrophilic, α,β-unsaturated ketone [165]. Despite the structural similarities between 15-oxo-LXA_4 and other AA-derived electrophilic lipids, including 15d-PGJ_2 and 15-oxoETE, the bioactive signaling abilities of 15-oxo-LXA_4 have not been critically examined. This study provides evidence that 15-oxo-LXA_4, but not LXA_4, can reduce LPS-induced inflammation in a murine macrophage cell line.

The primary metabolite of LXA_4 is oxidized to form 15-oxo-LXA_4, which was thought to be biologically inactive. However, the biological activity of 15-oxo-LXA_4 was only tested in one study (deemed inactive) in 2000 and has not been revisited [165]. Herein we demonstrate that

although 15-oxo-LXA$_4$ does appear to bind FPR2 (**Fig 12B**), the receptor responsible for LXA$_4$ activity, it promotes anti-inflammatory signaling through activation of the Nrf2-mediated antioxidant response and inhibition of LPS-driven pro-inflammatory signaling despite FPR2 inhibition (**Fig 12C-G**). 15-oxo-LXA$_4$ contains an α,β-unsaturated ketone moiety, conferring electrophilic signaling properties that are comparable to other AA metabolites such as 11- and 15-oxoETE, cyclopentanone prostaglandins, DMF, and nitro-lipids [116, 120, 147, 165]. These molecules also signal through GPCR-independent mechanism by forming reversible covalent Michael addition adducts with nucleophilic cysteines in redox regulatory transcription factors and enzymes [114, 119, 224]. Similar to other electrophilic lipids, 15-oxo-LXA$_4$ formed a glutathione adduct (**Fig 7**). Four prominent peaks with similar retention times (9.35, 9.53, 9.75, 10.15 min) between the adduct detected in cell media and a prepared 15-oxo-LXA$_4$-GS standard were observed, providing further evidence that 15-oxo-LXA$_4$ is electrophilic after release from the methyl ester derivative. Detection of a glutathione adduct as well as 15-oxo-LXA$_4$ and its reduced metabolite, 13,14-dihydro-15-oxo-LXA$_4$ (**Fig 6**) confirm the methyl ester releases the expected product *in vitro* and suggest it 15-oxo-LXA$_4$ is electrophilic.

15-oxo-LXA$_4$ reduced LPS-induced inflammation, but did not abolish total signaling (**Fig 8**). Both gene expression and protein levels of multiple pro-inflammatory cytokines (IL1β, IL6, MCP1) and NOS2 were significantly reduced at various time points during LPS-induced activation of a murine macrophage cell line in the presence of 15-oxo-LXA4 (**Fig 8**). However, TNFα production was not inhibited with 15-oxo-LXA$_4$ like the other cytokines (**Fig 9**). Together these data demonstrate 15-oxo-LXA$_4$ is active and can significantly lower aspects of LPS-induced inflammation without completely abolishing cytokine production. Importantly, LXA$_4$ was unable to dampen LPS-induced NOS expression or activate Nrf2, reinforcing the fact that these anti-

inflammatory effects were due to its electrophilic metabolite, 15-oxo-LXA_4 (**Fig 14**). These data corroborate the findings of other studies using electrophilic lipids to mitigate aspects of inflammation. The prostaglandin metabolite, 15d-PGJ_2 is highly efficient at reducing cytokine production and pro-inflammatory gene expression in both cell and animal models [113, 142, 222, 225, 226]. Another group of studies demonstrated that 15-oxoETE will reduce pro-inflammatory cytokine production in both murine and human macrophage/monocyte cells lines [143, 144]. Moreover, DMF (recently approved for MS as Tecfidera), an electrophilic fumarate analog, inhibits the generation of pro-inflammatory cytokines as well as NOS2 activity [213, 227]. The key and common factor between all of these electrophiles is their ability to minimize collateral damage from aberrant immune responses without inhibiting the normal function of immunity – highlighted when 15d-PGJ_2 is used to rescue mice from influenza-induced lung injury without impacting viral clearance [225]. Future studies will need to evaluate the role of 15-oxo-LXA_4 *in vivo*.

The activation of Nrf2 and its downstream target genes (e.g. NQO1, HO1, GCLM) results in antioxidant production, detoxification, and aids cells in returning to homeostasis after undergoing various stressors [86]. Many electrophiles, such as nitro-alkenes and α,β-unsaturated ketones will alkylate KEAP1 cysteines, resulting in Nrf2 nuclear translocation and the activation of the antioxidant response element [145, 228]. 15-oxo-LXA_4 greatly enhanced Nrf2 activity (**Fig 10**). The mRNA expression of *Nqo1*, *Gclm*, and *Ho1* were significantly enhanced by 15-oxo-LXA_4 at multiple time points after LPS administration (**Fig 10**). In corroboration with gene expression data, protein levels of each Nrf2 target gene were clearly induced by 15-oxo-LXA_4 at 6 and 12 hr after treatment (**Fig 10B, D, F**). Again, LXA_4 had no impact on HO1 (**Fig 14).** The ability to activate Nrf2 antioxidant responses seems to be another common attribute to electrophilic lipids.

The nitro-alkenes are highly efficient Nrf2 activators and are in phase II clinical trials for their ability to protect cells from injury and dampen inflammation [134, 145]. Many of the salient functions of DMF have been attributed to Nrf2 activation [169, 170, 227]. In fact, the Nrf2 an NF-κB pathways interact to regulate inflammation – linking the function of electrophilic lipids to core signaling mediators of immunity [93]. Finally, the cellular effects of pro-resolving lipid mediators, like LXA_4, mimic electrophilic lipids; however, 15-oxo-LXA_4, is the first electrophilic metabolite to be studied in the context of immunity.

Interestingly, both LXA_4 and 15-oxo-LXA_4 increased FPR2 activity in a similar manner that was significantly less than that of the positive control, WKYMVm (**Fig 12B**). However, the ability of 15-oxo-LXA_4 to inhibit NOS2 and activate Nrf2 target gene expression and protein production was not decreased when cells were pretreated with an FPR2 antagonist (**Fig 12**). Moreover, LXA_4 was unable to alter NOS2 or Nrf2 target genes to the same extent of 15-oxo-LXA_4 (**Fig 14**). These results suggest there may be FPR2-independent effects of 15-oxo-LXA_4 and its role in binding FPR2 needs to be examined further.

In conclusion, the electrophilic metabolite of LXA_4, 15-oxo-LXA_4, was able to activate Nrf2 and inhibit LPS-induced inflammation in RAW cells, a common *in vitro* model of inflammation. Moreover, LXA_4 did not mimic any of these changes, suggesting that 15-oxo-LXA_4, a metabolite previously thought to be inactive, may be responsible for some of its pro-resolving properties. In fact, many of the pro-resolving properties attributed to LXA_4 and other SPMs greatly overlap with electrophilic lipids (e.g. NF-κB inhibition and Nrf2 activation) – illustrated in **Fig 16**. Future studies need to address the metabolism of LXA_4 and better characterize the levels of 15-oxo-LXA_4 in addition to evaluating the pro-resolving properties of 15-oxo-LXA_4. A better characterization and delineation of the anti-inflammatory and tissue repairing effects of both LXA_4

and 15-oxo-LXA$_4$ needs to occur with other pharmaceutical and genetic models to separate the FPR2-depedent and alkylation-dependent actions of each lipid. Finally, other electrophilic metabolites are formed when pro-resolving mediators are added *in vivo*; however, nothing is known of their activity or tissue concentration. For example, 8-oxoRvD1 and 17-oxoRvD1 (from RvD1), and 18-oxoRvE1 (from RvE1) have all been detected, but not well characterized [229, 230]. A better understanding of pro-resolving mediator metabolism, along with the function of their electrophilic metabolites, will better inform the lipid community of their importance in pre-clinical animal models and optimize future clinical trials.

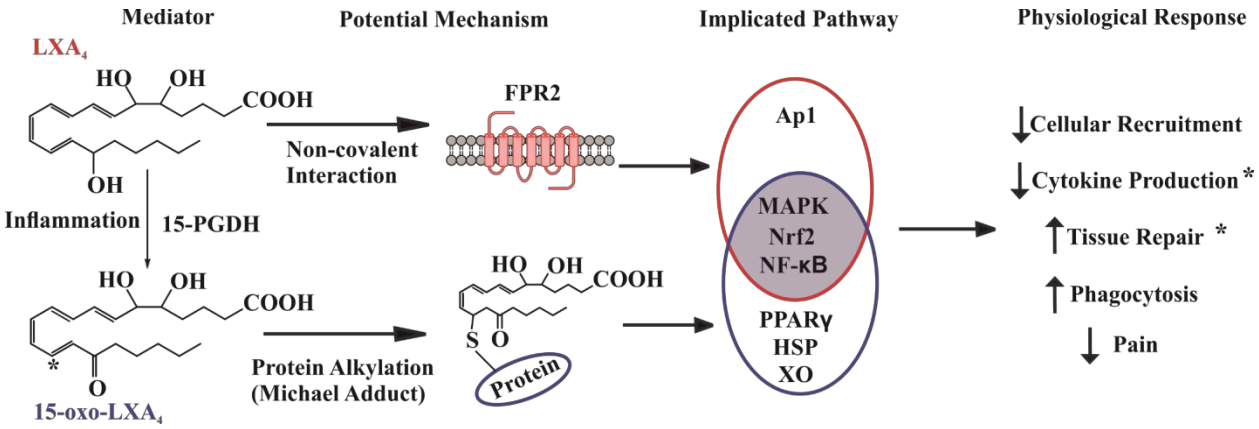

Figure 16: Schematic representation of LXA_4 and 15-oxo-LXA_4 signaling

LXA_4 is oxidized into 15-oxo-LXA_4 by 15-PGDH during inflammation. LXA_4 is thought mainly to signal by binding to the GPCR, FPR2 and intiating a variety of responses (red oval) that result in anti-inflammatory and cytoprotective actions. 15-oxo-LXA_4 and other electrophilic lipids alkylate key regulatory proteins (blue oval) by forming a Michael adduct between the electrophilic carbon (marked with the asterisk on 15-oxo-LXA_4) and a nucleophilic cysteine. Many of the implicated pathways overlap between LXA_4 and 15-oxo-LXA_4 (highlighted in purple) and elicit physiological responses that maintain cellular homeostasis after an inflammatory response. Cytokine production and tissue repair were analyzed in this manuscript so they are marked with an asterisk, while the other need to be evaluated in future studies.

4.0 Nitro-oleic acid inhibits dendritic cell function

Gregory J Buchan**, Veronika Cechova, Adolf Koudelka, James P O'Brien, Renee Anderko, Madeline Ellgass, Steven J Mullett, Robbie B Mailliard, Bruce A Freeman, Stacy G Wendell.* ***J Immunol *– In preparation.*

4.1 Introduction

Autoimmune diseases are difficult to treat due to their complexity and pervasive disruption of the immune system. Typically, self-recognition by T and B lymphocytes is aberrant and tissue destruction can result. For example, in MS, effector T cells recognize peptides composing the myelin sheath, resulting in breakdown of this protective layer and nervous system complications [24]. In systemic lupus erythematosus, loss of self-tolerance leads to the production of auto-antibodies, forming immune complexes that result in tissue injury [231]. Other autoimmune diseases include psoriasis, rheumatoid arthritis, and scleroderma– all of which involve a loss in tolerance, and abnormal activation of T and B lymphocytes. The pathogenesis of many chronic and autoimmune diseases is caused by irregularities in DC function that culminate in aberrant lymphocyte responses.

Recently, DMF was approved by the FDA for the treatment of MS (Tecfidera®) [166, 232]. DMF contains an electrophilic, α,β-unsaturated ketone and alkylates cysteine residues on various proteins as well as small molecular weight thiols (i.e. GSH) [61, 166, 208]. Known targets of DMF include C150/152 (mouse/human) of GAPDH [61], Cys151 of Keap1, Cys13 of IRAK4, and Cys75 of adenosine deaminase [166, 213]. Despite the promiscuity of DMF, it causes profound

changes in immune responses and ultimately, decreases DC and T cell activation, which is thought to be the reason for its success in treating MS and psoriasis. A successful therapeutic that forms covalent adducts is remarkable since these types of remedies have been ignored for decades because of their off-target and non-specific effects (e.g. many are used for chemotherapy and are highly toxic). However, recent strides have been made in identifying electrophile-sensitive targets and many "soft" electrophiles, such as DMF, that are generally non-toxic and possess immunomodulatory properties [117, 119, 233, 234]. Recent developments have also lauded the electrophile, itaconate for its potential in treating aberrant inflammatory disease [228, 235, 236]. In fact, several reviews have emerged describing the anti-inflammatory and tissue-repairing abilities of many electrophiles [116, 233, 237, 238]. More specifically, nitro-oleic acid (NO_2-OA), is currently in Phase II clinical trials for pulmonary hypertension as well as kidney disease (PRIMEx and FIRSTx). However, not much is known regarding NO_2-OA impact on DC function, a key component of most immune responses and auto-immune disorders.

We hypothesized that NO_2-OA, much like the electrophile DMF, would limit DC activation and function. Here we show that, NO_2OA efficiently limited DC activation at concentrations more than tenfold less than DMF. Common surface markers of activation, in addition to cytokine and chemokine production, were all decreased with the addition of NO_2-OA in LPS-activated DCs. Together, these data suggest that NO_2-OA rewires DC signaling to a passive state, likely through its ability to reversibly alkylate multiple proteins. These results implicate NO_2-OA is a suitable therapy for MS and other auto-immune disorders. Moreover, these suggest a common mechanism between other electrophiles, such as DMF, in modulating immunometabolism to confer their effects.

4.2 NO_2-OA does not impact GM-CSF-induced DC formation

Bone marrow derived monocytes were differentiated into BMDCs with GM-CSF (20 ng/mL) for 5 days. Oleic acid (a non-electrophilic control) or NO_2-OA were added at the same time as GM-CSF at a concentration of 5 μM on day 0. The surface phenotype was analyzed on day 5 (**Fig 17**). No significant differences were seen in viability (**Fig 19A**) and the percentage of CD11c+ cells remained the same among the treatment groups (**Fig 19B**). Moreover, the CD11b and MHCII distribution (**Fig 17A-C, Fig 19C**) were similar with or without lipid treatment and surface expression of CD80 and CD86 were unaltered (**Fig 17D, E**; **Fig 19D, E**). The gating strategy for this and subsequent experiments is shown in **Fig 18.** Recent studies have shown CD11c+ cells differentiated from bone marrow consist of macrophages, monocytes, and DCs; therefore, CD11c+CD11b+MHCII+ were deemed as DCs for their expression of CD80 and CD86 [46, 173]. These data demonstrate that NO_2-OA does not alter the GM-CSF-induced differentiation of monocytes into DCs.

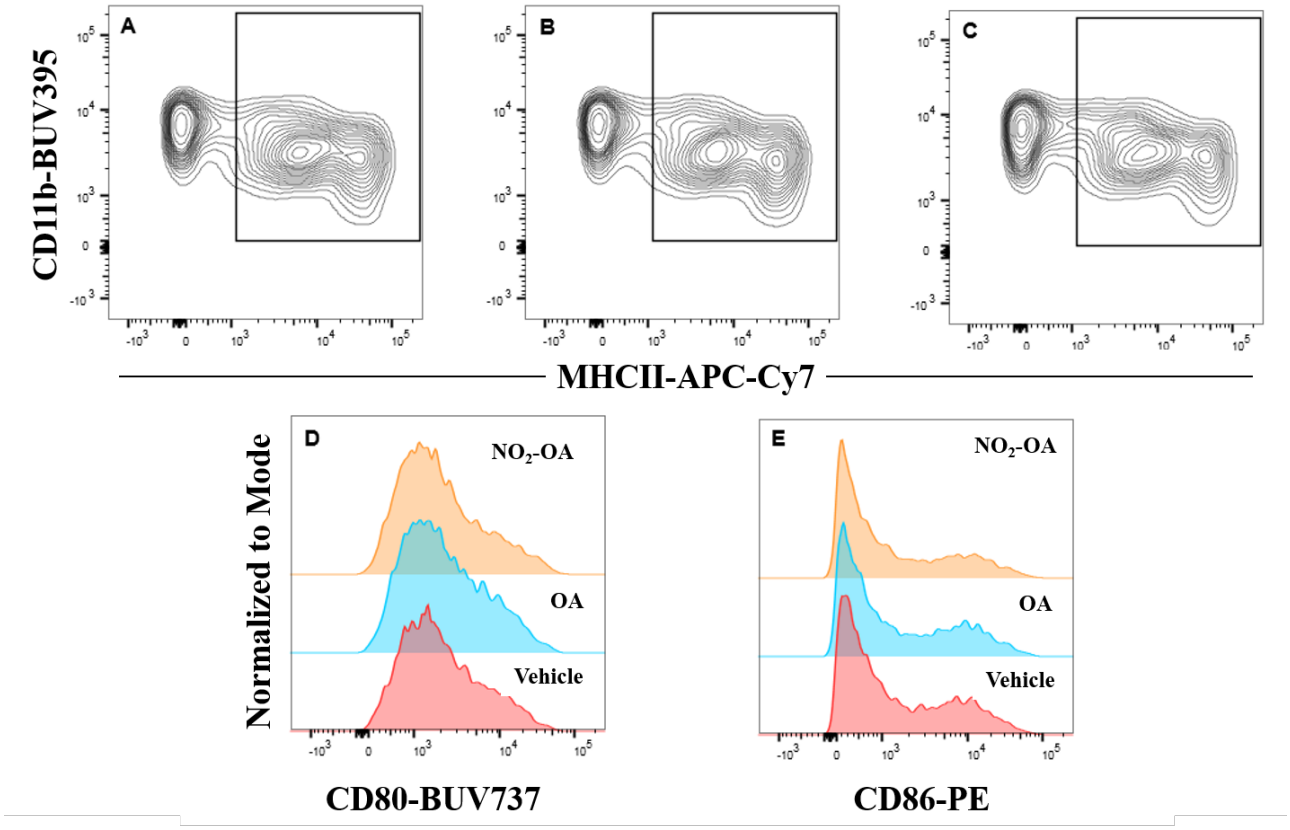

Figure 17: NO_2-OA does not inhibit GM-CSF induced DC differentiation

Bone marrow derived monocytes were treated with 20 ng/mL GM-CSF with or without 5 µM oleic acid or 5 µM NO_2-OA. On day 5, cells were collected and analyzed via flow cytometry. CD11c+ cells were characterized according to CD11b and MHCII expression with CD11b+MHCII+ cells deemed as DCs (Full gating shown in **Fig 18**). Cells were treated with vehicle (A), 5 µM oleic acid (B), or 5 µM NO_2-OA (C). CD11c+ CD11b+ MHCII+ DCs were also evaluated for CD80 (D) and CD86 expression (E).

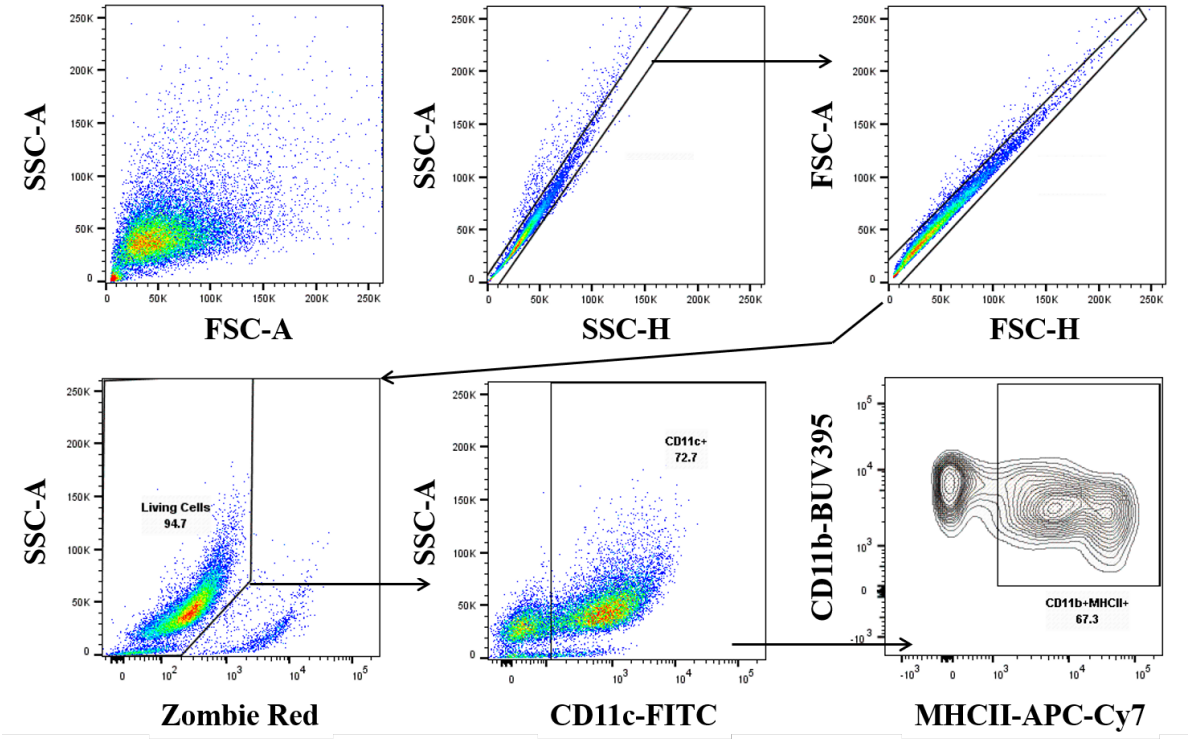

Figure 18: Gating Strategy

Cells were gated after excluding doublet populations and dead cells with the viability dye, Zombie Red. Then, CD11c+ cells were selected and BMDCs were characterized as CD11c+CD11b+MHCII+. The CD11c+CD11b+MHCII- population likely consists of macrophages and undifferentiated monocytes.

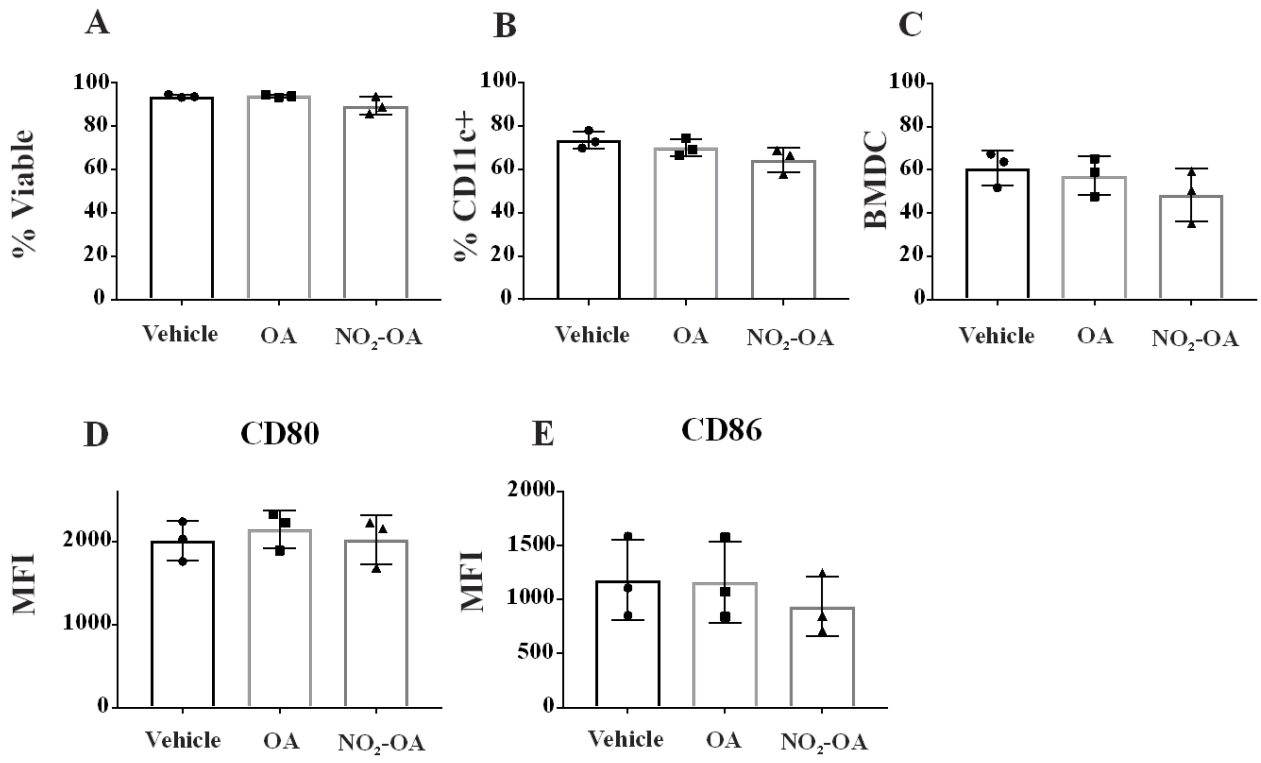

Figure 19: Supplement to Fig 17

Viability measured with Zombie Red dye (A). Percentage of Living, CD11c+ cells (B). Percentage of CD11c+CD11b+MHCII+ BMDCs (C). Median fluorescent intensity for CD80 (D) and CD86 (E) of BMDCs.

4.3 NO_2-OA inhibits LPS-induced DC activation

BMDCs were activated with 100 ng/mL LPS in the presence or absence of oleic acid (5 μM) or varying levels of NO_2-OA for 6 and 24 hr (**Fig 20**). The gating strategy is the same shown in **Fig 18**. It should be noted that during LPS-induced activation, there were no changes in the distribution of CD11c+ cells (**Fig 22, 23**). Indeed, NO_2-OA had no impact on the percentage of

CD11c+ cells at 6 or 24 hr (**Fig 23**). As expected, LPS did activate immature DCs as evidenced by a shift in MHCII (**Fig 22A, B**) and increases in CD40, CD80, and CD86 at both time points (**Fig 20, 21**). These data reinforce recent studies that show part of the CD11c+ population (MHCII-) are likely macrophages or undifferentiated monocytes [45, 46, 173]. LPS-induced activation was evaluated by analyzing surface expression of CD40, CD80, and CD86 – markers typically associated with DC activation. The surface phenotype of CD40 was decreased at 6 hr after administration with statistically significant changes with 2.5 and 5 μM NO_2-OA (**Fig 20A, D**). Likewise, 5 μM NO_2-OA significantly inhibited the expression of CD80 and CD86 with trending decreases in 1 and 2.5 μM (**Fig 20 B, C, E, F**). However, the decreases at 6 hr post LPS administration were not sustained as there were no significant decreases in any marker 24 hr after treatment (**Fig 21A-F**). It should be noted that decreases in viability were observed when 5 μM NO_2-OA was used and both 6 and 24 hr after treatment but 2.5 μM NO_2-OA or below did not alter viability (**Fig 23A, B**). Therefore, for the rest of the chapter, only 2.5 μM NO_2-OA results are shown. Although there was a loss in viability at 5 μM, there was a dose-dependent trend of inhibition at lower concentrations. These data demonstrate that NO_2-OA inhibits CD40, CD80, and CD86 expression – all classic markers for DC activation.

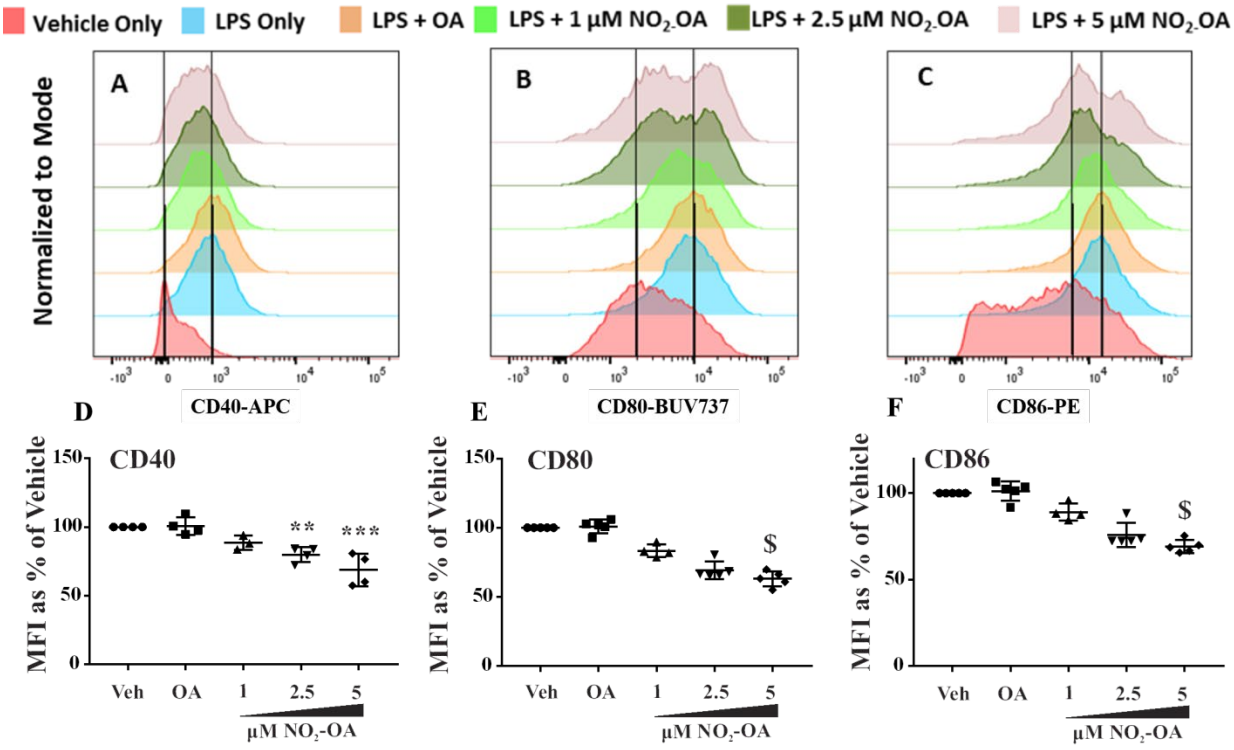

Figure 20: NO_2-OA inhibits LPS-induced DC activation 6 hr after treatment

On day 5, BMDCs were treated simultaneously with 100 ng/mL LPS with or without lipid treatment for 6 hrs. Cells were then collected and analyzed via flow cytometry. DCs were evaluated 6 hr after treatment based on CD40 (A, D), CD80 (B, E), and CD86 (C, F). **p<0.01, ***p<0.001 (normal, One-way ANOVA), $p<0.05 (Non-parametric, One-way ANOVA). Histogram data are representative of 4 independent experiments while MFI data are the combined percentages of those 4-5 experiments with error bars representing SD.

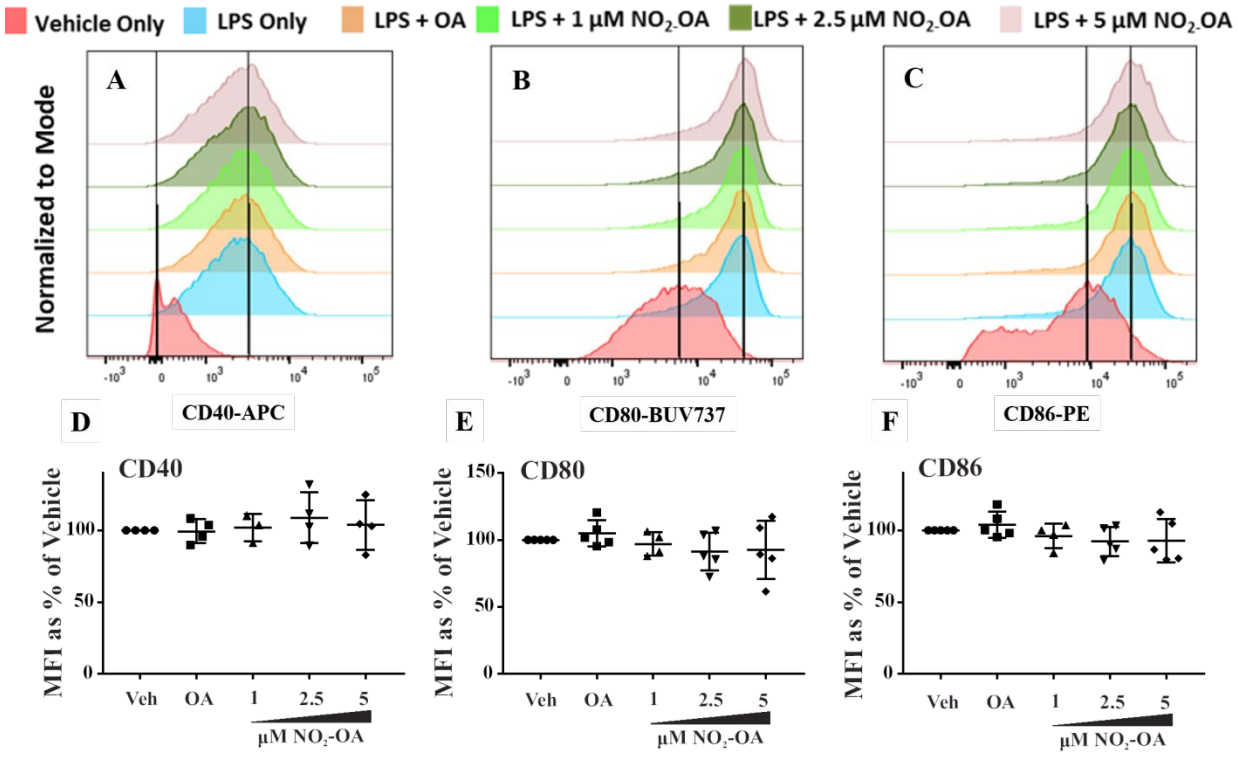

Figure 21: NO_2-OA does not inhibit surface marker activation 24 hr after treatment

On day 5, BMDCs were treated simultaneously with 100 ng/mL LPS with or without lipid treatment for 24 hrs. Cells were then collected and analyzed via flow cytometry DCs were evaluated 24 hr after treatment based on CD40 (A, D), CD80 (B, E), and CD86 (C, F). Histogram data are representative of 4 independent experiments while MFI data are the combined percentages of those 4-5 experiments.

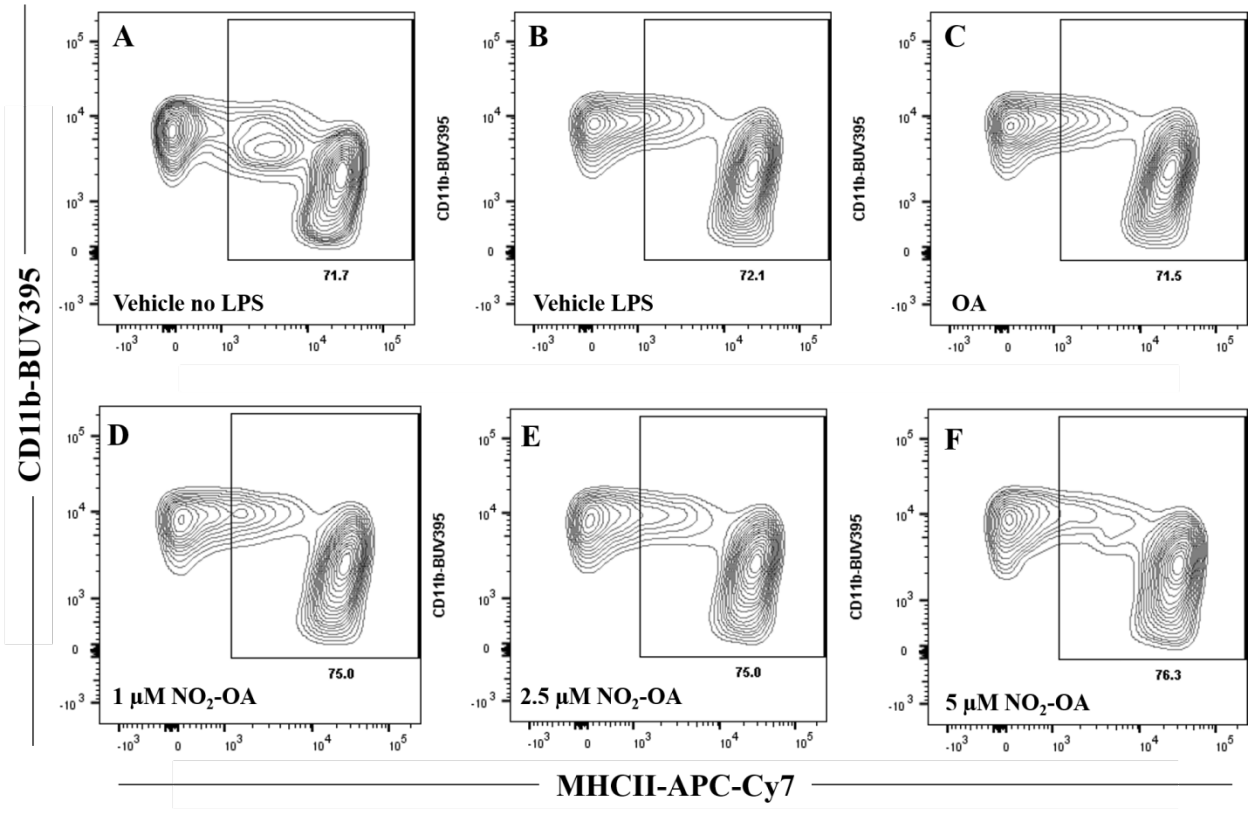

Figure 22: NO_2-OA does not alter cellular distribution during LPS treatment

GM-CSF-differentiated monocytes were activated with LPS and treated with increasing doses of NO_2-OA. The percentage of BMDCs, characterized as CD11c+CD11b+MHCII+ cells was not altered with treatment with the non-electrophilic OA control, nor NO_2-OA (B-F).

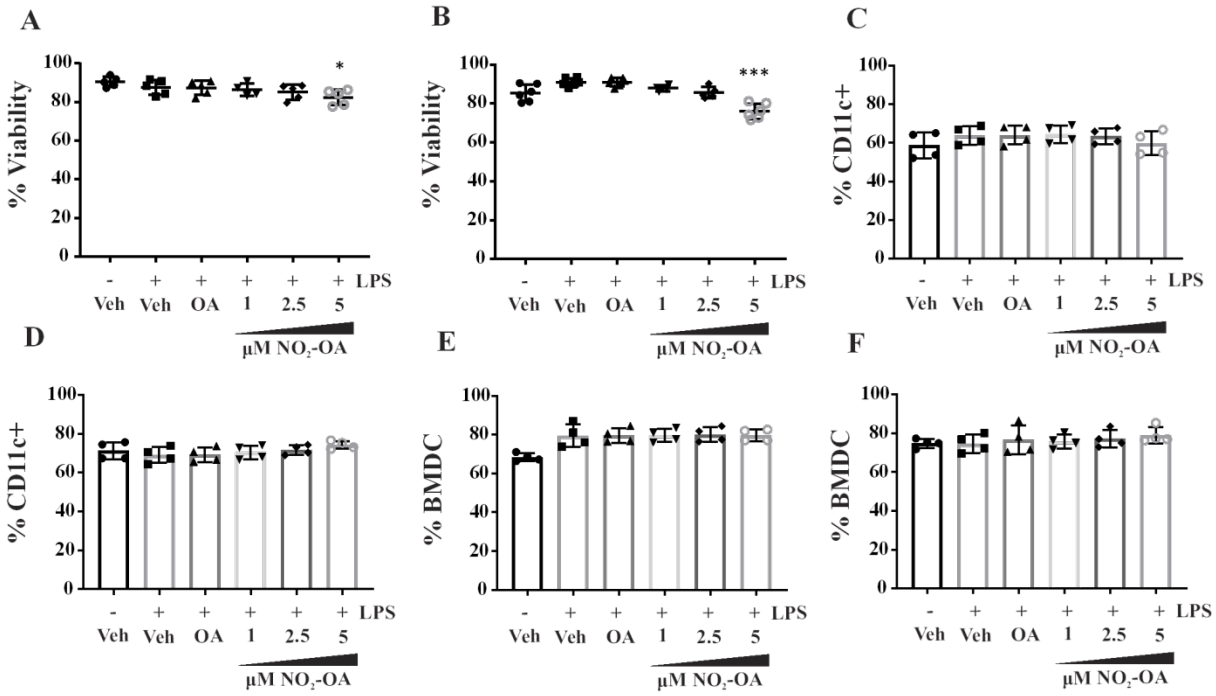

Figure 23: Supplement to Fig 20-22

Viability was measured at 6 (A) and 24 hr (B) after NO_2-OA and LPS treatment with Zombie Red viability dye. The percentage of CD11c+ cells are shown for 6 and 24 hr treatments (C, D). The percentage of CD11c+CD11b+MHCII+ (BMDCs) for 6 (E) and 24 hr (F) treatments. *$p<0.05$, ***$p<0.001$, One-way ANOVA. Results are combined from 4-5 independent experiments.

4.4 NO_2-OA limits cytokine production during DC activation

DCs were activated with LPS and simultaneously treated with NO_2-OA. Similar to the activation surface phenotype of BMDCs, NO_2-OA inhibited an array of cytokines at 6 and 24 hr post treatment in a dose-dependent manner (**Fig 24, 25**). Pro-inflammatory cytokines IL6, and IL1β, and were significantly decreased with 6 hr of treatment after LPS-induced activation (**Fig**

24A, B). Moreover, DC-specific inflammatory cytokines IL12 and IL23 were reduced to near non-detectable levels compared to vehicle controls (**Fig 24D, E**). Unexpectedly, IL10, typically classified as anti-inflammatory, was also decreased upon NO_2-OA treatment (**Fig 24C**). Most of these changes were sustained for up to 24 hr (**Fig 25**) with the exception of IL1β, which was no longer decreased at the later time point (**Fig 25A**). MCP1 was unaltered at both 6 and 24 hr (**Fig 24F, 25F**). Together, these data show that NO_2-OA inhibits several pro-inflammatory cytokines during LPS-induced DC activation. Importantly, DC-specific activation cytokines, IL12p70 and IL23, were inhibited while inhibition of the other cytokines could be from changes in macrophages or undifferentiated monocytes remaining in culture. Lastly, NO_2-OA did not completely suppress cytokine production as evidenced by no change in MCP1, IL1β, or IL10 at 24 hr (**Fig 25A, C, F**).

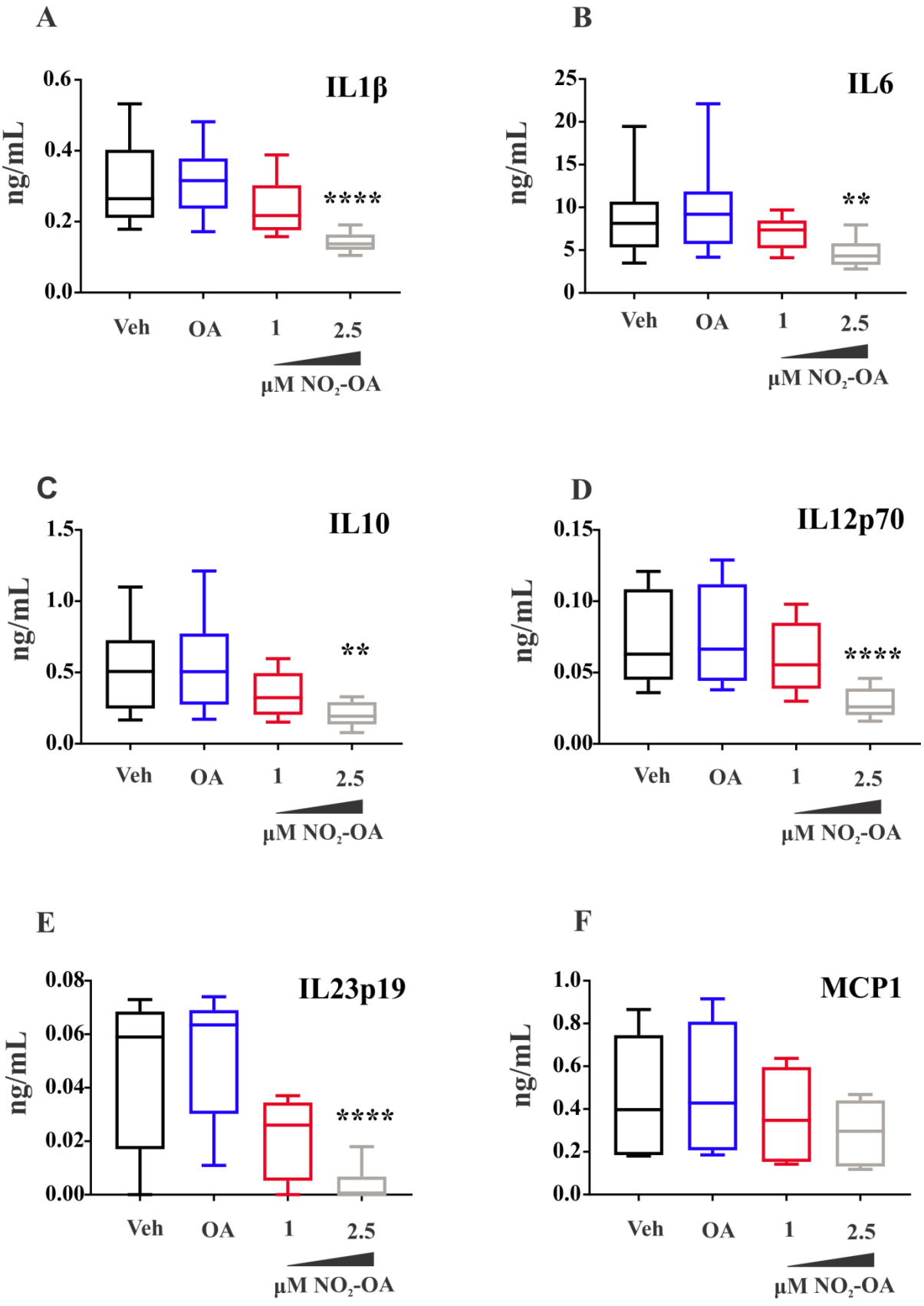
A
IL1β
ng/mL
0.6
0.4
0.2
0.0
****
Veh
OA
1
2.5
μM NO2-OA
B
IL6
ng/mL
25
20
15
10
5
0
**
Veh
OA
1
2.5
μM NO2-OA
C
IL10
ng/mL
1.5
1.0
0.5
0.0
**
Veh
OA
1
2.5
μM NO2-OA
D
IL12p70
ng/mL
0.15
0.10
0.05
0.00
****
Veh
OA
1
2.5
μM NO2-OA
E
IL23p19
ng/mL
0.08
0.06
0.04
0.02
0.00
****
Veh
OA
1
2.5
μM NO2-OA
F
MCP1
ng/mL
1.0
0.8
0.6
0.4
0.2
0.0
Veh
OA
1
2.5
μM NO2-OA

Figure 24: Cytokine generation is decreased after 6 hr NO_2-OA administration

On day 5, BMDCs were treated simultaneously with 100 ng/mL LPS with or without lipid treatment for 6 hrs. Media was then collected and frozen for analysis. ELISA analysis at 6 hr post treatment evaluated the level of IL1β (A), IL6 (B), IL10 (C), IL12p70 (D), IL23p19 (E), and MCP1 (F). *$p<0.05$, **$p<0.01$, ***$p<0.001$, ****$p<0.0001$. Data are from 3-4 independent experiments.

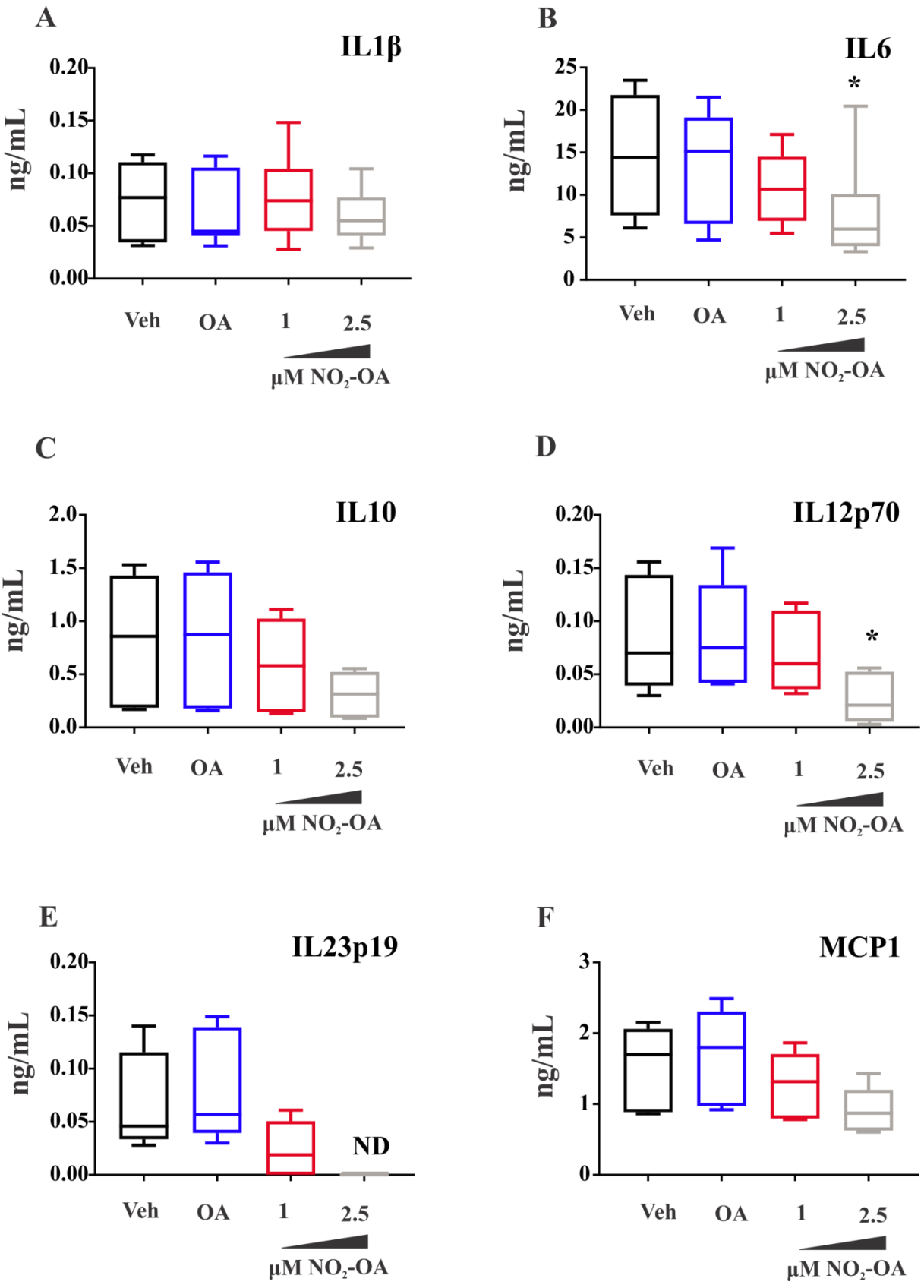
A
IL1β
ng/mL
0.20
0.15
0.10
0.05
0.00
Veh
OA
1
2.5
μM NO2-OA
B
IL6
ng/mL
25
20
15
10
5
0
*
Veh
OA
1
2.5
μM NO2-OA
C
IL10
ng/mL
2.0
1.5
1.0
0.5
0.0
Veh
OA
1
2.5
μM NO2-OA
D
IL12p70
ng/mL
0.20
0.15
0.10
0.05
0.00
*
Veh
OA
1
2.5
μM NO2-OA
E
IL23p19
ng/mL
0.20
0.15
0.10
0.05
0.00
ND
Veh
OA
1
2.5
μM NO2-OA
F
MCP1
ng/mL
3
2
1
0
Veh
OA
1
2.5
μM NO2-OA

Figure 25: Cytokine generation is decreased after 24 hr NO_2-OA administration

On day 5, BMDCs were treated simultaneously with 100 ng/mL LPS with or without lipid treatment for 24 hrs. Media was then collected and frozen for analysis. ELISA analysis at 6 hr post treatment evaluated the level of IL1β (A), IL6 (B), IL10 (C), IL12p70 (D), IL23p19 (E), and MCP1 (F). *p<0.05, **p<0.01, ***p<0.001, ****p<0.0001. Data are combined from 3-4 independent experiments.

4.5 NO_2-OA increases Nrf2 activity and inhibits NOS2 in BMDCs

Nrf2 activation was measured indirectly through the induction of NQO1, HO1, and GCLM. Interestingly, NO_2-OA induced HO1 3 hr after treatment **(FIG 26A**); however, NQO1 and GCLM were not detected. NQO1 and GCLM were induced 24 hr after treatment, compared to vehicle controls (**Fig 26C, D**). The increase in HO1 was sustained 24 hr after treatment but the vehicle group also induced HO1 as compared to the no LPS control (**Fig 26B**). Lastly, NOS2 was inhibited 24 hr after treatment with NO_2-OA (**FIG 26E**). These data suggest NO_2-OA can activate Nrf2-depedendent responses in BMDCs as well as inhibit NOS2 induction. Importantly, these results are consistent with the effects of NO_2-OA and other electrophilic lipids in many cellular and animal models of inflammation [113, 131, 140, 142-145, 147, 148, 155, 157, 222, 225, 239-246].

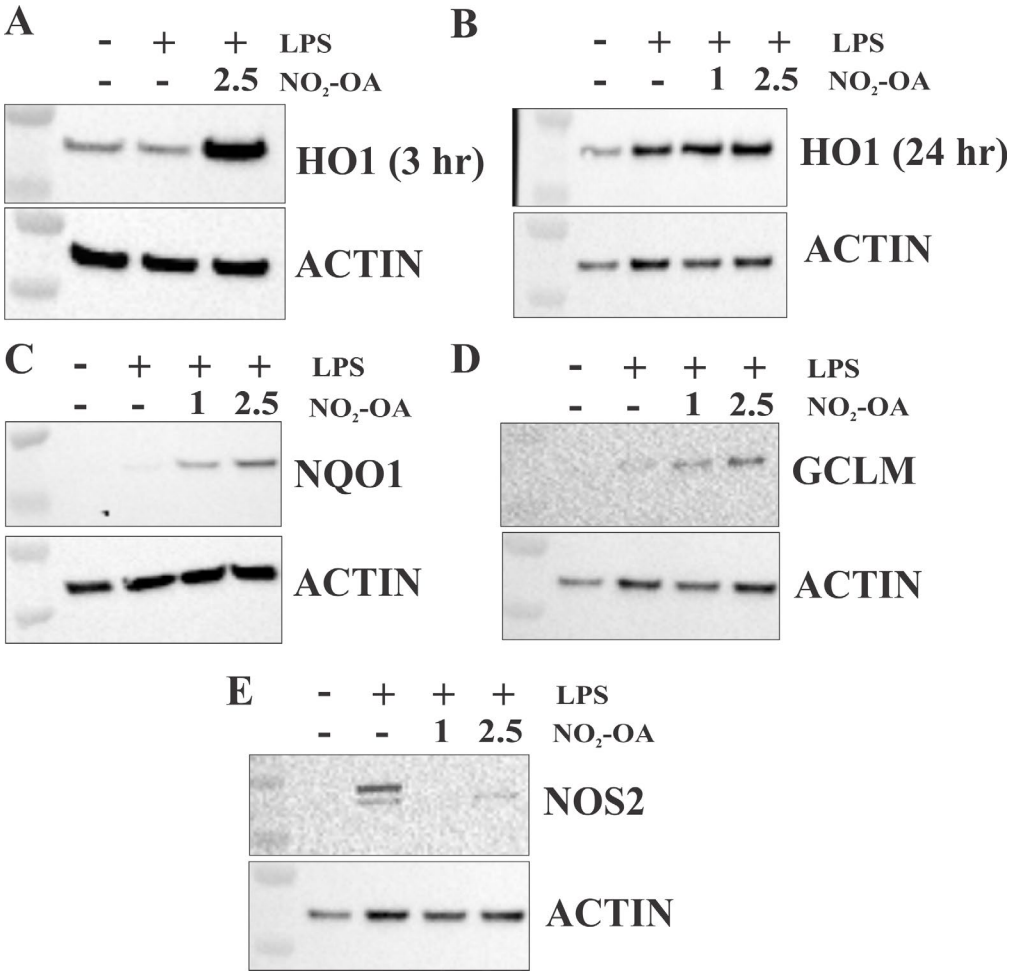

Figure 26: NO_2-OA activates Nrf2 and inhibits NOS2

On day 5, BMDCs were treated simultaneously with 100 ng/mL LPS with or without lipid treatment for 3-24 hrs. Cells were then collected and frozen for analysis. At 3 hr after treatment, HO1 expression was measured with western blot (A). HO1 (B), NQO1 (C), GCLM (D), and NOS2 (E) were analyzed 24 hr after treatment. Images are representative of 2-3 independent experiments. Full blots are shown in **Fig 27**.

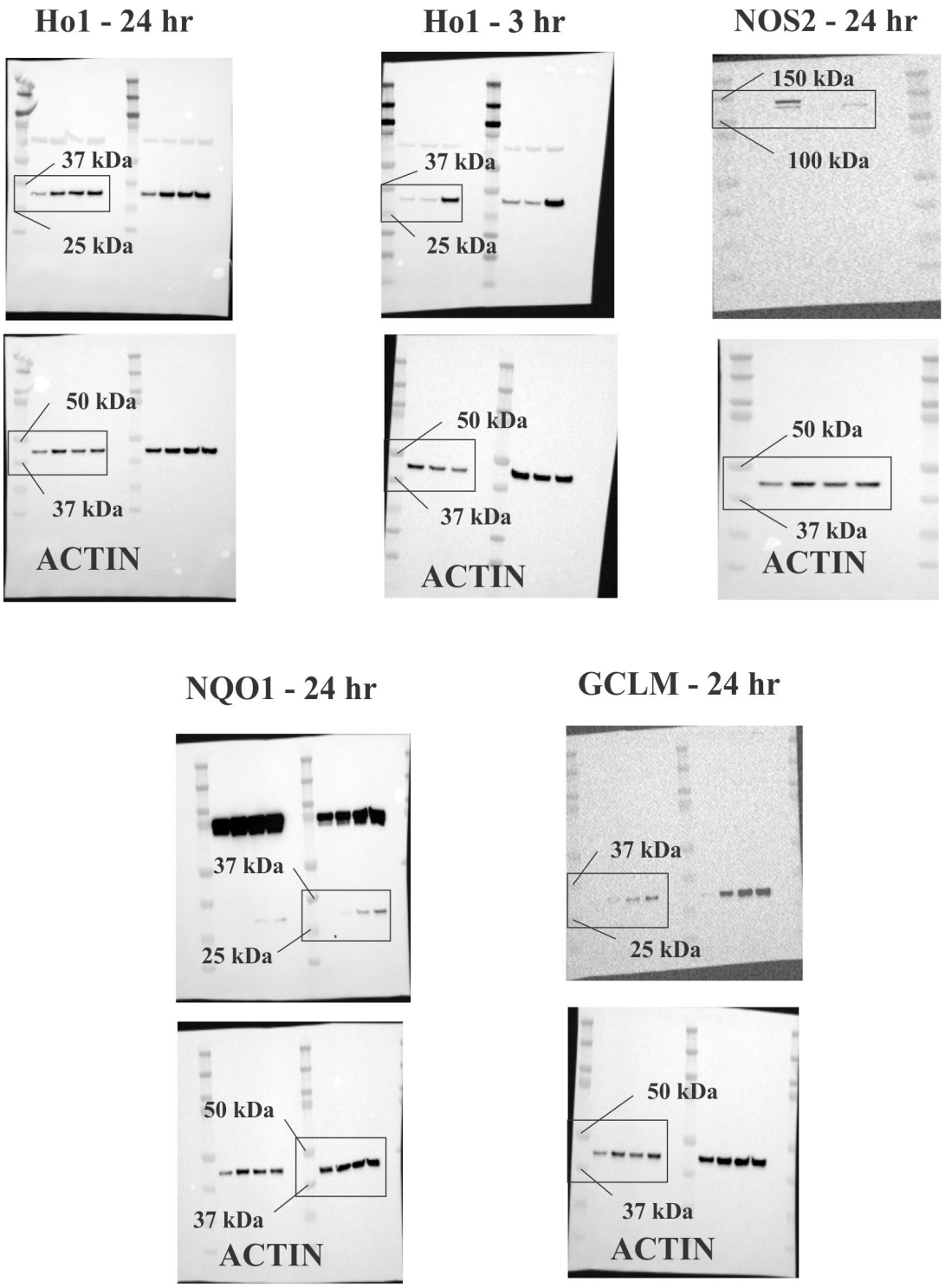

Figure 27: Full western blot images for Fig 26

4.6 NO_2-OA alters DC metabolism

Metabolomics analysis was performed on both lysate and media samples of DC cultures treated with or without LPS and NO_2-OA. Amino acids, citric acid cycle, and glycolytic analytes were measured and normalized to internal standard values (**Fig 28**). At 12 hr after treatment, lactate, succinate, and itaconate were all increased with LPS; however, NO_2-OA had no impact on their intracellular levels (**Fig 28A-C**). Interestingly, glutamate was decreased in cellular lysate when comparing vehicle and NO_2-OA groups that had been activated with LPS (**Fig 28D**). Moreover, citrulline production was significantly decreased with NO_2-OA treatment, alluding to NOS2 inhibition (**Fig 28E**). DCs and macrophages rely on aerobic glycolysis during activation and this process is partially regulated by Nrf2 and NF-κB [15, 61, 101, 102, 247]. These data suggest that NO_2-OA does not directly alter aerobic glycolysis through lactate or succinate levels; however, changes in glutamate and citrulline may contribute changes in DC activation.

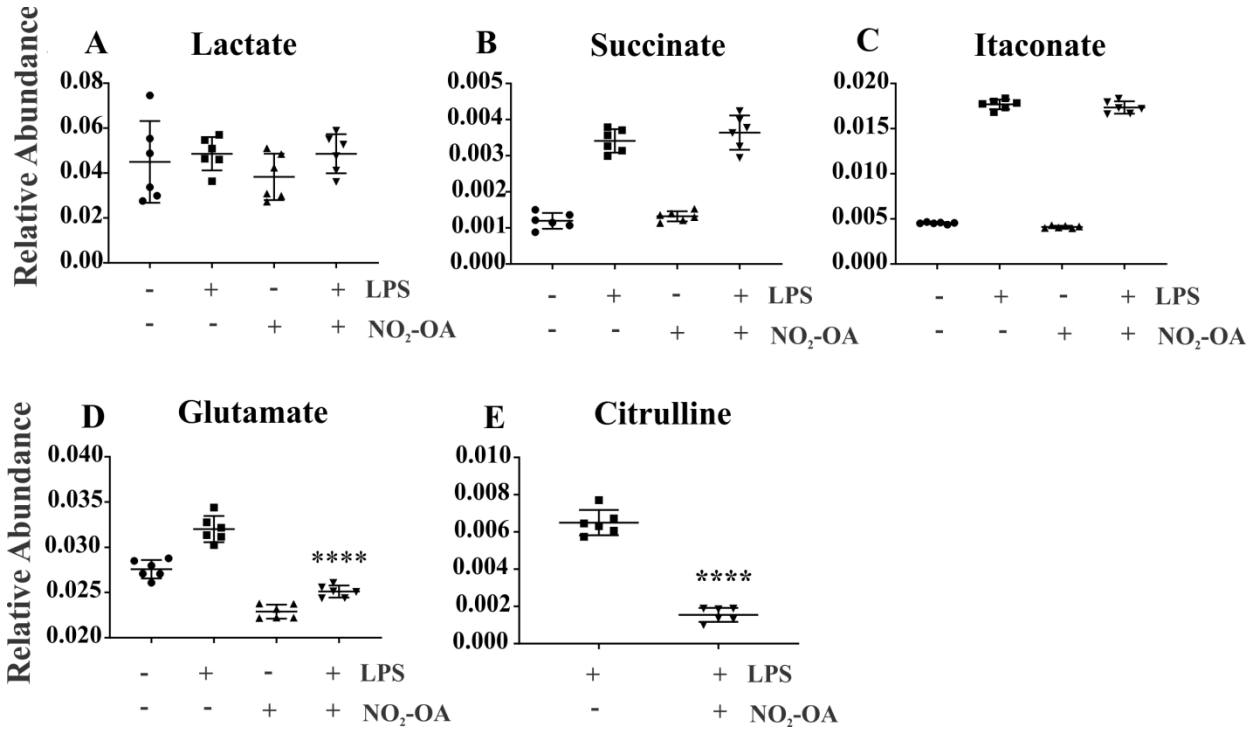

Figure 28: NO_2-OA alters DC metabolism

On day 5, BMDCs were treated simultaneously with 100 ng/mL LPS with or without lipid treatment for 12 hrs. Cells were then collected and frozen for analysis. LC/MS analysis evaluated intracellular levels of lactate (A), succinate (B), itaconate (C), glutamate (D), and citrulline (E). ****$p<0.0001$ One-way ANOVA. SD is shown and data is from one experiment (n=6). The cittrulline in non-LPS treated groups was not detectable.

4.7 Human DC IL12 production is limited by NO_2-OA treatment

Human DCs (HuDCs) were activated with either LPS or CD40L with or without IFNγ and then treated with 2.5 μM NO_2-OA. Interestingly, there were no significant differences between vehicle and NO_2-OA-treated groups for immature (iDC) or LPS/CD40L-stimulated DCs (**Fig 29**);

However, IL12 production from DCs activated with LPS/CD40L plus IFNγ was decreased in the NO_2-OA-treated group. These data demonstrate that decreases in DC activation caused by NO_2-OA may be translated to human DCs. Furthermore, NO_2-OA-dependent inhibition of DC activation may be dependent on IFNγ signaling.

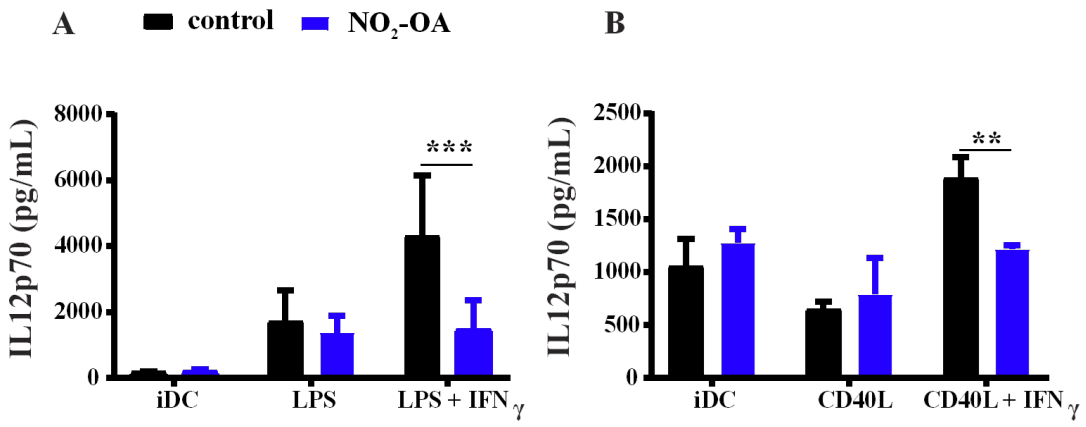

Figure 29: HuDC IL12 production is limited by NO_2-OA.

HuDCs were activated with LPS or CD40L with or without IFNγ and IL12p70 was measured from the media with ELISA. LPS data is combined from two independent experiments using two sets of DCs derived from different donors (n=5-6) while the CD40L data is from one experiment (n=3). **p<0.01, ***p<0.001 – normal, two-way ANOVA with multiple comparisons.

4.8 Discussion

DCs act as messengers between innate and adaptive immunity by detecting pathogens and tissue damage and presenting this signal to T and B lymphocytes [35, 248]. Upon activation, DCs will also exert their own defenses against inflammatory stimuli and alert innate immune cells

through the production of RS and pro-inflammatory cytokines like IL6, IL12, IL23, and IL1β [29, 249, 250]. At the center of an immune response, DCs are prime targets for therapeutics in a myriad of inflammatory diseases, including multiple sclerosis, influenza infection, and cancer [19, 23, 24, 251, 252]. In fact, DMF, an electrophilic α,β-unsaturated ketone, was recently approved for the treatment of MS and is known to limit DC activation, likely through the combination of altered metabolism, inhibition of NF-κB, and Nrf2 activation [37, 61, 96, 112, 166, 167, 170, 253, 254]. Electrophilic nitro-fatty acids limit inflammation at least in part to NF-κB inhibition and Nrf2 activation [133, 134, 145, 147]. Herein, we show evidence supporting that NO_2-OA, an exemplary nitro-fatty acid, inhibits DC activation. These results offer new insights into how nitro-fatty acids function in animal and human models of inflammatory disease as well as suggest a common role of electrophilic lipids to manipulate DC function.

To begin, BMDCs were harvested and matured in a manner similar to recent studies, confirming GM-CSF-induced CD11c+ cells are heterogenous (**Fig 17**) [46, 173]. There are clearly multiple CD11c+, CD11b+, MHCII+ "DC" populations when mouse bone marrow cells are differentiated for 5 days with GM-CSF (**Fig 17A-C, Fig 18**). In this study, BMDCs populations were defined as CD11c+, CD11b+, MHCII+ population for all flow cytometry experiments involving surface marker expression. NO_2-OA did not alter the cellular composition of GM-CSF-induced DC culture (**Fig 17A-C**). Moreover, NO_2-OA did not inhibit CD80 or CD86 expression in CD11c+CD11b+MHCII+ cells (referred to as DCs for the rest of the article, **Fig 17D, E**). Lastly, viability of GM-CSF-induced DCs was not impacted when NO_2-OA was added at the same time as GM-CSF (day 0 and day 3, **Fig 19 A**).

Next, the surface phenotype of LPS-activated DCs was evaluated upon NO_2-OA treatment (**Fig 20-23**). There were no significant differences in the cellular composition

(CD11c+CD11b+MHCII+) of DCs with increasing concentrations of NO_2-OA or the non-electrophilic lipid control, oleic acid (**Fig 22, Fig 23A-F**) at 6 or 24 hr after LPS administration and treatment. Although there were no significant differences between CD80, and CD86, decreases in CD40 expression were observed at 6 hr post LPS administration in CD40 with 2.5 NO_2-OA. The significant decreases of CD80 and CD86 at 5μM NO_2-OA may be attributed to a loss in viability of surrounding cells, but there were clear, dose-dependent trends in each marker (**Fig 20A-F**). However, all changes in surface marker phenotype were not sustained at 24 hr after treatment (**Fig 21A-F**). Together, these data suggest that NO_2-OA alters DC activation in a time-dependent manner without changing maturation.

DCs are primary responders to both DAMPs and PAMPs. Activation of DCs result in the production of pro-inflammatory cytokines in addition to RS. In corroboration with surface phenotype, NO_2-OA decreased the production of multiple cytokines (**Fig 24, 25**). Most cytokine levels were significantly decreased at 6 hr after treatment with 2.5 μM NO_2-OA while only IL6, IL12p70, and IL23p19 remained dampened at 24 hr (**Fig 24, 25**). The decreases observed with 1μM NO_2-OA were not statistically significant; however, they may suggest a dose-dependent response. TNFα levels were not altered with either concentration of NO_2-OA (data not shown). Together, these data provide evidence to support the claim that NO_2-OA can inhibition DC activation and signaling. Other lipid electrophiles such as 15d-PGJ_2 affect immune cells in a similar manner as well as the non-lipid electrophile, DMF, suggesting a common role amongst electrophiles to modulate immunity [37, 113, 142, 148].

The major antioxidant and cellular repair pathways mediated via Nrf2 signaling are becoming more important in the context of controlling inflammation [93, 103, 104, 255]. Many electrophilic lipids (e.g. 15-oxoETE, 15d-PGJ_2, nitro-fatty acids) are known activators of Nrf2 and

the non-lipid electrophile, DMF is FDA-approved treatment for MS (Tecfidera®) [38, 114, 134, 143, 148, 161, 256]. This study is the first to show NO_2-OA activates Nrf2 signaling in DCs (**Fig 26**). HO1 is induced as early as 3 hrs and NQO1 and GCLM are activated later and their levels are sustained for at least 24 hr (**Fig 26**). Moreover, NOS2 was inhibited 24 hr after treatment, suggesting NF-κB activity was suppressed (**Fig 26E**). These changes are consistent with a decade of studies in other cellular and animal models using NO_2-OA to decrease aspects of inflammation [116]. Changes in DC activation, along with Nrf2 activation and NOS2 inhibition, motivated an evaluation into DC metabolism, which is central to function.

Immunometabolism of macrophages and DCs is a rapidly growing field [47, 48, 51, 257]. Importantly, novel therapeutics are being designed to target the increased anaerobic metabolism that contributes to inflammation and cancer [258-261]. DMF was approved for treating MS and recent studies show that it can partially reverse the metabolic changes that accompany inflammation [61]. Furthermore, alterations in NF-κB or Nrf2 signaling can impact cellular metabolism [15, 101, 102, 106, 236]. DC metabolism was analyzed and LPS induced increases in lactate, itaconate, and succinate in DCs, confirming previous studies (**Fig 28A-C**) [262-265]. Interestingly, while NO_2-OA did not decrease lactate, succinate, or itaconate levels, glutamate and citrulline were decreased upon administration (**Fig 28**). A decrease in glutamate may signify a change in the glutamate/cystine transporter (xCT) that is regulated by Nrf2; however, future tests need to understand this further and measure glutathione and cystine levels [266, 267]. Changes in glutamate metabolism may effect DC activation in addition to downstream changes in T cell interactions, which need to be explored further [267, 268]. Decreases in citrulline verify a decrease in NOS2 expression; although, nitric oxide levels need to be analyzed in future studies to confirm inhibition in DCs.

Lastly, human DC IL12 production was also decreased with NO_2-OA suggesting this electrophilic lipid can play a role in human immunity (**Fig 29**). Interestingly, changes were only observed when cells were activated with both LPS and IFNγ in human DCs whereas significant changes were seen with only LPS in the murine DCs. Therefore, the role of NO_2-OA in IFNγ signaling will need to be further explored.

Future studies will examine the different CD11c+ cells subsets by sorting according to CD11b and MHCII and evaluate surface marker expression, cytokine production, and cellular metabolism in these specific subsets. This study analyzed early (6 hr) and late (24 hr) time points for flow and cytokine studies; however, more detailed, temporal analyses need to be performed, to better understand the sequence of cell signaling that occurs between NF-κB, Nrf2, and cellular metabolism. Lastly, T cell activation with or without DC involvement needs to be evaluated in the presence of NO_2-OA and will be the focus of future experiment. In conclusion, NO_2-OA is an effective inhibitor of DC activation and lays the groundwork for understanding the mechanism of action of NO_2-OA and other electrophilic lipids in the context of immunity.

5.0 Electrophilic lipids attenuate influenza pathogenesis

5.1 Introduction

Influenza A viruses (IAV) impose a significant burden on global health and economy. More than 250,000 deaths worldwide are reported annually and yearly costs attributed to IAV infection exceed $10 billion in the United States alone [269, 270]. Re-assortment of IAV's segmented genome and an error-prone RNA-dependent RNA polymerase increase the occurrence of mutations, promoting more facile zoonosis (e.g. H7N9, H5N1) and human-human transmission. Unlike seasonal IAV infection, severe IAV infection, from pandemic or zoonotic IAV strains, are resistant to tetravalent vaccines and antiviral agents [271, 272]. Furthermore, the incidence of highly pathogenic H7N9 avian influenza, omnipresent in migratory birds and poultry, led to over 650 deaths in 2013 and continues to pose a pandemic threat to humans [273, 274]. There have been four pandemics in the past century beginning with the 1918 Spanish Flu (H1N1) resulting in over 40 million deaths [269, 274, 275]. Pandemic IAV strains strongly promote pro-inflammatory cytokine and RS generation, leading to higher mortality than seasonal strains due to dysregulated inflammation (**Fig 30**) [276]. Lung injury occurs in response to neutrophil infiltration of the alveolar space, oxidative damage, and edema from disrupted tight junctions, leading to acute respiratory distress syndrome [16, 276-280]. Current strategies to alleviate the burden of IAV are not effective against pandemic strains and no drug strategies target the exacerbated host response [281-283]. Thus, new approaches to mitigate IAV pathogenesis are needed.

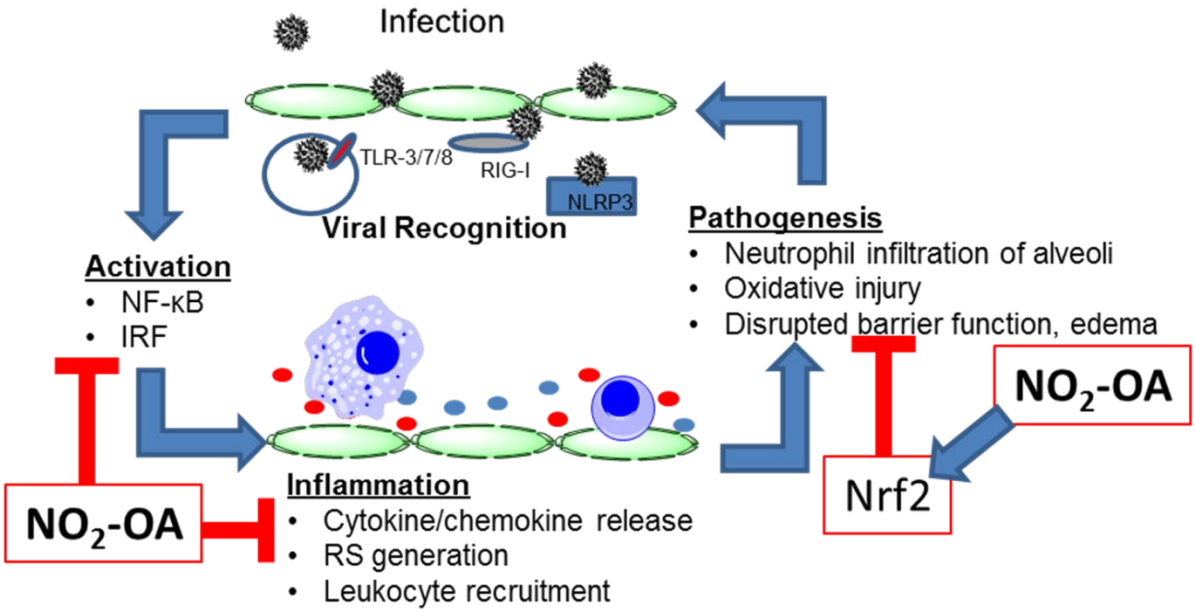

Figure 30: NO_2-OA can mitigate viral pathogenesis.

IAV is a segmented, negative stranded RNA orthomyxovirus that transcribes its genome in the nucleus [274, 284]. IAV stimulates both cytoplasmic (e.g. RIG-I, NLRP3) and endoplasmic (e.g. TLR3) pattern recognition receptors, leading to the production of cytokines and chemokines via nuclear factor kappa B (NF-κB) and interferon (IFN) response factors, igniting the innate immune response [285-290]. Viral proteins (e.g. hemagluttinin, HA) also play a role in perturbing the host-response. HA can overload translation machinery causing endoplasmic reticulum stress and production of RS [291, 292]. Basic polymerase (PB1-F2) and acid polymerase (PA-X) contribute to cell death and altered redox state in host cells [293-297]. Furthermore, Non structural protein 1 undermines the IFN response [298-300], with mutations in any one of these proteins increasing virulence [301]. Continual activation of the innate immune response from host and viral factors leads to a positive feedback response that enhances cytokine expression, RS production and infiltration of leukocytes promoting lung injury by evoking cell death, protein oxidation, and

damage to epithelial barriers [16, 275-277, 287, 302-306]. In severe cases (e.g. pandemics, elderly infection) these insults can lead to acute respiratory distress syndrome [277-279, 307]. Therefore, immunomodulatory agents that target an overwhelming host response have been gaining attention [308]. Examples include cyclooxygenase 2 (COX2) inhibitors [309, 310], suppression of RS generation [269, 282, 311-314], NOS2 inhibition [315], direct inhibition of NF-κB activation [316-319], and Nrf2 activation [320-323]. Electrophilic lipids broadly impact inflammation by covalently modifying regulatory proteins responsible for both propagating (e.g. NF-κB) and limiting (e.g. Nrf2) inflammatory injury [116, 145]. Due to a pleiotropic nature conferred by a high reactivity with functionally-significant cysteine moieties that regulate the transcriptional programs regulated by NF-κB and Nrf2, an electrophilic lipid-based therapeutic strategy designed to limit IAV-induced lung injury has strong merit.

NF-κB-mediated gene expression is inhibited via mechanisms involving Michael addition of the electrophilic fatty acid with nucleophilic Cys target residues [140, 164, 324, 325]. This in turn inhibits the expression of enzymes responsible for RS and lipid mediator release (e.g. NOS2 and COX2) and suppression of pro-inflammatory mediator expression (e.g. TNFα, MCP-1, IL-6) [116, 154, 164, 326-330]. Under basal conditions, Nrf2 is bound by Kelch-like ECH-associated protein 1 (Keap1), ubiquinylated, and degraded by the proteasome [331]. Keap1 Cys alkylation by electrophilic lipids induces Nrf2 release and subsequent nuclear translocation, where Nrf2 activates ARE-regulated expression of many cytoprotective proteins [145, 332]. Consequences of electrophilic lipid-mediated Nrf2 activation include increased a) biosythesis of GSH, b) expression of the antioxidant enzymes superoxide dismutase (SOD) and catalase and expression of the cytoprotective proteins NQO1 and HO1 [332]. Notably, the electrophilic lipid, NO_2-OA, decreases expression of the NF-κB target gene products TNFα, IL-6, and MCP1 [164, 333] and increases

Nrf2 target gene products NQO1 and HO-1 [145, 330, 334]. Other endogenous electrophilic lipids such as 15-oxoETE and 15d-PGJ_2 also activate Nrf2 and inhibit NF-κB via the same mechanisms [143, 164, 324]. Because of pleiotropic signaling properties, electrophilic lipids have the potential to abate the lung injury caused by an overzealous host response to IAV (**Fig 30**).

The synthetic electrophilic lipid, NO_2-OA, simultaneously activates Nrf2 and inhibits NF-κB signaling, has passed pre-clinical toxicology/pharmacokinetics testing following five FDA-approved early stage human safety/efficacy trials of both intravenous (IND 122583) and oral (IND 124524) formulations. Affirmation of Nrf2 and NF-κB pathway engagement in healthy obese humans also came from these Phase 1 trials. Lead drug candidates are now being evaluated by the Pitt-based Complexa, Inc. in FDA-approved Phase 2 trials in chronic lung and renal disorders. The experiments herein tested more acute applications of this lipid electrophile-based new drug strategy, with the objective of quickly translating pre-clinical studies into viable therapeutic trials. Electrophilic lipid-targetable pathways are critical in the pathogenesis of pandemic (pdmH1N1) [319, 321]. Excessive RS generation is associated with severe IAV pathogenesis and acute lung injury. In fact, suppression of the oxidant-producing enzymes NOX, NOS2, COX2, and XO increased survival in animal models [279, 309, 310, 312, 313, 315, 335-339]. Furthermore, alterations in redox state (e.g. via oxidative stress) are also attributed to enhanced IAV replication and GSH analogs were used to restore the reducing environment of epithelial cells [143, 292, 340-343] and decrease viral gene expression [292, 343-345]. Leukocyte infiltration, lung injury, and exacerbated cytokine production are associated with increased mortality and severe IAV infection, and are being evaluated as therapeutic targets [16, 19, 225, 279, 280, 304, 346-351]. Nrf2 activation strategies are also protective in cell models of IAV infection [320, 321] due to increased SOD, catalase and HO-1[352-355] and preservation of a reducing environment within cells by

increased expression of enzymes of GSH synthesis. Inhibition of the NF-κB signaling cascade limits several aspects of the IAV-induced adverse immune response since NF-κB is a key regulator of NOS2, COX2, and cytokine and chemokine production. The electrophilic lipid, 15d-PGJ_2 rescued mice from lethal IAV; however, its mechanism of action in the context of its electrophilic nature was not discussed [225]. Importantly, ablation of pro-inflammatory and RS-generating systems does not always negatively impact the host's ability to clear virus. Knockdown of type I IFN receptor paradoxically results in increased survival of mice infected with IAV [350, 356], and the same occurs with decreasing NOS2 or COX2 [309, 310, 339]. I hypothesized that electrophilic lipids will mitigate IAV-induced lung injury by promoting antioxidant responses and limiting inflammation.

5.2 Oral administration of NO_2-OA increase mouse survival during lethal influenza infection

Mice were infected with a lethal dose of influenza and treated with 25 mg/kg NO_2-OA, 60 mg/kg oseltamivir phosphate (Tamiflu), or vehicle control twice daily for 5 days after the infection starting 4 hr prior to infection (**Fig 31A**). Weight loss is shown as a percentage of original weight (**Fig 31B**). Remarkably, survival was significantly increased with NO_2-OA treatment (**Fig 31C**). Moreover, increases in survival were not accompanied with any significant changes in viral titer measured in BALF (**Fig 31D**). Together, these data show that NO_2-OA can improve mouse survival during lethal influenza infection without compromising viral clearance.

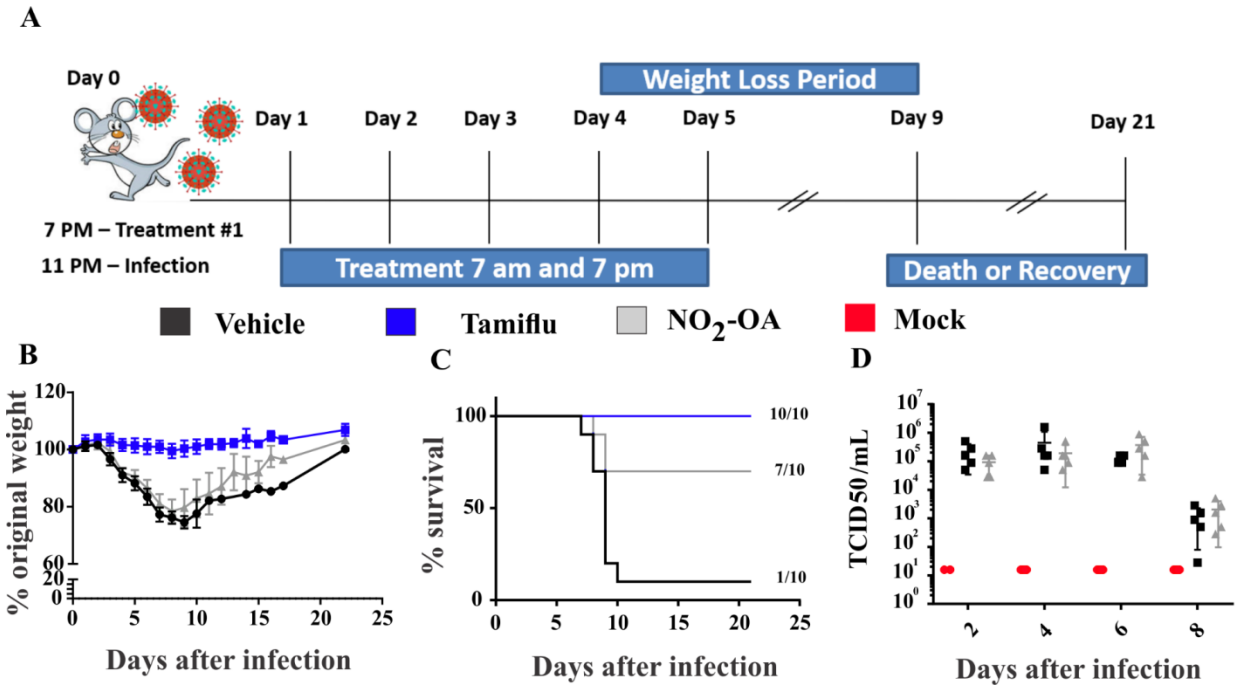

Figure 31: NO_2-OA increases survival of mice infected with lethal dose of influenza.

Female, Balb/cJ mice were infected with 300 TCID50 PR8, treated twice daily for 5 days after infection, and monitored for weight loss over time. Treatment regimen consisted of vehicle (glycerol trioleate), 60 mg/kg Tamiflu, or 25 mg/kg NO_2-OA (A). Weight loss (B) and survival (C) data are combined from two independent experiments (n=10). BALF titer is from a separate experiment in which mice were sacrificed on days 2, 4, 6, and 8 (n=5) in order to track viral load over time (D). SD is shown for weight loss and viral load. Significance for the survival study was determined using Log-rank (Mantel-Cox) test where p=.0092 between vehicle and NO_2-OA-treated groups (**).

5.3 NO_2-OA administration decreases cytokine production during influenza infection without completely suppressing immune responses

Cytokine responses were measured from BALF on days 2, 4, 6, and 8 after the infection (**Fig 32, 33**). No significant changes were seen in any cytokine measured 2 days after infection (**Fig 32, 33**). On day 4, GCSF and MCP1 were significantly decreased (**Fig 32G, I)**. Many changes were observed on day 6 including significant decreases in the production of IL4, IL10, IL12p70, MIP1β, TNFα, Eotaxin, MCP1, GM-CSF, G-CSF, and IFNγ (**Fig 32A-I, 33F**). Decreases in MIP1β, Eotaxin, and MCP1 were also observed 8 days after infection (**Fig 32D, F, G**). However, total suppression of cytokines did not occur since there was never a change in IL1β, MIP1α, or RANTES (**Fig 33A, B, D**). In fact, KC levels were increased on day 6 along with increases in KC, IL6, and IFNγ on day 8 **(Fig 33C, E, F**). Together these data suggest that NO_2-OA dampens inflammatory cytokine production during influenza infection without total suppression of the immune response.

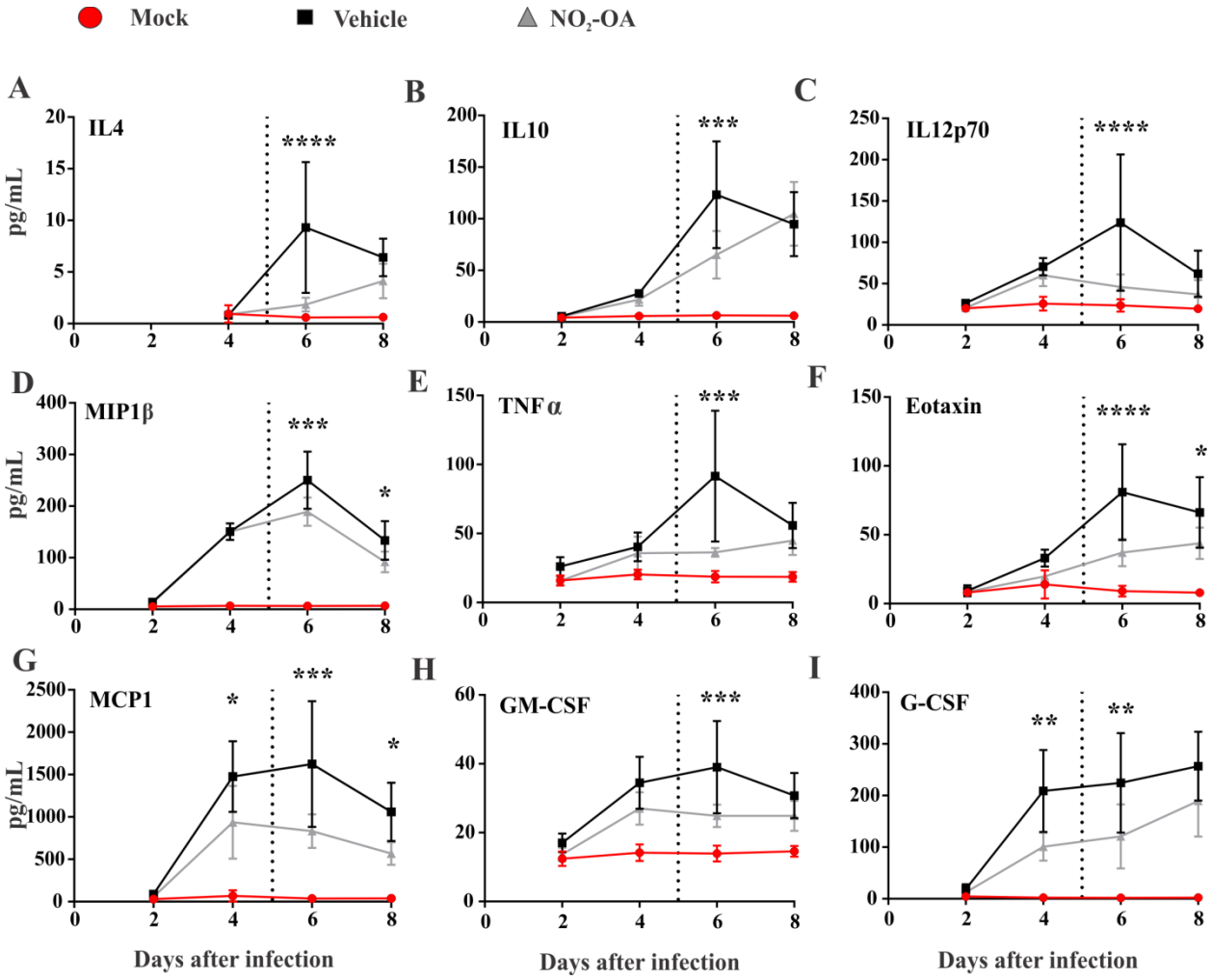

Figure 32: NO_2-OA decreases cytokine production during severe influenza infection.

Female, Balb/cJ mice were infected with a lethal dose of influenza (PR8 – 300 TCID50) and treated with 25 mg/kg NO_2-OA. Mock infected mice were given an intranasal injection of sterile PBS and vehicle mice were infected with PR8 and treated with glycerol trioleate. Treatment lasted 5 days and the dotted line in each graph represents the last day of treatment. BALF cytokines were measured and harvested on day 2, 4, 6, and 8 (n=5). Results are from one experiment. Significance was determined with a Two-way ANOVA where *p<0.05, **p<0.01, ***p<0.001, ****p<0.00001.

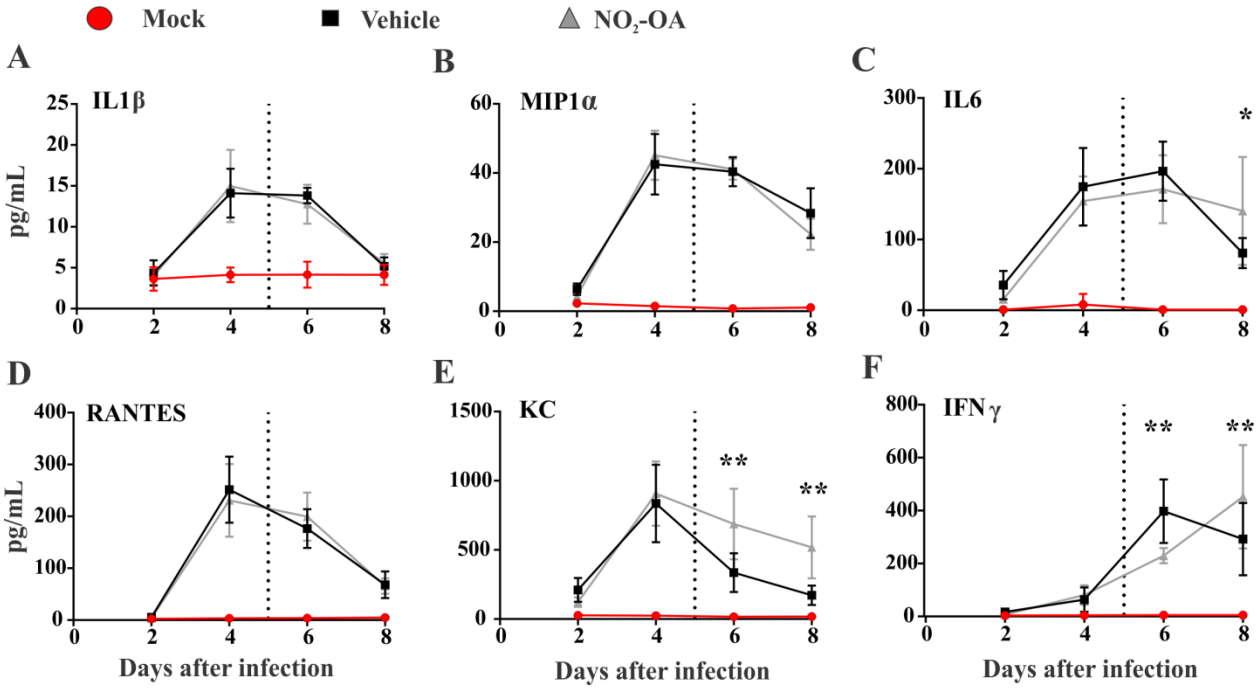

Figure 33: NO_2-OA cytokine effects do not result in total suppression of immune response.

Female, Balb/cJ mice were infected with a lethal dose of influenza (PR8 – 300 TCID50) and treated with 25 mg/kg NO_2-OA. Mock infected mice were given an intranasal injection of sterile PBS and vehicle mice were infected with PR8 and treated with glycerol trioleate. Treatment lasted 5 days and the dotted line in each graph represents the last day of treatment. BALF cytokines were measured and harvested on day 2, 4, 6, and 8 (n=5). Results are from one experiment. Significance was determined with a Two-way ANOVA where *p<0.05, **p<0.01, ***p<0.001, ****p<0.00001.

5.4 NO_2-OA decreases T cell recruitment without altering total cell count

Immune cell populations were analyzed from mouse BALF via flow cytometry on various days after infection and treatment (**Fig 34-37**). The gating strategy for innate immune cells is shown in **Fig 34, 35**. Living leukocytes (CD45+) cells were further gated according to CD11c and CD11b expression in order to distinguish myeloid and lymphoid subsets (**Fig 35**). Myeloid cells (CD11b+) consisted of mostly neutrophils (**Fig 35D**) along with TNFα and NOS2 producing DCs (TipDCs) (**Fig 35D**). It should be noted that without further markers (e.g. F4/80, Ly6c) these populations cannot be truly separated from interstitial macrophages and other inflammatory monocytes; however, TipDCs are prominent in influenza infection and would be included in this population [19, 357]. Lymphoid cells (CD11b- CD11c-) were then divided according to CD4 and CD8 expression (**Fig 35C**). Cells negative for CD11b, CD11c, CD4, and CD8 were then stratified with CD19 to identify B cells and possibly NK cells; however, CD49b would need to be included in future studies to validate NK populations (**Fig 35E**). It should also be noted that CD4 and CD8 populations are likely T cells but need further validation with CD3.

There were no differences in absolute cell count between vehicle and NO_2-OA-treated groups until 8 days after infection (**Fig 36B, C, 37A).** This change may be a reflection of significant decreases in both CD4 and CD8 T cells with the addition of NO_2-OA (**Fig 36H, I, 37D, E**). Interestingly, neutrophils and TipDCs were both increased on day 4 (**Fig 37B, C**).

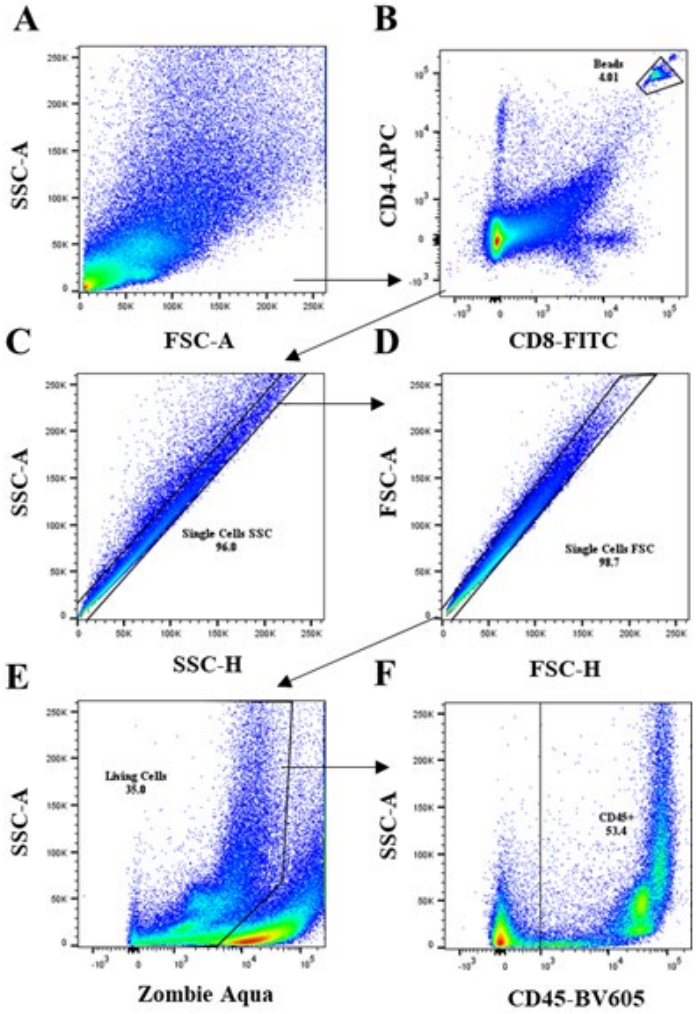

Figure 34: Gating strategy for influenza studies.

Granularity and size of cell populations are shown by SSC x FSC (A). Beads are highly fluorescent in ever channel and were gated according to APC and FITC (B) and then removed from subsequent analysis. Doublet exclusion based on SSC (C) and FSC (D) preceded live/dead analysis using Zombie Aqua (E). Living cells were then gated according to CD45 before characterizing more specific, leukocyte subsets (F). These data are from one experiment, representative of 5 mice per group.

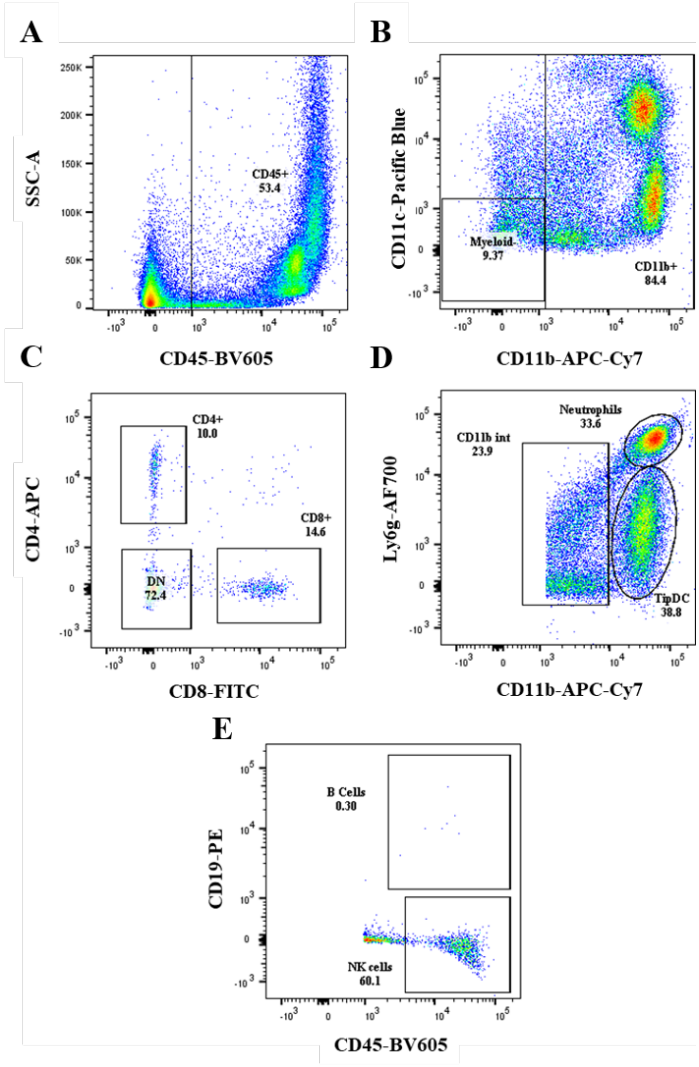

Figure 35: Gating strategy for individual leukocytes.

Living, CD45+ leukocytes (A) were gated according to CD11c and CD11b (B). Myeloid negative (CD11c- CD11b-) populations were further divided into CD4+ and CD8+ Cells (C). Myeloid cells were further divided into neutrophils (Ly6c+) and TipDCs (D). NK cells may be the CD19- arising from CD4 and CD8 double negative (DN) cells (E). These data are from one experiment, representative of 5 mice per group.

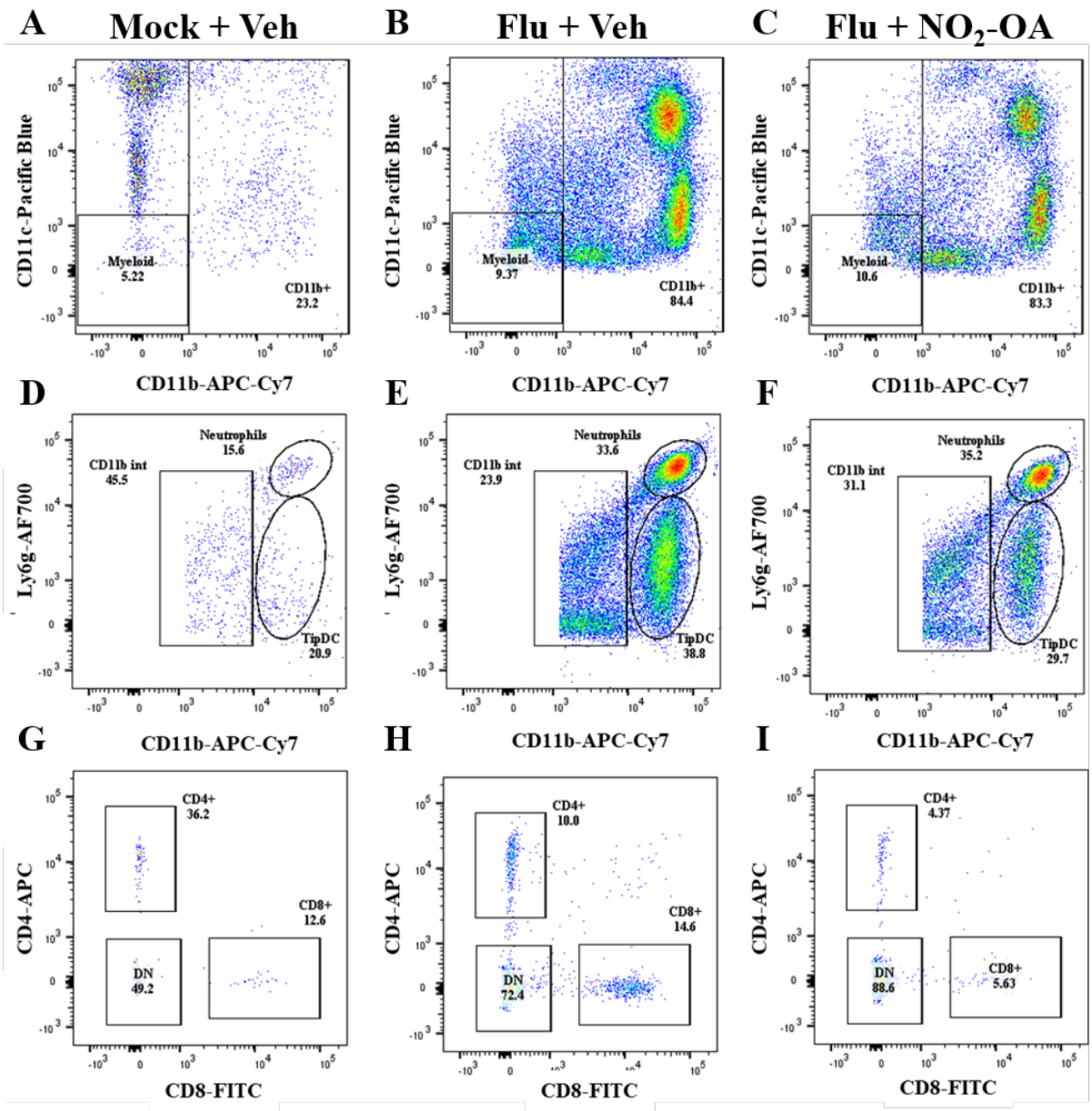

Figure 36: Flow cytometry analysis of cell subsets.

Gated populations are shown for mock + vehicle, flu + vehicle, and flu + NO_2-OA. Gating by CD11c x CD11b (A-C). Neutrophil and TipDC populations are shown (D-F). Pseudocolor plots of T cell counts (G-I). These data are from one experiment, representative of 5 mice per group.

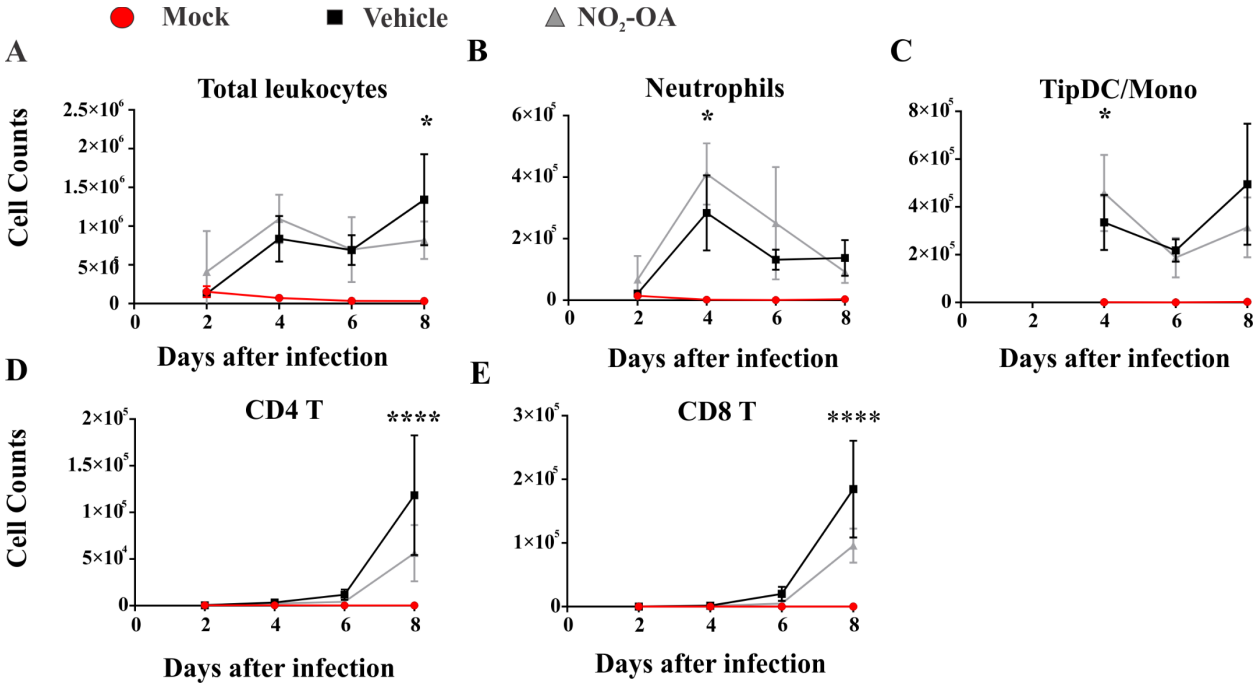

Figure 37: Absolute cell counts.

Total cell counts were evaluated by using Precision Count Beads (A). Neutrophils (CD11b+ Ly6g+), TipDC and other monocyte-derived cells (CD11b+ CD11c intermediate), CD4+ and CD8+ (CD11b- CD11c-) were all measured in BALF (B-E). Two-way ANOVA with Tukey's multiple comparisons was used to determine significance where *p<0.05, ****p<0.0001. These data are from one experiment with n=5.

5.5 Discussion

Influenza infection poses a significant threat to humanity and pathogenic strains (i.e. H5N1, H7N9) result in robust inflammatory responses that can lead to acute respiratory distress syndrome [20, 358-362]. Viral reassortment (antigenic shift) as well as accumulating mutations (antigen drift) in IAV strains make treatment difficult with current vaccine and antiviral strategies [274, 281, 363-367]. Moreover, excessive inflammation from the immune response is recalcitrant to antiviral treatment; therefore, novel strategies that target the host are being explored [212]. Examples include blocking TLR4 receptor signaling, activating Nrf2 responses, inhibiting NF-κB, and decreasing reactive oxygen and nitrogen species generation [19, 225, 255, 269, 282, 311-313, 315, 317, 319-321, 323, 336, 351, 352, 355, 368-372].

Electrophilic lipids, including NO_2-OA are known activators of Nrf2 and inhibit NF-κB responses [116]. Indeed, NO_2-OA increased the survival of mice infected with a lethal dose of IAV (**Fig 31**). Importantly, viral clearance was not affected as shown in the TCID50 measurements in **Fig 31D**. These results are similar to studies using 15d-PGJ_2, an electrophilic, α,β-unsaturated ketone, to ameliorate severe influenza infection [225]. It should be noted that NO_2-OA was added 4 hours prior to treatment in this model and future studies need to evaluate the efficacy when administered multiple days after infection – a time when antivirals become inefficient [338].

Oral administration of NO_2-OA decreased the production of multiple cytokines including, GM-CSF, G-CSF, TNFα, IL4, IL10, IL12p70, MCP1, MIP1β, IFNγ, and Eotaxin (**Fig 32**). However, not all cytokines were decreased (**Fig 33**). There were no changes in MIP1α, RANTES, or IL1β (**Fig 33A, B, D**). Interestingly, IL6 and KC were increased (**FIG 33C, E**) with NO_2-OA which is inconsistent with other *in vitro* and *in vivo* studies involving NO_2-OA [135, 245, 373]. Lastly, although IFNγ is decreased on day 6, day 8 levels are increased (**Fig 33F**). The differential

expression of cytokines could be due to the cessation of treatment on day 5. Specifically, in the case of IFNγ, it is possible that the effect of NO2-OA peaked around day 5/6 resulting in decreased production and then there was a rebounding effect that accounts for the increased production on day 8 (**Fig 33F**). Furthermore, each cytokine is likely regulated in a different manner via transcription, synthesis, and degradation – all of which could be affected by NO_2-OA to varying degrees.

Unlike a similar *in vivo* study using a zymosan-induced peritonitis model, NO_2-OA increased neutrophil recruitment (**FIG 37B**) [135]. I expected total cell recruitment to decrease in addition to neutrophils; however, this did not occur until day 8 with total cell recruitment (**Fig 37A**). Surprisingly, CD4+ and CD8+ T cells were significantly decreased with NO_2-OA treatment (**FIG 37D, E**). This is the first study to examine T cell recruitment with NO_2-OA delivery and I propose changes in DC activation are responsible. Although there were no significant changes in TipDC recruitment (**Fig 37C**), decreases in GM-CSF, G-CSF, MCP1, and IL12p70 could lead to altered monocyte recruitment, DC maturation and activation – all of which can impact T cell recruitment. Better flow cytometry with markers such as Ly6c, F4/80, CD103, CD80, CD40, and CD86 would provide more information regarding this proposal.

These studies were preliminary and need further optimization and analysis. The survival data shown here were repeated twice (n=10); however, cytokine and flow cytometry data are from one experiment. After these initial experiments, inconsistencies appeared in subsequent studies. A third attempt to repeat the survival data showed no significant changes. Further attempts were also made to repeat the T cell data but to no avail. These discrepancies could be due to inadequate verification of NO_2-OA (several different batches across several years). Moreover, freezer issues (-80C going down to -20C) resulted in moving IAV stocks between multiple freezers. Although,

stocks were propagated and TCID50 measurements were taken, other unknown effects may have occurred to the virus (e.g. sequence mutation) that contributed to the above reproducibility issues. Small sample size may also be an issue and I may have just observed a gradual regression to the mean. I believe that a new cyclodextrin-based delivery of NO_2-OA in the water may yield more consistent results. Lastly, better batch-to-batch LC/MS analysis needs to occur prior to treatment and influenza is now being stored in liquid nitrogen.

6.0 Final discussion and future directions

Inflammation is essential to our survival; however, aberrant immune responses contribute to a plethora of acute, chronic, and autoimmune diseases [374]. Severe infection, despite current antibiotic or antiviral therapies, often leads to irreversible organ damage (e.g. Sepsis, ARDS) due to excessive inflammation [20, 215, 287, 375-380]. Chronic inflammation from poor diet can lead to atherosclerosis and cardiac failure [3, 4, 15, 381-385]. Finally, autoimmune disorders are innately defined by aberrant inflammation – MS is a prime example of DC and T cells destroying the myelin sheath [23, 24, 231, 386-388]. Novel therapeutics, that dampen aberrant immune responses while maintaining necessary inflammation, are required to combat these diseases.

Our understanding of electrophilic lipid signaling is growing and it is clear that they are efficient immunomodulating agents. Two major classes of electrophilic lipids are the nitroalkenes and the α,β-unsaturated ketones – both with the ability to enhance the resolution of inflammation in addition to minimizing collateral damage from the original immune response [116, 131]. Electrophilic lipids have shown efficacy in a wide variety of inflammatory disease models including, acute lung injury caused by influenza infection, pulmonary hypertension, metabolic syndrome, and asthma [135, 137, 162, 222, 225, 389-391]. DMF (a non-lipid, electrophilic, α,β-unsaturated ketone) was recently approved for MS (Tecfidera®) and NO_2-OA (CXA-10) is in phase II clinical trials for pulmonary arterial hypertension, focal segmental glomerulosclerosis, and asthma (PRIMEx – NCT03449524, FIRSTx – NCT03422510, ALMA – NCT03680976). Moreover, this body of work, along with many others illustrate that electrophilic lipids are often formed *in vivo* during inflammation and likely play a central role in regulating immune responses [114, 115, 135, 392].

6.1 15-oxo-LXA_4, electrophilic metabolite of lipid mediator, LXA_4, is active

In chapter 3 of this dissertation, the activity of 15-oxo-LXA_4, the primary metabolite of LXA_4, was evaluated. I concluded that 15-oxo-LXA_4 was efficient in inhibiting aspects of LPS-induced activation of a murine macrophage cell line (**Fig 8**). Furthermore, 15-oxo-LXA_4 activated Nrf2-dependent target genes (**Fig 10**). The inhibition of pro-inflammatory gene expression and the induction of Nrf2 target genes were independent of the proposed receptor for the parent lipid, LXA_4 (**Fig 12**). This was the first study to ever evaluate either LXA_4 or 15-oxo-LXA_4 in RAW murine macrophages activated via LPS. Importantly, these data contradict the one study that demonstrated a lack of 15-oxo-LXA_4 activity in human neutrophils; however, the minimal 15-oxo-LXA_4 binding to FPR2 is consistent [165]. Differences between studies may be the result of using different cell lines but illustrate that further studies need to evaluate both LXA_4 and its metabolite, 15-oxo-LXA_4, to better understand their combined pharmacology.

Demonstrating that 15-oxo-LXA_4 is indeed active and, in fact, displays similar anti-inflammatory and pre-resolving properties of its parent lipid, LXA_4, begs the question: to what extent can the profound cellular effects of pro-resolving lipid mediators be attributed to their electrophilic metabolites? Of the 4 classes of specialized pro-resolving mediators identified (Lipoxins, Resolvins, Maresins, and Protectins) and decades of research, less than 10 studies measured their electrophilic metabolites, let alone analyzed their potential activity [165, 199, 200, 204, 230, 393]. Resolvins are further oxidized to 18-oxoRvE1, 12-oxoRvE1, 8-oxoRvD1, and 17-oxoRvD1 [229, 394]. Interestingly, 8-oxoRvD1 was just as effective as RvD1 in reducing PMN infiltration [229]. Furthermore, Maresin is metabolized into 14-oxoMaR1, but only one study evaluated its activity and concluded it is inactive [395]. Future studies need to evaluate both the electrophilic metabolite and the parent lipid to fully understand the immunomodulatory effects

seen in cell and animal studies. In depth LC/MS pharmacokinetics studied need to be performed in animal models using pro-resolving lipid mediators to characterize electrophilic lipid formation. Lastly, measures need to be taken (e.g. enzyme inhibition, receptor knock-out) to separate the effects of the parent lipid and electrophilic metabolite in cell and animal models.

In regards to 15-oxo-LXA_4, other models of inflammation need to be examined to confirm its anti-inflammatory and cytoprotective roles in immunity. This study only examined RAW macrophages but THP1 (human monocyte) cells are another great introductory model for basic inflammation studies. Then, primary cell models (e.g. bone marrow derived macrophages) need to be evaluated and finally, animal models can be used to compare 15-oxo-LXA_4 efficacy to that of LXA_4. The challenge in using an animal model will be synthesizing 15-oxo-LXA_4 to sufficient quantities. Due to their ability to alkylate proteins, bind glutathione, and even incorporate into lipid membranes – electrophilic lipids notoriously require higher doses to achieve intracellular quantities sufficient to signal [114, 396].

In addition to evaluating the major effects of 15-oxo-LXA_4 in multiple models of inflammation, a deeper understanding of its mechanism of action is required. Many electrophilic lipids (e.g. DMF, nitroalkenes) are known to alkylate NF-κB and Keap1 resulting in the inhibition of pro-inflammatory gene expression and activation of Nrf2, respectfully [116]. No study has determined if 15-oxo-LXA_4 alkylates proteins in a manner similar to other electrophilic lipids. In **Fig 7**, I demonstrate 15-oxo-LXA_4 forms a glutathione adduct; however, further studies can better characterize the fragmentation pattern of this species to confirm the adduct is covalent. Proteomic studies after immunoprecipitation experiments may better identify protein targets for 15-oxo-LXA_4 and confirm alkylation events. Moreover, novel click chemistry techniques are evolving that may "trap" electrophile-protein adducts, and evaluate them using LC/MS-based proteomics [233,

234, 397]. Although the observable effects are very similar, 15-oxo-LXA_4 could inhibit inflammation through a separate mechanism. Furthermore, genetic models such as $Keap1^{-/-}$ and $Nrf2^{-/-}$ could confirm Nrf2 activation seen in this study.

6.2 NO_2-OA alters DC Immunity

Chapter 4 of this dissertation demonstrated that NO_2-OA, an electrophilic nitroalkene, inhibits several aspects of DC activation. In addition to the canonical pro-inflammatory cytokines (e.g. IL6, MCP1), NO_2-OA inhibited the production of IL12p70 and IL23p19, two major cytokines linked to DC activation (**Fig 24, 25**). Moreover, the surface marker expression of CD40, CD80, and CD86 was also suppressed upon NO_2-OA administration during LPS-induced activation (**Fig 20**). This study is in line with similar research that examined nitroalkene pharmacodynamics in BMDCs in addition to BMDMs. Myself and colleagues demonstrated that IFN signaling was dampened upon treatment with NO_2-OA or NO_2-cLA in BMDMs stimulated with dsDNA or herpes simplex virus [115]. Moreover, IL6 production in BMDCs was decreased with NO_2-cLA treatment; however, DC-specific cytokines and surface marker phenotype were not evaluated. Together these results suggest DC activation is altered by nitroalkenes and they may act as novel therapeutics for diseases with a DC component – much like MS.

The NO_2-OA related effects on DC immunity mentioned above are currently attributed to a combination of at least Nrf2 activation and NF-κB inhibition. Both pathways are critical in the regulation of immunity in addition to DC function [99, 398]. The results at the end of this study demonstrate that target genes of Nrf2 were indeed activated by NO_2-OA (**Fig 26**). Furthermore, NOS2, a gene regulated by NF- κB was also inhibited (**Fig 26**). These results are consistent with

other electrophilic lipids such as 15d-PGJ_2 and 15-oxoETE [113, 142-144, 147-149, 226].Together these data reinforce the fact that electrophilic lipids may, as a class, act as efficient immunomodulators and be effective therapeutics for a myriad of inflammatory diseases. However, deeper mechanistic understanding is required.

Assays designed to validate the involvement of NF-κB and Nrf2 are needed. Examples include luciferase assays, western blots focused on nuclear translocation, genetic knock-out models, and LC/MS proteomic studies to confirm alkylation of each target by NO_2-OA. Cytokines are regulated by transcription factors other than NF-κB, such as activating protein 1 (AP1), IRFs, and PU.1 – none of which have every been directly evaluated during NO_2-OA administration. Differential targeting of transcription factors, in addition to time of sampling, may explain why some cytokines were altered and some were not at 6 and 24 hr. Furthermore, better temporal studies (i.e. before 6 hr and in between 6-24 hr) to better understand changes in cytokine production and surface marker expression. The same can be said for evaluating DC metabolism. I only looked at a few metabolites at 12 hr after treatment – more detailed analyses can be performed early and later during treatment. Lastly, a full pharmacokinetic study in DCs needs to take place to characterize the metabolism and half-life of NO_2-OA. Together, these experiments would add key mechanistic insight into how NO_2-OA and other electrophilic lipids can alter DC activation.

6.3 Electrophilic lipids play a role in viral pathogenesis

Myself and colleagues from Denmark were the first to demonstrate that viral-induced inflammation can result in electrophilic, nitroalkene formation [115]. Several electrophilic, α,β-unsaturated ketones (e.g. 13-oxoODE, 5-oxoETE) were reported to form during influenza infection; however, their electrophilic nature was not discussed [346, 399]. Most viral infections induce NOS2 and NOX enzymes that generate reactive oxygen and nitrogen species [22, 370, 400]. Moreover, during inflammation, cell membranes release unsaturated fatty acids that are prone to oxidation and nitration reactions that occur from the reactions described in the introduction of this dissertation. Furthermore, hydroxylated fatty acids derived from COX and LOX-dependent oxygenation of arachidonic acid and other unsaturated fatty acids are reported to form during the resolution of inflammation. Many of these lipids are likely metabolized into electrophilic lipids in a similar manner as reported for LXA_4 in Chapter 3 of this dissertation. Thus, the inflammatory environment is ideal for electrophilic lipid generation and future studies need to confirm their formation in a variety of viral infections.

The formation of electrophilic lipids during viral infection is remarkable because decades of studies have shown how these species can manipulate immune responses. In this report NO_2-OA was shown to inhibit cytokine responses and promote mouse survival in a lethal IAV infection model (**Fig 31-33**). Furthermore, Chapter 4 demonstrates how electrophilic lipids can inhibit DC activation, which may play a role in decreasing T cell recruitment in the influenza model (**Fig 36, 37**). These actions likely result from an accumulation of alkylation events that alter regulatory protein function. For instance, NF-κB is a known target for various electrophilic lipids and is essential in most immune cell signaling cascades [15, 37, 108, 109, 112, 113]. Nrf2 activation is also a target for electrophilic lipid-based alkylation and may regulate NF-κB as well [38, 93, 95,

98, 103, 134, 143, 145, 148, 169, 255, 320, 321, 398, 401, 402]. Additionally, electrophilic lipids will bind glutathione and can alter the redox state, another important factor in cellular outcome during infection [246, 297, 403-405].

6.4 A word on specificity

Clearly, a major limitation to studies involving electrophilic lipids is addressing the specificity. Gaining a complete knowledge of specificity will be difficult for the following reasons. First, hundreds of different proteins have cysteines that have the potential to form Michael adducts with electrophilic lipids (let alone histidine or lysine residues that can also be modified). Second, the availability of these cysteines will depend on the redox environment of the cell and vary according to protein structure and concentration. For instance, the tendency of an electrophilic lipid to form a cysteine adduct will depend on the pKa of that particular cysteine [224]. Furthermore, as the concentration of proteins change (e.g. NF-κB levels rise and fall during immune responses along with Nrf2), it is likely that electrophilic targets will change. The same applied to the redox state of the cell, which is highly dependent on GSH concentrations – a prime target of Michael adduct formation. Third, each point listed above will change during the course of an immune response and is likely cell and tissue-dependent. Lastly, electrophilic metabolism will play a role in specificity since some metabolites retain their electrophilicity and may occupy protein targets. Therefore, to truly ascertain target specificity, one must perform full detailed, temporal studies that analyze 1) GSH/GSSG levels and other aspects of redox state (e.g. NADPH/NADP+); 2) pharmacokinetics of the electrophilic lipid via LC/MS, 3) the levels of all proteins containing cysteines within the cell (as well as a proteomic analysis of electrophile

adducts), and 4) the response being analyzed. This is an extremely (if not impossible) task at this point.

Strides are being made in methods designed to detect protein adducts with electrophiles [122, 233, 234, 397]. These techniques, combined with LC/MS-based approaches can begin to tease apart mechanisms of action and specificity when combined with other molecular analyses. For example, take the LPS-induced activation model above, in RAW cells. A new study can focus on the first 6 hr of LPS and NO_2-OA treatment by taking samples every 30 minutes. At each time point, analyze cytokine production, pro-inflammatory gene and protein expression, GSH/GSSG ratio, and electrophile adducts. Each one of these experiments would have to be performed independently because you cannot use the same sample for PCR as western blot or for ELISA for LC/MS. These types of studies would then have to be carried out for the duration of the immune response and in each cell of interest. Only then, can an absolute specificity begin to be addressed.

6.5 Final remarks

In conclusion, electrophilic lipids are relevant immunomodulators. These species are formed during inflammation, augment immunological responses, bolster cellular recovery, and minimize tissue damage. In these studies, I show that a common class of pro-resolving lipid mediators (Lipoxins) are metabolized into electrophilic, α,β-unsaturated ketones that contribute to their anti-inflammatory and cytoprotective responses. Furthermore, DC activation is inhibited by NO_2-OA, in addition to other electrophilic lipids, demonstrating these class of potential therapeutics can alter both innate and adaptive immunity. Finally, I show how NO_2-OA can improve the survival of mice in model of influenza-induced acute lung injury. With more

mechanistic and pharmacological studies, electrophilic lipids have the potential to stave off diseases with a major inflammatory component – acute, chronic, or autoimmune.

Bibliography

1. Chen, G.Y. and G. Nunez, *Sterile inflammation: sensing and reacting to damage.* Nat Rev Immunol, 2010. **10**(12): p. 826-37.
2. Bennett, J.M., et al., *Inflammation-Nature's Way to Efficiently Respond to All Types of Challenges: Implications for Understanding and Managing "the Epidemic" of Chronic Diseases.* Front Med (Lausanne), 2018. **5**: p. 316.
3. Hotamisligil, G.S., *Inflammation, metaflammation and immunometabolic disorders.* Nature, 2017. **542**(7640): p. 177-185.
4. Kotas, M.E. and R. Medzhitov, *Homeostasis, inflammation, and disease susceptibility.* Cell, 2015. **160**(5): p. 816-827.
5. Chovatiya, R. and R. Medzhitov, *Stress, inflammation, and defense of homeostasis.* Mol Cell, 2014. **54**(2): p. 281-8.
6. Medzhitov, R., *Origin and physiological roles of inflammation.* Nature, 2008. **454**(7203): p. 428-35.
7. Akira, S., *Innate immunity to pathogens: diversity in receptors for microbial recognition.* Immunol Rev, 2009. **227**(1): p. 5-8.
8. Takeuchi, O. and S. Akira, *Innate immunity to virus infection.* Immunol Rev, 2009. **227**(1): p. 75-86.
9. Akira, S., *Pathogen recognition by innate immunity and its signaling.* Proc Jpn Acad Ser B Phys Biol Sci, 2009. **85**(4): p. 143-56.
10. Kumar, H., T. Kawai, and S. Akira, *Pathogen recognition in the innate immune response.* Biochem J, 2009. **420**(1): p. 1-16.
11. Kono, H., et al., *Uric acid promotes an acute inflammatory response to sterile cell death in mice.* J Clin Invest, 2010. **120**(6): p. 1939-49.
12. Alvarez, F., et al., *The alarmins IL-1 and IL-33 differentially regulate the functional specialisation of Foxp3(+) regulatory T cells during mucosal inflammation.* Mucosal Immunol, 2019. **12**(3): p. 746-760.

13. Bertheloot, D. and E. Latz, *HMGB1, IL-1alpha, IL-33 and S100 proteins: dual-function alarmins.* Cell Mol Immunol, 2017. **14**(1): p. 43-64.

14. Taniguchi, K. and M. Karin, *NF-kappaB, inflammation, immunity and cancer: coming of age.* Nat Rev Immunol, 2018. **18**(5): p. 309-324.

15. Tornatore, L., et al., *The nuclear factor kappa B signaling pathway: integrating metabolism with inflammation.* Trends Cell Biol, 2012. **22**(11): p. 557-66.

16. Liu, Q., Y.H. Zhou, and Z.Q. Yang, *The cytokine storm of severe influenza and development of immunomodulatory therapy.* Cell Mol Immunol, 2016. **13**(1): p. 3-10.

17. Dennis, E.A. and P.C. Norris, *Eicosanoid storm in infection and inflammation.* Nat Rev Immunol, 2015. **15**(8): p. 511-23.

18. Guo, X.J. and P.G. Thomas, *New fronts emerge in the influenza cytokine storm.* Semin Immunopathol, 2017. **39**(5): p. 541-550.

19. Aldridge, J.R., Jr., et al., *TNF/iNOS-producing dendritic cells are the necessary evil of lethal influenza virus infection.* Proc Natl Acad Sci U S A, 2009. **106**(13): p. 5306-11.

20. Short, K.R., et al., *Pathogenesis of influenza-induced acute respiratory distress syndrome.* Lancet Infect Dis, 2014. **14**(1): p. 57-69.

21. Narasaraju, T., et al., *Excessive neutrophils and neutrophil extracellular traps contribute to acute lung injury of influenza pneumonitis.* Am J Pathol, 2011. **179**(1): p. 199-210.

22. Akaike, T., et al., *Pathogenesis of influenza virus-induced pneumonia: involvement of both nitric oxide and oxygen radicals.* Proc Natl Acad Sci U S A, 1996. **93**(6): p. 2448-53.

23. Ganguly, D., et al., *The role of dendritic cells in autoimmunity.* Nat Rev Immunol, 2013. **13**(8): p. 566-77.

24. Dendrou, C.A., L. Fugger, and M.A. Friese, *Immunopathology of multiple sclerosis.* Nat Rev Immunol, 2015. **15**(9): p. 545-58.

25. Cella, M., et al., *Inflammatory stimuli induce accumulation of MHC class II complexes on dendritic cells.* Nature, 1997. **388**(6644): p. 782-7.

26. Savina, A. and S. Amigorena, *Phagocytosis and antigen presentation in dendritic cells.* Immunol Rev, 2007. **219**: p. 143-56.

27. Merad, M., et al., *The dendritic cell lineage: ontogeny and function of dendritic cells and their subsets in the steady state and the inflamed setting.* Annu Rev Immunol, 2013. **31**: p. 563-604.

28. Lutz, M.B., et al., *An advanced culture method for generating large quantities of highly pure dendritic cells from mouse bone marrow.* J Immunol Methods, 1999. **223**(1): p. 77-92.

29. Krawczyk, C.M., et al., *Toll-like receptor-induced changes in glycolytic metabolism regulate dendritic cell activation.* Blood, 2010. **115**(23): p. 4742-9.

30. Everts, B., et al., *Commitment to glycolysis sustains survival of NO-producing inflammatory dendritic cells.* Blood, 2012. **120**(7): p. 1422-31.

31. Everts, B., et al., *TLR-driven early glycolytic reprogramming via the kinases TBK1-IKKvarepsilon supports the anabolic demands of dendritic cell activation.* Nat Immunol, 2014. **15**(4): p. 323-32.

32. Guermonprez, P., et al., *Antigen presentation and T cell stimulation by dendritic cells.* Annu Rev Immunol, 2002. **20**: p. 621-67.

33. Ng, S.L., et al., *Type 1 Conventional CD103(+) Dendritic Cells Control Effector CD8(+) T Cell Migration, Survival, and Memory Responses During Influenza Infection.* Front Immunol, 2018. **9**: p. 3043.

34. Patente, T.A., L.R. Pelgrom, and B. Everts, *Dendritic cells are what they eat: how their metabolism shapes T helper cell polarization.* Curr Opin Immunol, 2019. **58**: p. 16-23.

35. Kreutz, M., P.J. Tacken, and C.G. Figdor, *Targeting dendritic cells--why bother?* Blood, 2013. **121**(15): p. 2836-44.

36. Ghoreschi, K., et al., *Fumarates improve psoriasis and multiple sclerosis by inducing type II dendritic cells.* J Exp Med, 2011. **208**(11): p. 2291-303.

37. Peng, H., et al., *Dimethyl fumarate inhibits dendritic cell maturation via nuclear factor kappaB (NF-kappaB) and extracellular signal-regulated kinase 1 and 2 (ERK1/2) and mitogen stress-activated kinase 1 (MSK1) signaling.* J Biol Chem, 2012. **287**(33): p. 28017-26.

38. Hammer, A., et al., *Role of Nuclear Factor (Erythroid-Derived 2)-Like 2 Signaling for Effects of Fumaric Acid Esters on Dendritic Cells.* Front Immunol, 2017. **8**: p. 1922.

39. Hume, D.A., *Differentiation and heterogeneity in the mononuclear phagocyte system.* Mucosal Immunol, 2008. **1**(6): p. 432-41.

40. Shi, C. and E.G. Pamer, *Monocyte recruitment during infection and inflammation.* Nat Rev Immunol, 2011. **11**(11): p. 762-74.

41. Guilliams, M., B.N. Lambrecht, and H. Hammad, *Division of labor between lung dendritic cells and macrophages in the defense against pulmonary infections.* Mucosal Immunol, 2013. **6**(3): p. 464-73.

42. Kelly, B. and L.A. O'Neill, *Metabolic reprogramming in macrophages and dendritic cells in innate immunity.* Cell Res, 2015. **25**(7): p. 771-84.

43. Collin, M. and V. Bigley, *Human dendritic cell subsets: an update.* Immunology, 2018. **154**(1): p. 3-20.

44. Chow, K.V., et al., *Heterogeneity, functional specialization and differentiation of monocyte-derived dendritic cells.* Immunol Cell Biol, 2017. **95**(3): p. 244-251.

45. Na, Y.R., et al., *GM-CSF Grown Bone Marrow Derived Cells Are Composed of Phenotypically Different Dendritic Cells and Macrophages.* Mol Cells, 2016. **39**(10): p. 734-741.

46. Helft, J., et al., *GM-CSF Mouse Bone Marrow Cultures Comprise a Heterogeneous Population of CD11c(+)MHCII(+) Macrophages and Dendritic Cells.* Immunity, 2015. **42**(6): p. 1197-211.

47. Lee, Y.S., J. Wollam, and J.M. Olefsky, *An Integrated View of Immunometabolism.* Cell, 2018. **172**(1-2): p. 22-40.

48. Pearce, E.J. and E.L. Pearce, *Immunometabolism in 2017: Driving immunity: all roads lead to metabolism.* Nat Rev Immunol, 2017.

49. O'Neill, L.A., R.J. Kishton, and J. Rathmell, *A guide to immunometabolism for immunologists.* Nat Rev Immunol, 2016. **16**(9): p. 553-65.

50. Rambold, A.S. and E.L. Pearce, *Mitochondrial Dynamics at the Interface of Immune Cell Metabolism and Function.* Trends Immunol, 2018. **39**(1): p. 6-18.

51. Buck, M.D., et al., *Metabolic Instruction of Immunity.* Cell, 2017. **169**(4): p. 570-586.

52. Stienstra, R., et al., *Specific and Complex Reprogramming of Cellular Metabolism in Myeloid Cells during Innate Immune Responses.* Cell Metab, 2017. **26**(1): p. 142-156.

53. Menk, A.V., et al., *Early TCR Signaling Induces Rapid Aerobic Glycolysis Enabling Distinct Acute T Cell Effector Functions.* Cell Rep, 2018. **22**(6): p. 1509-1521.

54. O'Neill, L.A. and E.J. Pearce, *Immunometabolism governs dendritic cell and macrophage function.* J Exp Med, 2016. **213**(1): p. 15-23.

55. Huang, S.C., et al., *Metabolic Reprogramming Mediated by the mTORC2-IRF4 Signaling Axis Is Essential for Macrophage Alternative Activation.* Immunity, 2016. **45**(4): p. 817-830.

56. Pearce, E.J. and B. Everts, *Dendritic cell metabolism.* Nat Rev Immunol, 2015. **15**(1): p. 18-29.

57. Nagy, C. and A. Haschemi, *Time and Demand are Two Critical Dimensions of Immunometabolism: The Process of Macrophage Activation and the Pentose Phosphate Pathway.* Front Immunol, 2015. **6**: p. 164.

58. Pearce, E.L. and E.J. Pearce, *Metabolic pathways in immune cell activation and quiescence.* Immunity, 2013. **38**(4): p. 633-43.

59. Buck, M.D., D. O'Sullivan, and E.L. Pearce, *T cell metabolism drives immunity.* J Exp Med, 2015. **212**(9): p. 1345-60.

60. Huang, S.C., et al., *Cell-intrinsic lysosomal lipolysis is essential for alternative activation of macrophages.* Nat Immunol, 2014. **15**(9): p. 846-55.

61. Kornberg, M.D., et al., *Dimethyl fumarate targets GAPDH and aerobic glycolysis to modulate immunity.* Science, 2018. **360**(6387): p. 449-453.

62. Millet, P., et al., *GAPDH Binding to TNF-alpha mRNA Contributes to Posttranscriptional Repression in Monocytes: A Novel Mechanism of Communication between Inflammation and Metabolism.* J Immunol, 2016. **196**(6): p. 2541-51.

63. Amiel, E., et al., *Mechanistic target of rapamycin inhibition extends cellular lifespan in dendritic cells by preserving mitochondrial function.* J Immunol, 2014. **193**(6): p. 2821-30.

64. Bekkering, S., et al., *Metabolic Induction of Trained Immunity through the Mevalonate Pathway.* Cell, 2018. **172**(1-2): p. 135-146 e9.

65. Byles, V., et al., *The TSC-mTOR pathway regulates macrophage polarization.* Nat Commun, 2013. **4**: p. 2834.

66. Chen, C., et al., *TSC-mTOR maintains quiescence and function of hematopoietic stem cells by repressing mitochondrial biogenesis and reactive oxygen species.* J Exp Med, 2008. **205**(10): p. 2397-408.

67. Cheng, S.C., et al., *mTOR- and HIF-1alpha-mediated aerobic glycolysis as metabolic basis for trained immunity.* Science, 2014. **345**(6204): p. 1250684.

68. Delgoffe, G.M., et al., *The mTOR kinase differentially regulates effector and regulatory T cell lineage commitment.* Immunity, 2009. **30**(6): p. 832-44.

69. Delgoffe, G.M. and J.D. Powell, *mTOR: taking cues from the immune microenvironment.* Immunology, 2009. **127**(4): p. 459-65.

70. Jones, R.G. and E.J. Pearce, *MenTORing Immunity: mTOR Signaling in the Development and Function of Tissue-Resident Immune Cells.* Immunity, 2017. **46**(5): p. 730-742.

71. Linke, M., et al., *mTORC1 and mTORC2 as regulators of cell metabolism in immunity.* FEBS Lett, 2017. **591**(19): p. 3089-3103.

72. Shi, L.Z., et al., *HIF1alpha-dependent glycolytic pathway orchestrates a metabolic checkpoint for the differentiation of TH17 and Treg cells.* J Exp Med, 2011. **208**(7): p. 1367-76.

73. Snyder, J.P. and E. Amiel, *Regulation of Dendritic Cell Immune Function and Metabolism by Cellular Nutrient Sensor Mammalian Target of Rapamycin (mTOR).* Front Immunol, 2018. **9**: p. 3145.

74. Sukhbaatar, N., M. Hengstschlager, and T. Weichhart, *mTOR-Mediated Regulation of Dendritic Cell Differentiation and Function.* Trends Immunol, 2016. **37**(11): p. 778-789.

75. Sun, Q., et al., *Mammalian target of rapamycin up-regulation of pyruvate kinase isoenzyme type M2 is critical for aerobic glycolysis and tumor growth.* Proc Natl Acad Sci U S A, 2011. **108**(10): p. 4129-34.

76. Weichhart, T., et al., *The TSC-mTOR signaling pathway regulates the innate inflammatory response.* Immunity, 2008. **29**(4): p. 565-77.

77. McCarthy, S.A., et al., *Metabolic reprogramming of the immune response in the tumor microenvironment.* Cancer Biol Ther, 2013. **14**(4): p. 315-8.

78. Serhan, C.N., *Discovery of specialized pro-resolving mediators marks the dawn of resolution physiology and pharmacology.* Mol Aspects Med, 2017. **58**: p. 1-11.

79. Arita, M., *Mediator lipidomics in acute inflammation and resolution.* J Biochem, 2012. **152**(4): p. 313-9.

80. Fullerton, J.N. and D.W. Gilroy, *Resolution of inflammation: a new therapeutic frontier.* Nat Rev Drug Discov, 2016. **15**(8): p. 551-67.

81. Perretti, M., *The resolution of inflammation: New mechanisms in patho-physiology open opportunities for pharmacology.* Semin Immunol, 2015. **27**(3): p. 145-8.

82. Serhan, C.N., et al., *Resolution of inflammation: state of the art, definitions and terms.* FASEB J, 2007. **21**(2): p. 325-32.

83. Sugimoto, M.A., et al., *Resolution of Inflammation: What Controls Its Onset?* Front Immunol, 2016. **7**: p. 160.

84. Itoh, K., et al., *Keap1 regulates both cytoplasmic-nuclear shuttling and degradation of Nrf2 in response to electrophiles.* Genes Cells, 2003. **8**(4): p. 379-91.

85. McMahon, M., et al., *Keap1-dependent proteasomal degradation of transcription factor Nrf2 contributes to the negative regulation of antioxidant response element-driven gene expression.* J Biol Chem, 2003. **278**(24): p. 21592-600.

86. Ma, Q., *Role of nrf2 in oxidative stress and toxicity.* Annu Rev Pharmacol Toxicol, 2013. **53**: p. 401-26.

87. Serhan, C.N., et al., *Lipid mediators in the resolution of inflammation.* Cold Spring Harb Perspect Biol, 2014. **7**(2): p. a016311.

88. Zhang, Q., M.J. Lenardo, and D. Baltimore, *30 Years of NF-kappaB: A Blossoming of Relevance to Human Pathobiology.* Cell, 2017. **168**(1-2): p. 37-57.

89. Serhan, C.N. and J. Savill, *Resolution of inflammation: the beginning programs the end.* Nat Immunol, 2005. **6**(12): p. 1191-7.

90. Nguyen, T., P. Nioi, and C.B. Pickett, *The Nrf2-antioxidant response element signaling pathway and its activation by oxidative stress.* J Biol Chem, 2009. **284**(20): p. 13291-5.

91. Chan, K., X.D. Han, and Y.W. Kan, *An important function of Nrf2 in combating oxidative stress: detoxification of acetaminophen.* Proc Natl Acad Sci U S A, 2001. **98**(8): p. 4611-6.

92. Kobayashi, A., et al., *Oxidative and electrophilic stresses activate Nrf2 through inhibition of ubiquitination activity of Keap1.* Mol Cell Biol, 2006. **26**(1): p. 221-9.

93. Cuadrado, A., et al., *Transcription Factor NRF2 as a Therapeutic Target for Chronic Diseases: A Systems Medicine Approach.* Pharmacol Rev, 2018. **70**(2): p. 348-383.

94. Rushworth, S.A., et al., *The high Nrf2 expression in human acute myeloid leukemia is driven by NF-kappaB and underlies its chemo-resistance.* Blood, 2012. **120**(26): p. 5188-98.

95. Ramezani, A., M.P. Nahad, and E. Faghihloo, *The role of Nrf2 transcription factor in viral infection.* J Cell Biochem, 2018.

96. Montes Diaz, G., et al., *Dimethyl fumarate treatment in multiple sclerosis: Recent advances in clinical and immunological studies.* Autoimmun Rev, 2018. **17**(12): p. 1240-1250.

97. Cuadrado, A., S. Kugler, and I. Lastres-Becker, *Pharmacological targeting of GSK-3 and NRF2 provides neuroprotection in a preclinical model of tauopathy.* Redox Biol, 2018. **14**: p. 522-534.

98. Nagai, N., et al., *Nrf2 is a critical modulator of the innate immune response in a model of uveitis.* Free Radic Biol Med, 2009. **47**(3): p. 300-6.

99. Williams, M.A., et al., *Disruption of the transcription factor Nrf2 promotes pro-oxidative dendritic cells that stimulate Th2-like immunoresponsiveness upon activation by ambient particulate matter.* J Immunol, 2008. **181**(7): p. 4545-59.

100. Pajares, M., et al., *Transcription factor NFE2L2/NRF2 modulates chaperone-mediated autophagy through the regulation of LAMP2A.* Autophagy, 2018. **14**(8): p. 1310-1322.

101. Olagnier, D., et al., *Nrf2 negatively regulates STING indicating a link between antiviral sensing and metabolic reprogramming.* Nat Commun, 2018. **9**(1): p. 3506.

102. Ohl, K., et al., *Nrf2 Is a Central Regulator of Metabolic Reprogramming of Myeloid-Derived Suppressor Cells in Steady State and Sepsis.* Front Immunol, 2018. **9**: p. 1552.

103. Kobayashi, E.H., et al., *Nrf2 suppresses macrophage inflammatory response by blocking proinflammatory cytokine transcription.* Nat Commun, 2016. **7**: p. 11624.

104. Yin, S. and W. Cao, *Toll-Like Receptor Signaling Induces Nrf2 Pathway Activation through p62-Triggered Keap1 Degradation.* Mol Cell Biol, 2015. **35**(15): p. 2673-83.

105. Hobbs, S., et al., *LPS-stimulated NF-kappaB p65 dynamic response marks the initiation of TNF expression and transition to IL-10 expression in RAW 264.7 macrophages.* Physiol Rep, 2018. **6**(21): p. e13914.

106. D'Ignazio, L., D. Bandarra, and S. Rocha, *NF-kappaB and HIF crosstalk in immune responses.* FEBS J, 2016. **283**(3): p. 413-24.

107. Ting, A.T. and M.J.M. Bertrand, *More to Life than NF-kappaB in TNFR1 Signaling.* Trends Immunol, 2016. **37**(8): p. 535-545.

108. Fitzpatrick, S.F., et al., *An intact canonical NF-kappaB pathway is required for inflammatory gene expression in response to hypoxia.* J Immunol, 2011. **186**(2): p. 1091-6.

109. Smale, S.T., *Hierarchies of NF-kappaB target-gene regulation.* Nat Immunol, 2011. **12**(8): p. 689-94.

110. Liu, T., et al., *NF-kappaB signaling in inflammation.* Signal Transduct Target Ther, 2017. **2**.

111. Sun, S.C., *The non-canonical NF-kappaB pathway in immunity and inflammation.* Nat Rev Immunol, 2017. **17**(9): p. 545-558.

112. Kastrati, I., et al., *Dimethyl Fumarate Inhibits the Nuclear Factor kappaB Pathway in Breast Cancer Cells by Covalent Modification of p65 Protein.* J Biol Chem, 2016. **291**(7): p. 3639-47.

113. Straus, D.S., et al., *15-deoxy-delta 12,14-prostaglandin J2 inhibits multiple steps in the NF-kappa B signaling pathway.* Proc Natl Acad Sci U S A, 2000. **97**(9): p. 4844-9.

114. Schopfer, F.J. and N.K.H. Khoo, *Nitro-Fatty Acid Logistics: Formation, Biodistribution, Signaling, and Pharmacology.* Trends Endocrinol Metab, 2019.

115. Hansen, A.L., et al., *Nitro-fatty acids are formed in response to virus infection and are potent inhibitors of STING palmitoylation and signaling.* Proc Natl Acad Sci U S A, 2018. **115**(33): p. E7768-E7775.

116. Schopfer, F.J., C. Cipollina, and B.A. Freeman, *Formation and signaling actions of electrophilic lipids.* Chem Rev, 2011. **111**(10): p. 5997-6021.

117. Lopachin, R.M., et al., *Application of the Hard and Soft, Acids and Bases (HSAB) theory to toxicant--target interactions.* Chem Res Toxicol, 2012. **25**(2): p. 239-51.

118. LoPachin, R.M. and T. Gavin, *Molecular mechanisms of aldehyde toxicity: a chemical perspective.* Chem Res Toxicol, 2014. **27**(7): p. 1081-91.

119. LoPachin, R.M., B.C. Geohagen, and L.U. Nordstroem, *Mechanisms of soft and hard electrophile toxicities.* Toxicology, 2019. **418**: p. 62-69.

120. Lin, D., S. Saleh, and D.C. Liebler, *Reversibility of covalent electrophile-protein adducts and chemical toxicity.* Chem Res Toxicol, 2008. **21**(12): p. 2361-9.

121. Chen, N.H., et al., *Formaldehyde Stress Responses in Bacterial Pathogens.* Front Microbiol, 2016. **7**: p. 257.

122. Parvez, S., et al., *Redox Signaling by Reactive Electrophiles and Oxidants.* Chem Rev, 2018. **118**(18): p. 8798-8888.

123. Proschak, E., H. Stark, and D. Merk, *Polypharmacology by Design: A Medicinal Chemist's Perspective on Multitargeting Compounds.* J Med Chem, 2019. **62**(2): p. 420-444.

124. Yin, H., L. Xu, and N.A. Porter, *Free radical lipid peroxidation: mechanisms and analysis.* Chem Rev, 2011. **111**(10): p. 5944-72.

125. Haeggstrom, J.Z. and C.D. Funk, *Lipoxygenase and leukotriene pathways: biochemistry, biology, and roles in disease.* Chem Rev, 2011. **111**(10): p. 5866-98.

126. Smith, W.L., Y. Urade, and P.J. Jakobsson, *Enzymes of the cyclooxygenase pathways of prostanoid biosynthesis.* Chem Rev, 2011. **111**(10): p. 5821-65.

127. Capdevila, J.H., J.R. Falck, and R.W. Estabrook, *Cytochrome P450 and the arachidonate cascade.* FASEB J, 1992. **6**(2): p. 731-6.

128. Hardy, K.D., et al., *Nonenzymatic free radical-catalyzed generation of 15-deoxy-Delta(12,14)-prostaglandin J(2)-like compounds (deoxy-J(2)-isoprostanes) in vivo.* J Lipid Res, 2011. **52**(1): p. 113-24.

129. Milne, G.L., et al., *Isoprostane generation and function.* Chem Rev, 2011. **111**(10): p. 5973-96.

130. Woodcock, S.R., et al., *Nitrated fatty acids: synthesis and measurement.* Free Radic Biol Med, 2013. **59**: p. 14-26.

131. Delmastro-Greenwood, M., B.A. Freeman, and S.G. Wendell, *Redox-dependent anti-inflammatory signaling actions of unsaturated fatty acids.* Annu Rev Physiol, 2014. **76**: p. 79-105.

132. Morgan, M.J. and Z.G. Liu, *Crosstalk of reactive oxygen species and NF-kappaB signaling.* Cell Res, 2011. **21**(1): p. 103-15.

133. Woodcock, C.C., et al., *Nitro-fatty acid inhibition of triple-negative breast cancer cell viability, migration, invasion, and tumor growth.* J Biol Chem, 2018. **293**(4): p. 1120-1137.

134. Khoo, N.K.H., et al., *Electrophilic fatty acid nitroalkenes regulate Nrf2 and NF-kappaB signaling:A medicinal chemistry investigation of structure-function relationships.* Sci Rep, 2018. **8**(1): p. 2295.

135. Villacorta, L., et al., *In situ generation, metabolism and immunomodulatory signaling actions of nitro-conjugated linoleic acid in a murine model of inflammation.* Redox Biol, 2018. **15**: p. 522-531.

136. Vitturi, D.A., et al., *Convergence of biological nitration and nitrosation via symmetrical nitrous anhydride.* Nat Chem Biol, 2015. **11**(7): p. 504-10.

137. Kelley, E.E., et al., *Fatty acid nitroalkenes ameliorate glucose intolerance and pulmonary hypertension in high-fat diet-induced obesity.* Cardiovasc Res, 2014. **101**(3): p. 352-63.

138. Vitturi, D.A., et al., *Modulation of nitro-fatty acid signaling: prostaglandin reductase-1 is a nitroalkene reductase.* J Biol Chem, 2013. **288**(35): p. 25626-37.

139. Rudolph, V., et al., *Endogenous generation and protective effects of nitro-fatty acids in a murine model of focal cardiac ischaemia and reperfusion.* Cardiovasc Res, 2010. **85**(1): p. 155-66.

140. Cui, T., et al., *Nitrated fatty acids: Endogenous anti-inflammatory signaling mediators.* J Biol Chem, 2006. **281**(47): p. 35686-98.

141. Rossi, A., et al., *Anti-inflammatory cyclopentenone prostaglandins are direct inhibitors of IkappaB kinase.* Nature, 2000. **403**(6765): p. 103-8.

142. Cernuda-Morollon, E., et al., *15-Deoxy-Delta 12,14-prostaglandin J2 inhibition of NF-kappaB-DNA binding through covalent modification of the p50 subunit.* J Biol Chem, 2001. **276**(38): p. 35530-6.

143. Snyder, N.W., et al., *15-Oxoeicosatetraenoic acid is a 15-hydroxyprostaglandin dehydrogenase-derived electrophilic mediator of inflammatory signaling pathways.* Chem Biol Interact, 2015. **234**: p. 144-53.

144. Wei, C., et al., *15-oxo-Eicosatetraenoic acid, a metabolite of macrophage 15-hydroxyprostaglandin dehydrogenase that inhibits endothelial cell proliferation.* Mol Pharmacol, 2009. **76**(3): p. 516-25.

145. Kansanen, E., et al., *Electrophilic nitro-fatty acids activate NRF2 by a KEAP1 cysteine 151-independent mechanism.* J Biol Chem, 2011. **286**(16): p. 14019-27.

146. Rachakonda, G., et al., *Covalent modification at Cys151 dissociates the electrophile sensor Keap1 from the ubiquitin ligase CUL3.* Chem Res Toxicol, 2008. **21**(3): p. 705-10.

147. Tsujita, T., et al., *Nitro-fatty acids and cyclopentenone prostaglandins share strategies to activate the Keap1-Nrf2 system: a study using green fluorescent protein transgenic zebrafish.* Genes Cells, 2011. **16**(1): p. 46-57.

148. Surh, Y.J., et al., *15-Deoxy-Delta(1)(2),(1)(4)-prostaglandin J(2), an electrophilic lipid mediator of anti-inflammatory and pro-resolving signaling.* Biochem Pharmacol, 2011. **82**(10): p. 1335-51.

149. Oh, J.Y., et al., *Accumulation of 15-deoxy-delta(12,14)-prostaglandin J2 adduct formation with Keap1 over time: effects on potency for intracellular antioxidant defence induction.* Biochem J, 2008. **411**(2): p. 297-306.

150. Cheng, W.Y., et al., *The cGas-Sting Signaling Pathway Is Required for the Innate Immune Response Against Ectromelia Virus.* Front Immunol, 2018. **9**: p. 1297.

151. Haag, S.M., et al., *Targeting STING with covalent small-molecule inhibitors.* Nature, 2018. **559**(7713): p. 269-273.

152. Ishikawa, H. and G.N. Barber, *The STING pathway and regulation of innate immune signaling in response to DNA pathogens.* Cell Mol Life Sci, 2011. **68**(7): p. 1157-65.

153. Liu, D., et al., *STING directly activates autophagy to tune the innate immune response.* Cell Death Differ, 2018.

154. Kelley, E.E., et al., *Nitro-oleic acid, a novel and irreversible inhibitor of xanthine oxidoreductase.* J Biol Chem, 2008. **283**(52): p. 36176-84.

155. Kansanen, E., et al., *Nrf2-dependent and -independent responses to nitro-fatty acids in human endothelial cells: identification of heat shock response as the major pathway activated by nitro-oleic acid.* J Biol Chem, 2009. **284**(48): p. 33233-41.

156. Schopfer, F.J., et al., *Covalent peroxisome proliferator-activated receptor gamma adduction by nitro-fatty acids: selective ligand activity and anti-diabetic signaling actions.* J Biol Chem, 2010. **285**(16): p. 12321-33.

157. Baker, P.R., et al., *Convergence of nitric oxide and lipid signaling: anti-inflammatory nitro-fatty acids.* Free Radic Biol Med, 2009. **46**(8): p. 989-1003.

158. Burnett, J.P., et al., *Sulforaphane enhances the anticancer activity of taxanes against triple negative breast cancer by killing cancer stem cells.* Cancer Lett, 2017. **394**: p. 52-64.

159. Geisel, J., et al., *Sulforaphane protects from T cell-mediated autoimmune disease by inhibition of IL-23 and IL-12 in dendritic cells.* J Immunol, 2014. **192**(8): p. 3530-9.

160. Koo, J.E., et al., *Sulforaphane inhibits the engagement of LPS with TLR4/MD2 complex by preferential binding to Cys133 in MD2.* Biochem Biophys Res Commun, 2013. **434**(3): p. 600-5.

161. Schopfer, F.J., et al., *Nitro-fatty acids: New drug candidates for chronic inflammatory and fibrotic diseases.* Nitric Oxide, 2018.

162. Rudolph, T.K., et al., *Nitro-fatty acids reduce atherosclerosis in apolipoprotein E-deficient mice.* Arterioscler Thromb Vasc Biol, 2010. **30**(5): p. 938-45.

163. Rom, O., et al., *Nitro-fatty acids protect against steatosis and fibrosis during development of nonalcoholic fatty liver disease in mice.* EBioMedicine, 2019. **41**: p. 62-72.

164. Groeger, A.L., et al., *Cyclooxygenase-2 generates anti-inflammatory mediators from omega-3 fatty acids.* Nat Chem Biol, 2010. **6**(6): p. 433-41.

165. Clish, C.B., et al., *Oxidoreductases in lipoxin A4 metabolic inactivation: a novel role for 15-onoprostaglandin 13-reductase/leukotriene B4 12-hydroxydehydrogenase in inflammation.* J Biol Chem, 2000. **275**(33): p. 25372-80.

166. Zaro, B.W., et al., *Dimethyl Fumarate Disrupts Human Innate Immune Signaling by Targeting the IRAK4-MyD88 Complex.* J Immunol, 2019.

167. Hosseini, A., et al., *Dimethyl fumarate: Regulatory effects on the immune system in the treatment of multiple sclerosis.* J Cell Physiol, 2019. **234**(7): p. 9943-9955.

168. Blewett, M.M., et al., *Chemical proteomic map of dimethyl fumarate-sensitive cysteines in primary human T cells.* Sci Signal, 2016. **9**(445): p. rs10.

169. Brennan, M.S., et al., *Dimethyl fumarate and monoethyl fumarate exhibit differential effects on KEAP1, NRF2 activation, and glutathione depletion in vitro.* PLoS One, 2015. **10**(3): p. e0120254.

170. Gold, R., R.A. Linker, and M. Stangel, *Fumaric acid and its esters: an emerging treatment for multiple sclerosis with antioxidative mechanism of action.* Clin Immunol, 2012. **142**(1): p. 44-8.

171. Woodcock, S.R., et al., *Synthesis of an Electrophilic Keto-Tetraene 15-oxo-Lipoxin A4 Methyl Ester via a MIDA Boronate.* Tetrahedron Lett, 2018. **59**(39): p. 3524-3527.

172. Sun, L., et al., *GM-CSF Quantity Has a Selective Effect on Granulocytic vs. Monocytic Myeloid Development and Function.* Front Immunol, 2018. **9**: p. 1922.

173. Erlich, Z., et al., *Macrophages, rather than DCs, are responsible for inflammasome activity in the GM-CSF BMDC model.* Nat Immunol, 2019.

174. Mailliard, R.B., et al., *alpha-type-1 polarized dendritic cells: a novel immunization tool with optimized CTL-inducing activity.* Cancer Res, 2004. **64**(17): p. 5934-7.

175. Livak, K.J. and T.D. Schmittgen, *Analysis of relative gene expression data using real-time quantitative PCR and the 2(-Delta Delta C(T)) Method.* Methods, 2001. **25**(4): p. 402-8.

176. Balish, A.L., J.M. Katz, and A.I. Klimov, *Influenza: propagation, quantification, and storage.* Curr Protoc Microbiol, 2013. **Chapter 15**: p. Unit 15G 1.

177. Basil, M.C. and B.D. Levy, *Specialized pro-resolving mediators: endogenous regulators of infection and inflammation.* Nat Rev Immunol, 2016. **16**(1): p. 51-67.

178. Serhan, C.N., M. Hamberg, and B. Samuelsson, *Lipoxins: novel series of biologically active compounds formed from arachidonic acid in human leukocytes.* Proc Natl Acad Sci U S A, 1984. **81**(17): p. 5335-9.

179. Serhan, C.N., M. Hamberg, and B. Samuelsson, *Trihydroxytetraenes: a novel series of compounds formed from arachidonic acid in human leukocytes.* Biochem Biophys Res Commun, 1984. **118**(3): p. 943-9.

180. Edenius, C., J. Haeggstrom, and J.A. Lindgren, *Transcellular conversion of endogenous arachidonic acid to lipoxins in mixed human platelet-granulocyte suspensions.* Biochem Biophys Res Commun, 1988. **157**(2): p. 801-7.

181. Romano, M. and C.N. Serhan, *Lipoxin generation by permeabilized human platelets.* Biochemistry, 1992. **31**(35): p. 8269-77.

182. Claria, J. and C.N. Serhan, *Aspirin triggers previously undescribed bioactive eicosanoids by human endothelial cell-leukocyte interactions.* Proc Natl Acad Sci U S A, 1995. **92**(21): p. 9475-9.

183. Claria, J., M.H. Lee, and C.N. Serhan, *Aspirin-triggered lipoxins (15-epi-LX) are generated by the human lung adenocarcinoma cell line (A549)-neutrophil interactions and are potent inhibitors of cell proliferation.* Mol Med, 1996. **2**(5): p. 583-96.

184. Fiore, S., et al., *Identification of a human cDNA encoding a functional high affinity lipoxin A4 receptor.* J Exp Med, 1994. **180**(1): p. 253-60.

185. Sham, H.P., et al., *15-epi-Lipoxin A4, Resolvin D2, and Resolvin D3 Induce NF-kappaB Regulators in Bacterial Pneumonia.* J Immunol, 2018. **200**(8): p. 2757-2766.

186. Seki, H., et al., *The anti-inflammatory and proresolving mediator resolvin E1 protects mice from bacterial pneumonia and acute lung injury.* J Immunol, 2010. **184**(2): p. 836-43.

187. Levy, B.D., et al., *Lipoxin A4 stable analogs reduce allergic airway responses via mechanisms distinct from CysLT1 receptor antagonism.* FASEB J, 2007. **21**(14): p. 3877-84.

188. Vieira, A.M., et al., *ATL-1, a synthetic analog of lipoxin, modulates endothelial permeability and interaction with tumor cells through a VEGF-dependent mechanism.* Biochem Pharmacol, 2014. **90**(4): p. 388-96.

189. Kieran, N.E., et al., *Modification of the transcriptomic response to renal ischemia/reperfusion injury by lipoxin analog.* Kidney Int, 2003. **64**(2): p. 480-92.

190. Guo, Z., et al., *Lipoxin A4 Reduces Inflammation Through Formyl Peptide Receptor 2/p38 MAPK Signaling Pathway in Subarachnoid Hemorrhage Rats.* Stroke, 2016. **47**(2): p. 490-7.

191. Liu, L., et al., *LXA4 Ameliorates Cerebrovascular Endothelial Dysfunction by Reducing Acute Inflammation after Subarachnoid Hemorrhage in Rats.* Neuroscience, 2019.

192. Serhan, C.N. and N. Chiang, *Endogenous pro-resolving and anti-inflammatory lipid mediators: a new pharmacologic genus.* Br J Pharmacol, 2008. **153 Suppl 1**: p. S200-15.

193. Buckley, C.D., D.W. Gilroy, and C.N. Serhan, *Proresolving lipid mediators and mechanisms in the resolution of acute inflammation.* Immunity, 2014. **40**(3): p. 315-27.

194. Serhan, C.N., *Resolution phase of inflammation: novel endogenous anti-inflammatory and proresolving lipid mediators and pathways.* Annu Rev Immunol, 2007. **25**: p. 101-37.

195. Serhan, C.N. and N.A. Petasis, *Resolvins and protectins in inflammation resolution.* Chem Rev, 2011. **111**(10): p. 5922-43.

196. Kong, X., et al., *Pilot application of lipoxin A4 analog and lipoxin A4 receptor agonist in asthmatic children with acute episodes.* Exp Ther Med, 2017. **14**(3): p. 2284-2290.

197. Wu, S.H., et al., *Efficacy and safety of 15(R/S)-methyl-lipoxin A(4) in topical treatment of infantile eczema.* Br J Dermatol, 2013. **168**(1): p. 172-8.

198. Christie, P.E., B.W. Spur, and T.H. Lee, *The effects of lipoxin A4 on airway responses in asthmatic subjects.* Am Rev Respir Dis, 1992. **145**(6): p. 1281-4.

199. Boucher, J.L., M. Delaforge, and D. Mansuy, *Metabolism of lipoxins A4 and B4 and of their all-trans isomers by human leukocytes and rat liver microsomes.* Biochem Biophys Res Commun, 1991. **177**(1): p. 134-9.

200. Serhan, C.N., et al., *Lipoxin A4 metabolism by differentiated HL-60 cells and human monocytes: conversion to novel 15-oxo and dihydro products.* Biochemistry, 1993. **32**(25): p. 6313-9.

201. Clish, C.B., Y.P. Sun, and C.N. Serhan, *Identification of dual cyclooxygenase-eicosanoid oxidoreductase inhibitors: NSAIDs that inhibit PG-LX reductase/LTB(4) dehydrogenase.* Biochem Biophys Res Commun, 2001. **288**(4): p. 868-74.

202. Clish, C.B., et al., *Local and systemic delivery of a stable aspirin-triggered lipoxin prevents neutrophil recruitment in vivo.* Proc Natl Acad Sci U S A, 1999. **96**(14): p. 8247-52.

203. Maddox, J.F., et al., *Lipoxin A4 stable analogs are potent mimetics that stimulate human monocytes and THP-1 cells via a G-protein-linked lipoxin A4 receptor.* J Biol Chem, 1997. **272**(11): p. 6972-8.

204. Maddox, J.F. and C.N. Serhan, *Lipoxin A4 and B4 are potent stimuli for human monocyte migration and adhesion: selective inactivation by dehydrogenation and reduction.* J Exp Med, 1996. **183**(1): p. 137-46.

205. Tai, H.H., et al., *NAD+-linked 15-hydroxyprostaglandin dehydrogenase: structure and biological functions.* Curr Pharm Des, 2006. **12**(8): p. 955-62.

206. Snyder, N.W., et al., *Cellular uptake and antiproliferative effects of 11-oxo-eicosatetraenoic acid.* J Lipid Res, 2013. **54**(11): p. 3070-7.

207. Freeman, B.A., V.B. O'Donnell, and F.J. Schopfer, *The discovery of nitro-fatty acids as products of metabolic and inflammatory reactions and mediators of adaptive cell signaling.* Nitric Oxide, 2018. **77**: p. 106-111.

208. Mrowietz, U., et al., *The Pharmacokinetics of Fumaric Acid Esters Reveal Their In Vivo Effects.* Trends Pharmacol Sci, 2018. **39**(1): p. 1-12.

209. Wendell, S.G., et al., *15-Hydroxyprostaglandin dehydrogenase generation of electrophilic lipid signaling mediators from hydroxy omega-3 fatty acids.* J Biol Chem, 2015. **290**(9): p. 5868-80.

210. Yacoubian, S. and C.N. Serhan, *New endogenous anti-inflammatory and proresolving lipid mediators: implications for rheumatic diseases.* Nat Clin Pract Rheumatol, 2007. **3**(10): p. 570-9; quiz 1 p following 589.

211. Bannenberg, G., M. Arita, and C.N. Serhan, *Endogenous receptor agonists: resolving inflammation.* ScientificWorldJournal, 2007. **7**: p. 1440-62.

212. Baillie, J.K. and P. Digard, *Influenza--time to target the host?* N Engl J Med, 2013. **369**(2): p. 191-3.

213. Schulze-Topphoff, U., et al., *Dimethyl fumarate treatment induces adaptive and innate immune modulation independent of Nrf2.* Proc Natl Acad Sci U S A, 2016. **113**(17): p. 4777-82.

214. Fukunaga, K., et al., *Cyclooxygenase 2 plays a pivotal role in the resolution of acute lung injury.* J Immunol, 2005. **174**(8): p. 5033-9.

215. Matthay, M.A. and R.L. Zemans, *The acute respiratory distress syndrome: pathogenesis and treatment.* Annu Rev Pathol, 2011. **6**: p. 147-63.

216. Reddy, A.T., S.P. Lakshmi, and R.C. Reddy, *The Nitrated Fatty Acid 10-Nitro-oleate Diminishes Severity of LPS-Induced Acute Lung Injury in Mice.* PPAR Res, 2012. **2012**: p. 617063.

217. Gong, J., et al., *BML-111, a lipoxin receptor agonist, protects haemorrhagic shock-induced acute lung injury in rats.* Resuscitation, 2012. **83**(7): p. 907-12.

218. Eber, E., et al., *Leflunomide, a novel immunomodulating agent, prevents the development of allergic sensitization in an animal model of allergic asthma.* Clin Exp Allergy, 1998. **28**(3): p. 376-84.

219. Hammad, H., et al., *Activation of the D prostanoid 1 receptor suppresses asthma by modulation of lung dendritic cell function and induction of regulatory T cells.* J Exp Med, 2007. **204**(2): p. 357-67.

220. McGuire, V.A., et al., *Dimethyl fumarate blocks pro-inflammatory cytokine production via inhibition of TLR induced M1 and K63 ubiquitin chain formation.* Sci Rep, 2016. **6**: p. 31159.

221. Mazzola, M.A., et al., *Monomethyl fumarate treatment impairs maturation of human myeloid dendritic cells and their ability to activate T cells.* Mult Scler, 2017: p. 1352458517740213.

222. Gilroy, D.W., et al., *Inducible cyclooxygenase-derived 15-deoxy(Delta)12-14PGJ2 brings about acute inflammatory resolution in rat pleurisy by inducing neutrophil and macrophage apoptosis.* FASEB J, 2003. **17**(15): p. 2269-71.

223. Bonacci, G., et al., *Conjugated linoleic acid is a preferential substrate for fatty acid nitration.* J Biol Chem, 2012. **287**(53): p. 44071-82.

224. Turell, L., et al., *The Chemical Basis of Thiol Addition to Nitro-conjugated Linoleic Acid, a Protective Cell-signaling Lipid.* J Biol Chem, 2017. **292**(4): p. 1145-1159.

225. Cloutier, A., et al., *The prostanoid 15-deoxy-Delta12,14-prostaglandin-j2 reduces lung inflammation and protects mice against lethal influenza infection.* J Infect Dis, 2012. **205**(4): p. 621-30.

226. Fionda, C., et al., *Inhibition of trail gene expression by cyclopentenonic prostaglandin 15-deoxy-delta12,14-prostaglandin J2 in T lymphocytes.* Mol Pharmacol, 2007. **72**(5): p. 1246-57.

227. Giustina, A.D., et al., *Dimethyl Fumarate Modulates Oxidative Stress and Inflammation in Organs After Sepsis in Rats.* Inflammation, 2018. **41**(1): p. 315-327.

228. Mills, E.L., et al., *Itaconate is an anti-inflammatory metabolite that activates Nrf2 via alkylation of KEAP1.* Nature, 2018.

229. Sun, Y.P., et al., *Resolvin D1 and its aspirin-triggered 17R epimer. Stereochemical assignments, anti-inflammatory properties, and enzymatic inactivation.* J Biol Chem, 2007. **282**(13): p. 9323-34.

230. Arita, M., et al., *Metabolic inactivation of resolvin E1 and stabilization of its anti-inflammatory actions.* J Biol Chem, 2006. **281**(32): p. 22847-54.

231. Choi, J., S.T. Kim, and J. Craft, *The pathogenesis of systemic lupus erythematosus-an update.* Curr Opin Immunol, 2012. **24**(6): p. 651-7.

232. Montes Diaz, G., et al., *Dimethyl fumarate induces a persistent change in the composition of the innate and adaptive immune system in multiple sclerosis patients.* Sci Rep, 2018. **8**(1): p. 8194.

233. Long, M.J.C. and Y. Aye, *Privileged Electrophile Sensors: A Resource for Covalent Drug Development.* Cell Chem Biol, 2017. **24**(7): p. 787-800.

234. Liu, X., M.J.C. Long, and Y. Aye, *Proteomics and Beyond: Cell Decision-Making Shaped by Reactive Electrophiles.* Trends Biochem Sci, 2019. **44**(1): p. 75-89.

235. Lampropoulou, V., et al., *Itaconate Links Inhibition of Succinate Dehydrogenase with Macrophage Metabolic Remodeling and Regulation of Inflammation.* Cell Metab, 2016. **24**(1): p. 158-66.

236. Bambouskova, M., et al., *Electrophilic properties of itaconate and derivatives regulate the IkappaBzeta-ATF3 inflammatory axis.* Nature, 2018. **556**(7702): p. 501-504.

237. Groeger, A.L. and B.A. Freeman, *Signaling actions of electrophiles: anti-inflammatory therapeutic candidates.* Mol Interv, 2010. **10**(1): p. 39-50.

238. Arshad, L., et al., *Immunosuppressive Effects of Natural alpha,beta-Unsaturated Carbonyl-Based Compounds, and Their Analogs and Derivatives, on Immune Cells: A Review.* Front Pharmacol, 2017. **8**: p. 22.

239. Batthyany, C., et al., *Reversible post-translational modification of proteins by nitrated fatty acids in vivo.* J Biol Chem, 2006. **281**(29): p. 20450-63.

240. Freeman, B.A., et al., *Nitro-fatty acid formation and signaling.* J Biol Chem, 2008. **283**(23): p. 15515-9.

241. Ichikawa, T., et al., *Nitroalkenes suppress lipopolysaccharide-induced signal transducer and activator of transcription signaling in macrophages: a critical role of mitogen-activated protein kinase phosphatase 1.* Endocrinology, 2008. **149**(8): p. 4086-94.

242. Villacorta, L., et al., *Electrophilic nitro-fatty acids inhibit vascular inflammation by disrupting LPS-dependent TLR4 signalling in lipid rafts.* Cardiovasc Res, 2013. **98**(1): p. 116-24.

243. Gonzalez-Perilli, L., et al., *Nitroarachidonic acid prevents NADPH oxidase assembly and superoxide radical production in activated macrophages.* Free Radic Biol Med, 2013. **58**: p. 126-33.

244. Ambrozova, G., et al., *Nitro-oleic acid inhibits vascular endothelial inflammatory responses and the endothelial-mesenchymal transition.* Biochim Biophys Acta, 2016. **1860**(11 Pt A): p. 2428-2437.

245. Ambrozova, G., et al., *Nitro-oleic acid modulates classical and regulatory activation of macrophages and their involvement in pro-fibrotic responses.* Free Radic Biol Med, 2016. **90**: p. 252-260.

246. Woodcock, C.C., et al., *Nitro-fatty acid inhibition of triple negative breast cancer cell viability, migration, invasion and tumor growth.* J Biol Chem, 2017.

247. Rius, J., et al., *NF-kappaB links innate immunity to the hypoxic response through transcriptional regulation of HIF-1alpha.* Nature, 2008. **453**(7196): p. 807-11.

248. Eisenbarth, S.C., *Dendritic cell subsets in T cell programming: location dictates function.* Nat Rev Immunol, 2019. **19**(2): p. 89-103.

249. van de Laar, L., P.J. Coffer, and A.M. Woltman, *Regulation of dendritic cell development by GM-CSF: molecular control and implications for immune homeostasis and therapy.* Blood, 2012. **119**(15): p. 3383-93.

250. Dearman, R.J., et al., *Toll-like receptor ligand activation of murine bone marrow-derived dendritic cells.* Immunology, 2009. **126**(4): p. 475-84.

251. Lehmann, C.H., et al., *Direct Delivery of Antigens to Dendritic Cells via Antibodies Specific for Endocytic Receptors as a Promising Strategy for Future Therapies.* Vaccines (Basel), 2016. **4**(2).

252. Fehres, C.M., et al., *Understanding the biology of antigen cross-presentation for the design of vaccines against cancer.* Front Immunol, 2014. **5**: p. 149.

253. Selman, M., et al., *Dimethyl fumarate potentiates oncolytic virotherapy through NF-kappaB inhibition.* Sci Transl Med, 2018. **10**(425).

254. Linker, R.A., et al., *Fumaric acid esters exert neuroprotective effects in neuroinflammation via activation of the Nrf2 antioxidant pathway.* Brain, 2011. **134**(Pt 3): p. 678-92.

255. Yageta, Y., et al., *Role of Nrf2 in host defense against influenza virus in cigarette smoke-exposed mice.* J Virol, 2011. **85**(10): p. 4679-90.

256. Rodriguez-Duarte, J., et al., *Electrophilic nitroalkene-tocopherol derivatives: synthesis, physicochemical characterization and evaluation of anti-inflammatory signaling responses.* Sci Rep, 2018. **8**(1): p. 12784.

257. Wculek, S.K., et al., *Metabolic Control of Dendritic Cell Functions: Digesting Information.* Front Immunol, 2019. **10**: p. 775.

258. Boergeling, Y. and S. Ludwig, *Targeting a metabolic pathway to fight the flu.* FEBS J, 2017. **284**(2): p. 218-221.

259. Arts, R.J., et al., *Cellular metabolism of myeloid cells in sepsis.* J Leukoc Biol, 2017. **101**(1): p. 151-164.

260. Munger, J., et al., *Systems-level metabolic flux profiling identifies fatty acid synthesis as a target for antiviral therapy.* Nat Biotechnol, 2008. **26**(10): p. 1179-86.

261. Palsson-McDermott, E.M., et al., *Pyruvate kinase M2 regulates Hif-1alpha activity and IL-1beta induction and is a critical determinant of the warburg effect in LPS-activated macrophages.* Cell Metab, 2015. **21**(1): p. 65-80.

262. Tannahill, G.M., et al., *Succinate is an inflammatory signal that induces IL-1beta through HIF-1alpha.* Nature, 2013. **496**(7444): p. 238-42.

263. Michelucci, A., et al., *Immune-responsive gene 1 protein links metabolism to immunity by catalyzing itaconic acid production.* Proc Natl Acad Sci U S A, 2013. **110**(19): p. 7820-5.

264. Perrin-Cocon, L., et al., *Toll-like Receptor 4-Induced Glycolytic Burst in Human Monocyte-Derived Dendritic Cells Results from p38-Dependent Stabilization of HIF-1alpha and Increased Hexokinase II Expression.* J Immunol, 2018. **201**(5): p. 1510-1521.

265. Guak, H., et al., *Glycolytic metabolism is essential for CCR7 oligomerization and dendritic cell migration.* Nat Commun, 2018. **9**(1): p. 2463.

266. Habib, E., et al., *Expression of xCT and activity of system xc(-) are regulated by NRF2 in human breast cancer cells in response to oxidative stress.* Redox Biol, 2015. **5**: p. 33-42.

267. D'Angelo, J.A., et al., *The cystine/glutamate antiporter regulates dendritic cell differentiation and antigen presentation.* J Immunol, 2010. **185**(6): p. 3217-26.

268. Pacheco, R., et al., *Glutamate released by dendritic cells as a novel modulator of T cell activation.* J Immunol, 2006. **177**(10): p. 6695-704.

269. Kash, J.C., et al., *Treatment with the reactive oxygen species scavenger EUK-207 reduces lung damage and increases survival during 1918 influenza virus infection in mice.* Free Radic Biol Med, 2014. **67**: p. 235-47.

270. Zhai, Y., et al., *Host Transcriptional Response to Influenza and Other Acute Respiratory Viral Infections--A Prospective Cohort Study.* PLoS Pathog, 2015. **11**(6): p. e1004869.

271. Ishikawa, T., Y. Ito, and M. Kawai-Yamada, *Molecular characterization and targeted quantitative profiling of the sphingolipidome in rice.* Plant J, 2016. **88**(4): p. 681-693.

272. Korteweg, C. and J. Gu, *Pathology, molecular biology, and pathogenesis of avian influenza A (H5N1) infection in humans.* Am J Pathol, 2008. **172**(5): p. 1155-70.

273. Tanner, W.D., D.J. Toth, and A.V. Gundlapalli, *The pandemic potential of avian influenza A(H7N9) virus: a review.* Epidemiol Infect, 2015. **143**(16): p. 3359-74.

274. Palese, P., *Influenza: old and new threats.* Nat Med, 2004. **10**(12 Suppl): p. S82-7.

275. Kash, J.C., et al., *Genomic analysis of increased host immune and cell death responses induced by 1918 influenza virus.* Nature, 2006. **443**(7111): p. 578-81.

276. Kobasa, D., et al., *Aberrant innate immune response in lethal infection of macaques with the 1918 influenza virus.* Nature, 2007. **445**(7125): p. 319-23.

277. Mauad, T., et al., *Lung pathology in fatal novel human influenza A (H1N1) infection.* Am J Respir Crit Care Med, 2010. **181**(1): p. 72-9.

278. Short, K.R., et al., *Influenza virus damages the alveolar barrier by disrupting epithelial cell tight junctions.* Eur Respir J, 2016. **47**(3): p. 954-66.

279. Short, K.R., et al., *Pathogenesis of influenza-induced acute respiratory distress syndrome.* The Lancet Infectious Diseases, 2014. **14**(1): p. 57-69.

280. To, K.K., et al., *Delayed clearance of viral load and marked cytokine activation in severe cases of pandemic H1N1 2009 influenza virus infection.* Clin Infect Dis, 2010. **50**(6): p. 850-9.

281. Hurt, A.C., *The epidemiology and spread of drug resistant human influenza viruses.* Curr Opin Virol, 2014. **8**: p. 22-9.

282. Vlahos, R., J. Stambas, and S. Selemidis, *Suppressing production of reactive oxygen species (ROS) for influenza A virus therapy.* Trends Pharmacol Sci, 2012. **33**(1): p. 3-8.

283. Barrera-Ramirez, J., et al., *Micro-RNA Profiling of Exosomes from Marrow-Derived Mesenchymal Stromal Cells in Patients with Acute Myeloid Leukemia: Implications in Leukemogenesis.* Stem Cell Rev, 2017. **13**(6): p. 817-825.

284. Taubenberger, J.K. and D.M. Morens, *The pathology of influenza virus infections.* Annu Rev Pathol, 2008. **3**: p. 499-522.

285. Tripathi, S., M.R. White, and K.L. Hartshorn, *The amazing innate immune response to influenza A virus infection.* Innate Immun, 2015. **21**(1): p. 73-98.

286. Goraya, M.U., et al., *Induction of innate immunity and its perturbation by influenza viruses.* Protein Cell, 2015. **6**(10): p. 712-21.

287. Peiris, J.S., et al., *Innate immune responses to influenza A H5N1: friend or foe?* Trends Immunol, 2009. **30**(12): p. 574-84.

288. Pulendran, B. and M.S. Maddur, *Innate immune sensing and response to influenza.* Curr Top Microbiol Immunol, 2015. **386**: p. 23-71.

289. Iwasaki, A. and P.S. Pillai, *Innate immunity to influenza virus infection.* Nat Rev Immunol, 2014. **14**(5): p. 315-28.

290. Wang, J., et al., *NF-kappa B RelA subunit is crucial for early IFN-beta expression and resistance to RNA virus replication.* J Immunol, 2010. **185**(3): p. 1720-9.

291. Hrincius, E.R., et al., *Acute Lung Injury Results from Innate Sensing of Viruses by an ER Stress Pathway.* Cell Rep, 2015. **11**(10): p. 1591-603.

292. Sgarbanti, R., et al., *Redox regulation of the influenza hemagglutinin maturation process: a new cell-mediated strategy for anti-influenza therapy.* Antioxid Redox Signal, 2011. **15**(3): p. 593-606.

293. Le Goffic, R., et al., *Influenza A virus protein PB1-F2 exacerbates IFN-beta expression of human respiratory epithelial cells.* J Immunol, 2010. **185**(8): p. 4812-23.

294. Zamarin, D., et al., *Influenza virus PB1-F2 protein induces cell death through mitochondrial ANT3 and VDAC1.* PLoS Pathog, 2005. **1**(1): p. e4.

295. Vidy, A., et al., *The Influenza Virus Protein PB1-F2 Increases Viral Pathogenesis through Neutrophil Recruitment and NK Cells Inhibition.* PLoS One, 2016. **11**(10): p. e0165361.

296. Gao, H., et al., *The contribution of PA-X to the virulence of pandemic 2009 H1N1 and highly pathogenic H5N1 avian influenza viruses.* Sci Rep, 2015. **5**: p. 8262.

297. Shin, N., et al., *Influenza A virus PB1-F2 is involved in regulation of cellular redox state in alveolar epithelial cells.* Biochem Biophys Res Commun, 2015. **459**(4): p. 699-705.

298. Geiss, G.K., et al., *Cellular transcriptional profiling in influenza A virus-infected lung epithelial cells: the role of the nonstructural NS1 protein in the evasion of the host innate defense and its potential contribution to pandemic influenza.* Proc Natl Acad Sci U S A, 2002. **99**(16): p. 10736-41.

299. Wolff, T. and S. Ludwig, *Influenza viruses control the vertebrate type I interferon system: factors, mechanisms, and consequences.* J Interferon Cytokine Res, 2009. **29**(9): p. 549-57.

300. Haye, K., et al., *The NS1 protein of a human influenza virus inhibits type I interferon production and the induction of antiviral responses in primary human dendritic and respiratory epithelial cells.* J Virol, 2009. **83**(13): p. 6849-62.

301. Schrauwen, E.J. and R.A. Fouchier, *Host adaptation and transmission of influenza A viruses in mammals.* Emerg Microbes Infect, 2014. **3**(2): p. e9.

302. Ling, J.X., et al., *Amelioration of influenza virus-induced reactive oxygen species formation by epigallocatechin gallate derived from green tea.* Acta Pharmacol Sin, 2012. **33**(12): p. 1533-41.

303. Viemann, D., et al., *H5N1 virus activates signaling pathways in human endothelial cells resulting in a specific imbalanced inflammatory response.* J Immunol, 2011. **186**(1): p. 164-73.

304. Imai, Y., et al., *Identification of oxidative stress and Toll-like receptor 4 signaling as a key pathway of acute lung injury.* Cell, 2008. **133**(2): p. 235-49.

305. Cilloniz, C., et al., *Lethal dissemination of H5N1 influenza virus is associated with dysregulation of inflammation and lipoxin signaling in a mouse model of infection.* J Virol, 2010. **84**(15): p. 7613-24.

306. Neumann G, S.K., Kawaoka Y, *molecular pathogenesis of H5N1 influenza virus infections.* Antivir Ther, 2007. **12**(4): p. 617-626.

307. Nin, N., et al., *Lung histopathological findings in fatal pandemic influenza A (H1N1).* Med Intensiva, 2012. **36**(1): p. 24-31.

308. Baillie, J.K. and P. Digard, *Influenza - time to target the host.* N Engl J Med, 2013. **369**: p. 191-193.

309. Lauder, S.N., et al., *Paracetamol reduces influenza-induced immunopathology in a mouse model of infection without compromising virus clearance or the generation of protective immunity.* Thorax, 2011. **66**(5): p. 368-74.

310. Carey, M.A., et al., *Pharmacologic inhibition of COX-1 and COX-2 in influenza A viral infection in mice.* PLoS One, 2010. **5**(7): p. e11610.

311. Snelgrove, R.J., et al., *An absence of reactive oxygen species improves the resolution of lung influenza infection.* Eur J Immunol, 2006. **36**(6): p. 1364-73.

312. Oostwoud, L.C., et al., *Apocynin and ebselen reduce influenza A virus-induced lung inflammation in cigarette smoke-exposed mice.* Sci Rep, 2016. **6**: p. 20983.

313. Vlahos, R., et al., *Inhibition of Nox2 oxidase activity ameliorates influenza A virus-induced lung inflammation.* PLoS Pathog, 2011. **7**(2): p. e1001271.

314. van der Vliet, A., *NADPH oxidases in lung biology and pathology: host defense enzymes, and more.* Free Radic Biol Med, 2008. **44**(6): p. 938-55.

315. Burggraaf, S., et al., *Increased inducible nitric oxide synthase expression in organs is associated with a higher severity of H5N1 influenza virus infection.* PLoS One, 2011. **6**(1): p. e14561.

316. Cai, W., et al., *14-Deoxy-11,12-didehydroandrographolide attenuates excessive inflammatory responses and protects mice lethally challenged with highly pathogenic A(H5N1) influenza viruses.* Antiviral Res, 2016. **133**: p. 95-105.

317. Nimmerjahn, F., et al., *Active NF-kappaB signalling is a prerequisite for influenza virus infection.* J Gen Virol, 2004. **85**(Pt 8): p. 2347-56.

318. Bernasconi, D., et al., *The IkappaB kinase is a key factor in triggering influenza A virus-induced inflammatory cytokine production in airway epithelial cells.* J Biol Chem, 2005. **280**(25): p. 24127-34.

319. Ludwig, S. and O. Planz, *Influenza viruses and the NF-kappaB signaling pathway - towards a novel concept of antiviral therapy.* Biol Chem, 2008. **389**(10): p. 1307-12.

320. Kosmider, B., et al., *Nrf2 protects human alveolar epithelial cells against injury induced by influenza A virus.* Respir Res, 2012. **13**: p. 43.

321. Kesic, M.J., et al., *Nrf2 expression modifies influenza A entry and replication in nasal epithelial cells.* Free Radic Biol Med, 2011. **51**(2): p. 444-53.

322. Muller, L., et al., *Effect of Broccoli Sprouts and Live Attenuated Influenza Virus on Peripheral Blood Natural Killer Cells: A Randomized, Double-Blind Study.* PLoS One, 2016. **11**(1): p. e0147742.

323. Noah, T.L., et al., *Effect of broccoli sprouts on nasal response to live attenuated influenza virus in smokers: a randomized, double-blind study.* PLoS One, 2014. **9**(6): p. e98671.

324. Straus, D.S., et al., *15-deoxy-prostaglandin J2 inhibits multiple steps in the NF-kB pathway.* PNAS, 2000. **97**(9): p. 4844-4849.

325. Rizkalla, N.A., et al., *High-frequency percussive ventilation improves oxygenation and ventilation in pediatric patients with acute respiratory failure.* J Crit Care, 2014. **29**(2): p. 314 e1-7.

326. Cipollina, C., et al., *Dual anti-oxidant and anti-inflammatory actions of the electrophilic cyclooxygenase-2-derived 17-oxo-DHA in lipopolysaccharide- and cigarette smoke-induced inflammation.* Biochim Biophys Acta, 2014. **1840**(7): p. 2299-309.

327. Musiek, E.S., et al., *Electrophilic cyclopentenone neuroprostanes are anti-inflammatory mediators formed from the peroxidation of the omega-3 polyunsaturated fatty acid docosahexaenoic acid.* J Biol Chem, 2008. **283**(29): p. 19927-35.

328. Bonacci, G., et al., *Electrophilic fatty acids regulate matrix metalloproteinase activity and expression.* J Biol Chem, 2011. **286**(18): p. 16074-81.

329. Trostchansky, A., et al., *synthesis, isomer characterization, and anti-inflammatory properties of nitroarachidonate.* Biochemistry, 2007. **46**: p. 4645-4653.

330. Awwad, K., et al., *Electrophilic fatty acid species inhibit 5-lipoxygenase and attenuate sepsis-induced pulmonary inflammation.* Antioxid Redox Signal, 2014. **20**(17): p. 2667-80.

331. Kensler, T.W., N. Wakabayashi, and S. Biswal, *Cell survival responses to environmental stresses via the Keap1-Nrf2-ARE pathway.* Annu Rev Pharmacol Toxicol, 2007. **47**: p. 89-116.

332. Levonen, A.L., et al., *Redox regulation of antioxidants, autophagy, and the response to stress: implications for electrophile therapeutics.* Free Radic Biol Med, 2014. **71**: p. 196-207.

333. Wang, G., et al., *Nitro-oleic acid downregulates lipoprotein-associated phospholipase A2 expression via the p42/p44 MAPK and NFkappaB pathways.* Sci Rep, 2014. **4**: p. 4905.

334. Wang, H., et al., *Nitro-oleic acid protects against endotoxin-induced endotoxemia and multiorgan injury in mice.* Am J Physiol Renal Physiol, 2010. **298**(3): p. F754-62.

335. Akaike, T., et al., *Dependence on O2 generation by XO of pathogenesis of influenza in mice.* J. Clin. Invest., 1990. **85**: p. 739-745.

336. Akaike, T., et al., *Pathogenesis of influenza virus-induced pneumonia-involvement of both nitric oxide and oxygen radicals.* Proc Natl Acad Sci U S A, 1996. **93**: p. 2448-2453.

337. Lee, S.M., et al., *Hyperinduction of cyclooxygenase-2-mediated proinflammatory cascade: a mechanism for the pathogenesis of avian influenza H5N1 infection.* J Infect Dis, 2008. **198**(4): p. 525-35.

338. Zheng, B.J., et al., *Delayed antiviral plus immunomodulator treatment still reduces mortality in mice infected by high inoculum of influenza A/H5N1 virus.* Proc Natl Acad Sci U S A, 2008. **105**(23): p. 8091-6.

339. Perrone, L.A., et al., *Inducible nitric oxide contributes to viral pathogenesis following highly pathogenic influenza virus infection in mice.* J Infect Dis, 2013. **207**(10): p. 1576-84.

340. Checconi, P., et al., *The Environmental Pollutant Cadmium Promotes Influenza Virus Replication in MDCK Cells by Altering Their Redox State.* Int J Mol Sci, 2013. **14**(2): p. 4148-62.

341. Cai, J., et al., *Inhibition of influenza infection by glutathione.* Free Radical Biology and Medicine, 2003. **34**(7): p. 928-936.

342. Checconi, P., et al., *Redox proteomics of the inflammatory secretome identifies a common set of redoxins and other glutathionylated proteins released in inflammation, influenza virus infection and oxidative stress.* PLoS One, 2015. **10**(5): p. e0127086.

343. Hennet, T., E. Peterhans, and R. Stocker, *Alterations in antioxidant defences in lung and liver of mice infected with influenza A virus.* Journal of General Virology, 1992. **73**: p. 39-46.

344. Amatore, D., et al., *Influenza virus replication in lung epithelial cells depends on redox-sensitive pathways activated by NOX4-derived ROS.* Cell Microbiol, 2015. **17**(1): p. 131-45.

345. Nencioni, L., et al., *Influenza a virus replication is dependent on an antioxidant pathway that involves GSH and bcl2.* FASEB J, 2003. **17**(6): p. 758-760.

346. Morita, M., et al., *The lipid mediator protectin D1 inhibits influenza virus replication and improves severe influenza.* Cell, 2013. **153**(1): p. 112-25.

347. Teijaro, J.R., et al., *Endothelial cells are central orchestrators of cytokine amplification during influenza virus infection.* Cell, 2011. **146**(6): p. 980-91.

348. Brandes, M., et al., *A systems analysis identifies a feedforward inflammatory circuit leading to lethal influenza infection.* Cell, 2013. **154**(1): p. 197-212.

349. Salomon, R., E. Hoffmann, and R.G. Webster, *Inhibition of the cytokine response does not protect against lethal H5N1 influenza infection.* Proc Natl Acad Sci U S A, 2007. **104**(30): p. 12479-81.

350. Davidson, S., et al., *Pathogenic potential of interferon alphabeta in acute influenza infection.* Nat Commun, 2014. **5**: p. 3864.

351. Shirey, K.A., et al., *The TLR4 antagonist Eritoran protects mice from lethal influenza infection.* Nature, 2013. **497**(7450): p. 498-502.

352. Cummins, N.W., et al., *Heme oxygenase-1 regulates the immune response to influenza virus infection and vaccination in aged mice.* FASEB J, 2012. **26**(7): p. 2911-8.

353. Uchide, N. and H. Toyoda, *Antioxidant therapy as a potential approach to severe influenza-associated complications.* Molecules, 2011. **16**(3): p. 2032-52.

354. Shi, X.L., et al., *Therapeutic effect of recombinant human catalase on H1N1 influenza-induced pneumonia in mice.* Inflammation, 2010. **33**(3): p. 166-72.

355. Oda, T., et al., *Oxygen radicals in influenza-induced pathogenesis and treatment with pyran polymer-conjugated SOD.* Science, 1989. **244**(4907): p. 974-6.

356. Crotta, S., et al., *Type I and type III interferons drive redundant amplification loops to induce a transcriptional signature in influenza-infected airway epithelia.* PLoS Pathog, 2013. **9**(11): p. e1003773.

357. Dominguez, P.M. and C. Ardavin, *Differentiation and function of mouse monocyte-derived dendritic cells in steady state and inflammation.* Immunol Rev, 2010. **234**(1): p. 90-104.

358. Herold, S., et al., *Influenza virus-induced lung injury: pathogenesis and implications for treatment.* Eur Respir J, 2015. **45**(5): p. 1463-78.

359. La Gruta, N.L., et al., *A question of self-preservation: immunopathology in influenza virus infection.* Immunol Cell Biol, 2007. **85**(2): p. 85-92.

360. Newton, A.H., A. Cardani, and T.J. Braciale, *The host immune response in respiratory virus infection: balancing virus clearance and immunopathology.* Semin Immunopathol, 2016. **38**(4): p. 471-82.

361. Perrone, L.A., et al., *H5N1 and 1918 pandemic influenza virus infection results in early and excessive infiltration of macrophages and neutrophils in the lungs of mice.* PLoS Pathog, 2008. **4**(8): p. e1000115.

362. Simon, P.F., et al., *Highly Pathogenic H5N1 and Novel H7N9 Influenza A Viruses Induce More Profound Proteomic Host Responses than Seasonal and Pandemic H1N1 Strains.* J Proteome Res, 2015. **14**(11): p. 4511-23.

363. Doherty, P.C., et al., *Influenza and the challenge for immunology.* Nat Immunol, 2006. **7**(5): p. 449-55.

364. Dunning, J., et al., *Antiviral combinations for severe influenza.* Lancet Infect Dis, 2014. **14**(12): p. 1259-70.

365. Gambotto, A., et al., *Human infection with highly pathogenic H5N1 influenza virus.* Lancet, 2008. **371**(9622): p. 1464-75.

366. Itoh, Y., et al., *In vitro and in vivo characterization of new swine-origin H1N1 influenza viruses.* Nature, 2009. **460**(7258): p. 1021-5.

367. Memoli, M.J., et al., *Multidrug-resistant 2009 pandemic influenza A(H1N1) viruses maintain fitness and transmissibility in ferrets.* J Infect Dis, 2011. **203**(3): p. 348-57.

368. Akaike, T., et al., *Dependence on O2- generation by xanthine oxidase of pathogenesis of influenza virus infection in mice.* J Clin Invest, 1990. **85**(3): p. 739-45.

369. Abdul-Careem, M.F., et al., *Critical role of natural killer cells in lung immunopathology during influenza infection in mice.* J Infect Dis, 2012. **206**(2): p. 167-77.

370. Akaike, T., *Role of free radicals in viral pathogenesis and mutation.* Rev Med Virol, 2001. **11**(2): p. 87-101.

371. Perrin-Cocon, L., et al., *TLR4 antagonist FP7 inhibits LPS-induced cytokine production and glycolytic reprogramming in dendritic cells, and protects mice from lethal influenza infection.* Sci Rep, 2017. **7**: p. 40791.

372. Xu, Y. and L. Liu, *Curcumin alleviates macrophage activation and lung inflammation induced by influenza virus infection through inhibiting the NF-kappaB signaling pathway.* Influenza Other Respir Viruses, 2017. **11**(5): p. 457-463.

373. Verescakova, H., et al., *Nitro-oleic acid regulates growth factor-induced differentiation of bone marrow-derived macrophages.* Free Radic Biol Med, 2017. **104**: p. 10-19.

374. Nathan, C. and A. Ding, *Nonresolving inflammation.* Cell, 2010. **140**(6): p. 871-82.

375. Netea, M.G., et al., *Proinflammatory cytokines and sepsis syndrome: not enough, or too much of a good thing?* Trends Immunol, 2003. **24**(5): p. 254-8.

376. Matute-Bello, G., C.W. Frevert, and T.R. Martin, *Animal models of acute lung injury.* Am J Physiol Lung Cell Mol Physiol, 2008. **295**(3): p. L379-99.

377. Bosmann, M. and P.A. Ward, *The inflammatory response in sepsis.* Trends Immunol, 2013. **34**(3): p. 129-36.

378. van der Poll, T., et al., *The immunopathology of sepsis and potential therapeutic targets.* Nat Rev Immunol, 2017. **17**(7): p. 407-420.

379. Raghavendran, K., et al., *Pharmacotherapy of acute lung injury and acute respiratory distress syndrome.* Curr Med Chem, 2008. **15**(19): p. 1911-24.

380. Sapru, A., et al., *Pathobiology of acute respiratory distress syndrome.* Pediatr Crit Care Med, 2015. **16**(5 Suppl 1): p. S6-22.

381. Liu, Y.Z., Y.X. Wang, and C.L. Jiang, *Inflammation: The Common Pathway of Stress-Related Diseases.* Front Hum Neurosci, 2017. **11**: p. 316.

382. Conte, M.S., et al., *Pro-resolving lipid mediators in vascular disease.* J Clin Invest, 2018. **128**(9): p. 3727-3735.

383. Shore, S.A., *Obesity, airway hyperresponsiveness, and inflammation.* J Appl Physiol (1985), 2010. **108**(3): p. 735-43.

384. Sideleva, O., et al., *Obesity and asthma: an inflammatory disease of adipose tissue not the airway.* Am J Respir Crit Care Med, 2012. **186**(7): p. 598-605.

385. Endo, Y., et al., *Obesity Drives Th17 Cell Differentiation by Inducing the Lipid Metabolic Kinase, ACC1.* Cell Rep, 2015. **12**(6): p. 1042-55.

386. Steinman, R.M. and J. Banchereau, *Taking dendritic cells into medicine.* Nature, 2007. **449**(7161): p. 419-26.

387. Theofilopoulos, A.N., D.H. Kono, and R. Baccala, *The multiple pathways to autoimmunity.* Nat Immunol, 2017. **18**(7): p. 716-724.

388. Ah Kioon, M.D., et al., *Plasmacytoid dendritic cells promote systemic sclerosis with a key role for TLR8.* Sci Transl Med, 2018. **10**(423).

389. Koudelka, A., et al., *Nitro-Oleic Acid Prevents Hypoxia- and Asymmetric Dimethylarginine-Induced Pulmonary Endothelial Dysfunction.* Cardiovasc Drugs Ther, 2016. **30**(6): p. 579-586.

390. Hughan, K.S., et al., *Conjugated Linoleic Acid Modulates Clinical Responses to Oral Nitrite and Nitrate.* Hypertension, 2017.

391. Delmastro-Greenwood, M., et al., *Nitrite and nitrate-dependent generation of anti-inflammatory fatty acid nitroalkenes.* Free Radic Biol Med, 2015. **89**: p. 333-41.

392. Buchan, G.J., et al., *Nitro-fatty acid formation and metabolism.* Nitric Oxide, 2018. **79**: p. 38-44.

393. Luo, B., et al., *Resolvin D1 Programs Inflammation Resolution by Increasing TGF-beta Expression Induced by Dying Cell Clearance in Experimental Autoimmune Neuritis.* J Neurosci, 2016. **36**(37): p. 9590-603.

394. Hong, S., et al., *Resolvin E1 metabolome in local inactivation during inflammation-resolution.* J Immunol, 2008. **180**(5): p. 3512-9.

395. Colas, R.A., et al., *Identification and Actions of the Maresin 1 Metabolome in Infectious Inflammation.* J Immunol, 2016. **197**(11): p. 4444-4452.

396. Fazzari, M., et al., *Electrophilic fatty acid nitroalkenes are systemically transported and distributed upon esterification to complex lipids.* J Lipid Res, 2019. **60**(2): p. 388-399.

397. Fang, X., et al., *Temporally controlled targeting of 4-hydroxynonenal to specific proteins in living cells.* J Am Chem Soc, 2013. **135**(39): p. 14496-9.

398. Aw Yeang, H.X., et al., *Loss of transcription factor nuclear factor-erythroid 2 (NF-E2) p45-related factor-2 (Nrf2) leads to dysregulation of immune functions, redox homeostasis, and intracellular signaling in dendritic cells.* J Biol Chem, 2012. **287**(13): p. 10556-64.

399. Tam, V.C., et al., *Lipidomic profiling of influenza infection identifies mediators that induce and resolve inflammation.* Cell, 2013. **154**(1): p. 213-27.

400. Hosakote, Y.M., et al., *Respiratory syncytial virus induces oxidative stress by modulating antioxidant enzymes.* Am J Respir Cell Mol Biol, 2009. **41**(3): p. 348-57.

401. Cho, H.Y., et al., *Antiviral activity of Nrf2 in a murine model of respiratory syncytial virus disease.* Am J Respir Crit Care Med, 2009. **179**(2): p. 138-50.

402. Sun, T., et al., *Respiratory syncytial virus infection up-regulates TLR7 expression by inducing oxidative stress via the Nrf2/ARE pathway in A549 cells.* Arch Virol, 2018.

403. Palamara, A.T., et al., *Inhibition of influenza A virus replication by resveratrol.* J Infect Dis, 2005. **191**(10): p. 1719-29.

404. Sgarbanti, R., et al., *Intracellular redox state as target for anti-influenza therapy: are antioxidants always effective?* Curr Top Med Chem, 2014. **14**(22): p. 2529-41.

405. Jobbagy, S., et al., *Electrophiles modulate glutathione reductase activity via alkylation and upregulation of glutathione biosynthesis.* Redox Biol, 2019. **21**: p. 101050.